九州大学学術情報リポジトリ
Kyushu University Institutional Repository

SEPARATION AND RECOVERY OF PLATINUM GROUP METALS FROM AUTOMOTIVE CATALYSTS USING POLYMER INCLUSION MEMBRANES CONTAINING IONIC LIQUIDS

アドロイト, トリク, ヌル, ファジャール

https://hdl.handle.net/2324/4496037

出版情報：九州大学, 2021, 博士（工学）, 課程博士
バージョン：
権利関係：

SEPARATION AND RECOVERY OF PLATINUM GROUP METALS FROM AUTOMOTIVE CATALYSTS USING POLYMER INCLUSION MEMBRANES CONTAINING IONIC LIQUIDS

Adroit Toriq Nur Fajar

Department of Chemical System & Engineering

Faculty of Engineering

Kyushu University

June 2021

TABLE OF CONTENTS

CHAPTER 1. GENERAL INTRODUCTION

1.1 Platinum Group Metals (PGMs)

Platinum group metals (PGMs) are six precious metals in the *d*-block of the periodic table consist of ruthenium ($_{44}$Ru), rhodium ($_{45}$Rh), palladium ($_{46}$Pd), osmium ($_{76}$Os), iridium ($_{77}$Ir), and platinum ($_{78}$Pt). These metals exhibit excellent physical and chemical properties such as outstanding catalytic activities [1,2], stable electrical properties [3], resistance to corrosion [4], and high thermal durability [5]. PGMs are also frequently used as an additive for mixtures of metals to form high-quality alloys [6]. Owing to these unique natures, PGMs have become an essential component in the manufacture of various modern products, particularly in the automotive and electronic device industries. Unfortunately, PGMs are extremely scarce elements with strictly limited mining sites [7]. Moreover, the role of PGMs in nowadays applications is rarely substituted, if not irreplaceable, by the other elements or compounds. These circumstances lead the price of PGMs, especially Pt, Pd, and Rh, steadily increasing over the years; and thus, becoming a highly treasurable commodity.

1.1.1 Global supply and demand for PGMs

The annual supply and the demand for PGMs in recent years were always unbalanced. According to the Johnson Matthey's report in February 2021 [8], the PGM supply in 2020 was 4,888,000 oz, 6,167,000 oz, and 583,000 oz for Pt, Pd, and Rh, respectively. This supply is mainly produced from mining sites in Russia and South Africa. On the other hand, the PGM demand in 2020 was 6,920,000 oz, 9,894,000 oz, and 1,005,000 oz for Pt, Pd, and Rh, respectively. The demand exceeded the supply by approximately 30%. A significant portion of this demand was attributed to the production of automotive catalytic converters, and the rest is distributed to fine chemical productions, electronic devices, jewelry, investments, bio-medical applications, and others. Figure 1.1 shows the market distribution of PGMs in 2020.

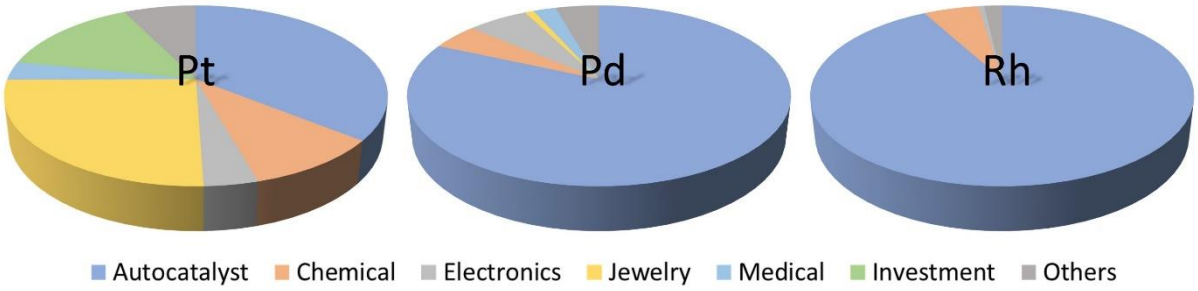

Figure 1.1. Global market distribution of PGMs in 2020. Compiled from the Johnson Matthey's report in February 2021 [8].

Despite the scarcity and high prices, the market of PGMs in the future is predicted to continuously increasing. Recently, Jasiński et al. reported a forecasting study on the supply and demand for PGMs and lithium (Li) until 2070 using a surplus cost potential as the indicator [9]. The market of PGMs and Li will be on a treadmill depending on the direction of car technologies. Continuously using gasoline cars will increase the demand for PGMs, while democratizing affordable electric vehicles will reduce the growing demand for PGMs and increase the demand for the Li battery. The latter option would be favorable in the viewpoint of environmental ethics and considering the threats of climate changes. However, the current electric car technology, particularly the battery's performance, still requires much improvement. Furthermore, the high price hinders the use of electric cars become mainstream, especially in developing countries. The third option is to move to the green and clean hydrogen energy. As for automotive industries, the hydrogen energy would be mainly produced using fuel cells, which requiring PGMs, especially Pt, as the electrode. A combination of gasoline, electric, and hydrogen energy is expected to happen in the upcoming future, at least for decades before the zero-emission goals could be achieved. Therefore, the demand for PGMs will be continuously growing for decades.

1.1.2 PGM secondary resources: automotive catalysts

To fill the gap between the supply and demand as well as to maintain the sustainability of the PGM stock, metal recycling or recovery from secondary resources is one of the best options. In fact, the concentration of a PGM, Pd for example, in secondary sources such as automotive catalysts (2 kg/ton), mobile phones (0.35 kg/ton), and computer motherboards (80 g/ton) is much higher than that of the primary ore (<10 g/ton) [10]. Thus, the recovery of PGMs from secondary sources would be profitable and feasible from an economic point of view. Moreover, the PGM recovery also would be favorable from the perspective of environmental ethics since it can decrease carbon emission, energy consumption, and landfill excavation in the mining processes. The production of noble metals requires more energy and a lot of carbon emission compared to common metals. For instance, the production of 1 kg Rh is equivalent to the emission of 35,100 kg CO_2 to the atmosphere, while the production of 1 kg Fe is equivalent to 1.5 kg CO_2 emission [11]. Therefore, PGM recycling is crucial since it would preserve the metal stock, economically profitable, and environmentally favorable at the same time.

As mentioned above, spent automotive catalysts (SACs) are the most abundant PGM secondary resource. Automotive catalysts were first introduced in the 1970s to regulate exhaust gases from a car, such as converting toxic CO gas to CO_2 [12]. Commonly, automotive catalysts are fabricated in the shape of a honeycomb structure, containing cordierite ($2MgO.2Al_2O_3{\cdot}5SiO_2$), gamma-alumina layers (γ-Al_2O_3), PGMs as catalytically active metals, and some additives (alkaline earth metals, rare earth metals, and transition metals) [13]. Recovery of PGMs from SACs in a conventional process requires many stages, high energy, and hazardous chemicals as it combines pyrometallurgical and hydrometallurgical approaches. Figure 1.2 shows a schematic representation of PGM recovery processes from SACs. In the effort to simplify metal recycling processes, currently, some alternative methods are being

developed, such as direct solvent extraction using ionic liquids [14], solvo-metallurgy [15], and separation using a membrane technology [16].

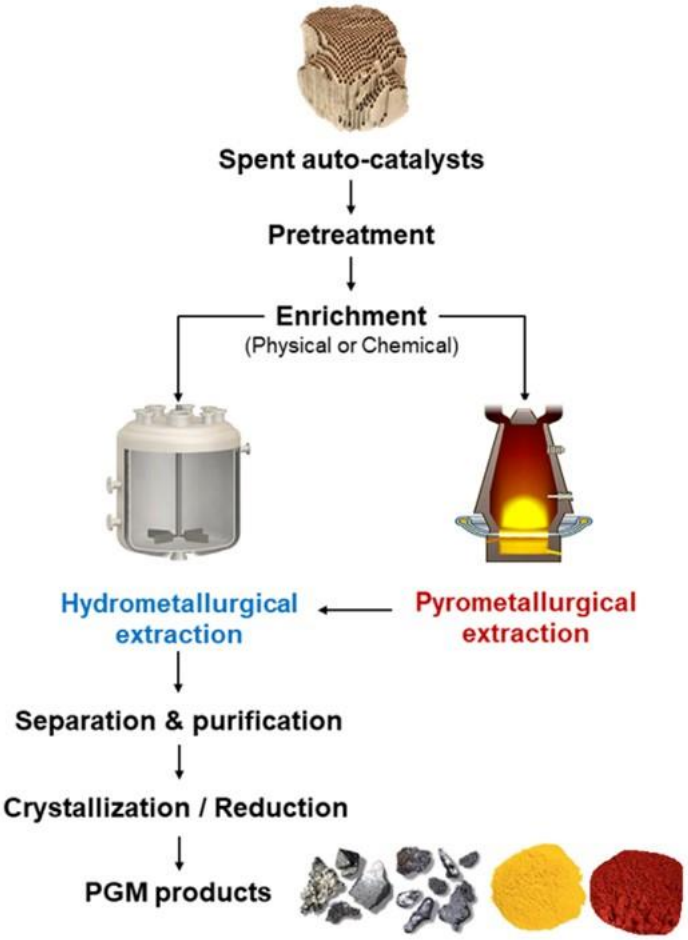

Figure 1.2. Schematic representation of PGMs recycling processes. Reproduced from ref. [13] with permission. Copyright 2020 Elsevier.

1.2 Ionic Liquids (ILs)

Ionic liquids (ILs) are defined as a class of compounds entirely composed of ions with a melting point below 100 °C [17]. By this definition, any inorganic and organic salt liquids at a temperature below 100 °C can be classified as ILs. Nowadays, the term IL is often used to refer to liquid salts at room temperature composed of organics or a combination of organic and inorganic ions. Since the first discovery of IL (ethyl ammonium nitrate) in 1914 by Paul Walden [18], the research on ILs has been tremendously growing, especially in the past few decades where ILs are produced commercially and applied in various fields. In recent years,

thousands of studies had reported new structures, synthesis techniques, and the application of ILs [19]. Depending on the structure design and the combination of cations and anions, the properties of ILs can be easily tuned, thus often considered as a designer solvent. Furthermore, the majority of ILs shows "green" properties such as non-volatile, non-flammable, and arguably less hazardous compare to conventional organic solvents.

In the field of metal extraction, the initial attempt in using an IL to extract metals was reported by Dai et al. in 1999 [20]. They reported a solvent extraction of strontium using an IL crown ether dissolved in IL 1,3-dialkylimidazolium, which showed distinguish extraction behaviors compare to that of conventional organic extractants. Since then, many other attempts have been pursued. Related to PGMs, several ionic liquids structures have been developed in the laboratory as well as applying the commercially available ones [21]. Frequently used cations were imidazolium, ammonium, phosphonium, and pyridinium-based ions. As for anions, bis(trifluoromethane-sulfonyl) imide (Tf_2N), bis(2,4,4-trymethylpentyl)-phosphinate (BTMPP), hexafluorophosphate (PF_6), and halides (Cl^- and Br^-) were often used in recent years. Figure 1.3 shows the commonly used IL cations and anions in the metal extraction, particularly PGMs.

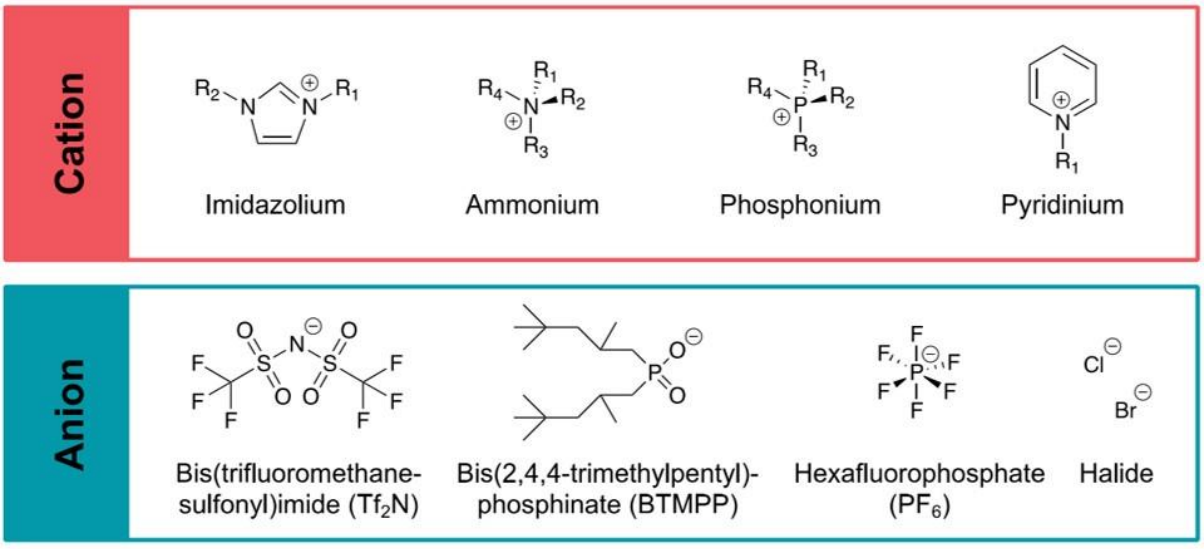

Figure 1.3. Common structures of ionic liquid's cations and anions studied for PGM separation. Reproduced from ref. [21], copyright 2020 J-STAGE.

In our laboratory, a novel IL specifically designed to carry out solvent extraction of PGMs had been developed, namely trioctyltetradecyl phosphonium chloride ($P_{88812}Cl$). As reported by Firmansyah et al., the IL demonstrated outstanding performance in the extraction of Pt(IV), Pd(II), and Rh(III) from a chloride solution [22]. Investigation on the extraction mechanism showed that the metal complexes were extracted from the aqueous phase to the organic phase via an ion-exchange mechanism as described in equations (1.1) – (1.3). Subsequently, Firmansyah et al. reported the application of the $P_{88812}Cl$ IL for the recovery of PGMs from automotive catalysts [14,23]. The results were quite promising and opening the possibilities to be implemented in industries. These insights were inspiring us to further utilize the IL for developing a greener and less expensive technology for metal separation, i.e., the membrane-based technology.

$$[PtCl_6]^{2-} + 2\left(P_{88812}{}^{+}Cl^{-}\right) \rightleftharpoons \left(P_{88812}{}^{+}\right)_2[PtCl_6]^{2-} + 2Cl^{-} \quad (1.1)$$

$$[PdCl_4]^{2-} + 2\left(P_{88812}{}^{+}Cl^{-}\right) \rightleftharpoons \left(P_{88812}{}^{+}\right)_2[PdCl_4]^{2-} + 2Cl^{-} \quad (1.2)$$

$$[RhCl_5(H_2O)]^{2-} + 2\left(P_{88812}{}^{+}Cl^{-}\right) \rightleftharpoons \left(P_{88812}{}^{+}\right)_2[RhCl_5(H_2O)]^{2-} + 2Cl^{-} \quad (1.3)$$

1.3 Polymer Inclusion Membranes (PIMs)

The concept of polymer inclusion membranes (PIMs) is based on supported-liquid membranes (SLMs), which were introduced in the 1950s [24,25]. SLMs are prepared by immersing a porous polymer membrane into a liquid extractant so that the liquid would incorporate into the membrane within the pores. As such, the extractant is the active reagent to act as a carrier targeting specific analytes, while the polymer framework functions as a solid support/framework to construct self-standing liquid membranes. The liquid phase is expected to be maintained inside the polymer pores owing to the capillary force. However, the membranes are often unstable due to the leakage of the extractant from the membrane.

Apparently, the capillary force is frequently not enough to hold back the other forces pulling the extractant molecules, such as a chemical affinity.

PIMs were then developed to enhance the stability of SLMs. Instead of immersing polymer membranes into liquid extractants, the extractants were directly included in the membrane matrix by mixing them with the dissolved polymers. Typically, this is carried out by solvent casting methods, i.e., dissolving a polymer and an extractant in a volatile solvent, casting the mixture onto a flat plate, then allows the solvent to evaporate, thus resulting in a thin solid membrane. Since the polymer and the extractant are homogeneously mixed, the interaction between them is expected to be stronger than in SLMs. The extractant molecules are well entrapped between the entanglement of the polymer chains and chemically interacted via Van der Waals force. Hence, the leakage of extractant during membrane operations can be prevented. Furthermore, PIM is also considered as a green technology compare to the use of extractant in liquid-liquid extraction counterparts owing to markedly fewer required carriers and the absence of any organic solvents. From the economic viewpoint, membrane-facilitated processes are arguably less expensive and less time-consuming compare to the other approaches. This is mainly related to reagents and energy consumptions and the simplicity or complexity of the engineering processes.

Historically, the concept of PIM had emerged between 1970 to 1980, but the first use of the term “polymer inclusion membrane” was coined by Schow et al. in 1996 [26]. Later on, since the early 2000s, Kolev and co-workers have been intensively investigating lots kind of PIMs and expanding the application into various fields [16]. Nowadays, PIMs are applied or studied for sensing application, separation, sample pre-concentration, and passive sampling (see Figure 1.4).

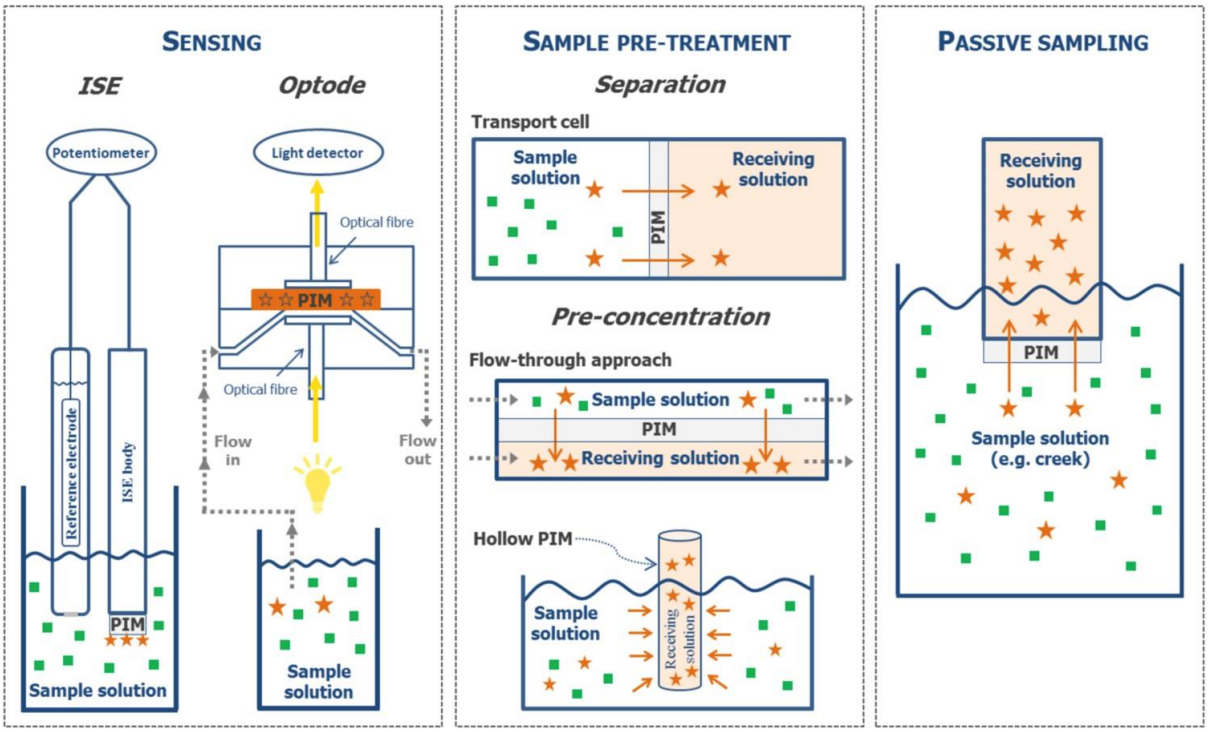

Figure 1.4. Application of polymer inclusion membranes in various fields. Reproduced from ref. [16] with permission. Copyright 2017 Elsevier.

Since PIMs work based on carrier-mediated transport mechanisms, the selection of extractants/carriers is crucial to the membrane performances. In the last decade, the use of PIMs for metal separation has been undertaken, particularly employing ILs as the metal carrier since they show promising and distinctive behavior in solvent extractions. The pioneers of this fascinating research include Regel-Rosocka and co-workers [27–29], Pospiech [30–32], and our group—Goto and co-workers [33–35]. In the present thesis, the author was studying the IL previously investigated by Firmansyah et al. for liquid-liquid extraction of PGMs, the $P_{88812}Cl$, as a metal carrier within PIMs. The possibilities of developing durable membranes with a high performance for selective separation of PGMs were systematically studied. Subsequently, the whole process for the recovery of PGMs from SACs using the PIM technology has been demonstrated.

1.4 Aim and Outline of The Thesis

This research aims to develop an effective process for selective separation and the recovery of platinum group metals from an automotive catalyst waste employing the polymer inclusion membrane technology, using the ionic liquid as the metal carrier. To achieve the goals within reasonable timeframe, the research was divided into three projects sequel, which would be elaborated comprehensively in the following chapters of this thesis.

The present thesis consists of 5 chapters, i.e., a general introduction (Chapter 1), the research achievements (Chapter 2, Chapter 3, and Chapter 4), and general conclusions (Chapter 5). References are provided at the end of each chapter, and Appendixes (Supporting Information) are presented within each chapter of the research achievements.

In the Chapter 1, a general introduction to platinum group metals, ionic liquids, and polymer inclusion membranes is presented. The author briefly reviewed the scientific literature on the topics, including the first discovery, recent progress, and position of the present study in advancing the field.

Chapter 2 discusses the development of polymer inclusion membranes containing phosphonium-based ionic liquids. The performance of membranes containing the ionic liquid developed in our laboratory ($P_{88812}Cl$) and a commercially available ionic liquid with an analog structure ($P_{66614}Cl$) for selective separation of Pd(II) and Rh(III) was systematically investigated.

Chapter 3 discusses the use of the optimized membrane and process developed in Chapter 2 to carry out a more complicated separation system, which was the separation of Pt(IV), Pd(II), and Rh(III). To selectively separate those three metals from each other using one membrane, a sequential membrane transport strategy was proposed. Plausible transport mechanisms are also discussed in this chapter.

Chapter 4 discusses the application of the membrane transport system developed in Chapter 2 & Chapter 3 to perform a selective recovery of Pt, Pd, and Rh from an actual waste—a spent automotive catalyst. The possibility of modifying membrane morphologies to enhance the transport performance is also discussed in this chapter.

In the Chapter 5, a summary of the entire research achievements is presented. In addition, the author also provided a brief outlook on the future potentials of this study from the perspective of industrial interests as well as the challenge to develop more sophisticated membrane transport theories.

In addition, the author would like to point out that permissions from publishers have been granted to reuse published materials from references. In the Chapter 1, copyright statements are provided in the captions of each corresponding figure. Chapter 2, Chapter 3, and Chapter 4 are original works conducted by the author and co-workers initially published in peer-reviewed journals (see ref. [33–35]). The publishers have granted permissions to reuse the whole articles for the present thesis, and the copyrights are declared on the first page of those chapters.

References

[1] P.B. Kettler, Platinum Group Metals in Catalysis: Fabrication of Catalysts and Catalyst Precursors, *Org. Process Res. Dev*. 7 (2003) 342–354.

[2] J. Zhang, Y. Zhao, X. Guo, C. Chen, C.-L. Dong, R.-S. Liu, C.-P. Han, Y. Li, Y. Gogotsi, G. Wang, Single platinum atoms immobilized on an MXene as an efficient catalyst for the hydrogen evolution reaction, *Nat. Catal*. 1 (2018) 985–992.

[3] C. Simonnet, A. Grandjean, J. Phalippou, Electrical behavior of platinum-group metals in glass-forming oxide melts, *J. Nucl. Mater*. 336 (2005) 243–250.

[4] I.A. Mwamba, L.A. Cornish, E. van der Lingen, Effect of platinum group metal addition on microstructure and corrosion behaviour of Ti–47·5 at-%Al, *Corros. Eng. Sci. Technol*. 49 (2014) 180–188.

[5] T. Tsuda, K. Miura, A. Hikasa, K. Hosoi, F. Kimata, Improvement of the Thermal Durability of an Exhaust Gas Purifying Catalyst Using Size-Controlled Pt-Hydroxide Clusters, *SAE Int. J. Engines*. 9 (2016) 2442–2450.

[6] K. Kusada, D. Wu, H. Kitagawa, New Aspects of Platinum Group Metal-Based Solid-Solution Alloy Nanoparticles: Binary to High-Entropy Alloys, *Chem. – A Eur. J*. 26 (2020) 5105–5130.

[7] H. Dong, J. Zhao, J. Chen, Y. Wu, B. Li, Recovery of platinum group metals from spent catalysts: A review, *Int. J. Miner. Process*. 145 (2015) 108–113.

[8] PGM Market Report 2020 - Reported in February 2021, *Johnson Matthey* (2021) 1–48.

[9] D. Jasiński, J. Meredith, K. Kirwan, The life cycle impact for platinum group metals and lithium to 2070 via surplus cost potential, I*nt. J. Life Cycle Assess*. 23 (2018) 773–786.

[10] C. Hagelüken, Recycling the Platinum Group Metals, *Platin. Met. Rev*. 56 (2012) 29–35.

[11] P. Nuss, M.J. Eckelman, Life cycle assessment of metals: A scientific synthesis, *PLoS One*. 9 (2014) 1–12.

[12] J. Kašpar, P. Fornasiero, N. Hickey, Automotive: catalytic converters current status, *Catal. Today*. 77 (2003) 419–449.

[13] H.B. Trinh, J. chun Lee, Y. jae Suh, J. Lee, A review on the recycling processes of spent auto-catalysts: Towards the development of sustainable metallurgy, *Waste Manag*. 114 (2020) 148–165.

[14] M.L. Firmansyah, F. Kubota, W. Yoshida, M. Goto, Application of a Novel Phosphonium-Based Ionic Liquid to the Separation of Platinum Group Metals from Automobile Catalyst Leach Liquor, *Ind. Eng. Chem. Res*. 58 (2019) 3845–3852.

[15] V.T. Nguyen, S. Riaño, E. Aktan, C. Deferm, J. Fransaer, K. Binnemans, Solvometallurgical Recovery of Platinum Group Metals from Spent Automotive Catalysts, *ACS Sustain. Chem. Eng*. 9 (2021) 337–350.

[16] M.I.G.S. Almeida, R.W. Cattrall, S.D. Kolev, Polymer inclusion membranes (PIMs) in chemical analysis - A review, *Anal. Chim. Acta*. 987 (2017) 1–14.

[17] Z. Lei, B. Chen, Y.M. Koo, D.R. Macfarlane, Introduction: Ionic Liquids, *Chem. Rev*. 117 (2017) 6633–6635.

[18] V.N. Emel'Yanenko, G. Boeck, S.P. Verevkin, R. Ludwig, Volatile times for the very first ionic liquid: Understanding the vapor pressures and enthalpies of vaporization of ethylammonium nitrate, *Chem. - A Eur. J.* 20 (2014) 11640–11645.

[19] K. Dong, X. Liu, H. Dong, X. Zhang, S. Zhang, Multiscale Studies on Ionic Liquids, *Chem. Rev*. 117 (2017) 6636–6695.

[20] S. Dai, Y.H. Ju, C.E. Barnes, Solvent extraction of strontium nitrate by a crown ether using room-temperature ionic liquids, J. Chem. Soc. - *Dalt. Trans*. 2 (1999) 1201–1202.

[21] M.L. Firmansyah, W. Yoshida, T. Hanada, M. Goto, Application of ionic liquids in solvent extraction of platinum group metals, *Solvent Extr. Res. Dev*. 27 (2020) 1–24.

[22] M.L. Firmansyah, F. Kubota, M. Goto, Solvent extraction of Pt (IV), Pd (II), and Rh (III) with the ionic liquid trioctyl (dodecyl) phosphonium chloride, *J. Chem. Technol. Biotechnol*. 93 (2018) 1714–1721.

[23] M.L. Firmansyah, F. Kubota, M. Goto, Selective recovery of platinum group metals from spent automotive catalysts by leaching and solvent extraction, *J. Chem. Eng. Japan*. 52 (2019) 835–842.

[24] R.E. Kesting, W.J. Subcasky, J.D. Paton, Liquid membranes at the cellulose acetate membrane/saline solution interface in reverse osmosis, *J. Colloid Interface Sci*. 28 (1968) 156–160.

[25] K. Srinivasan, G.A. Rechnitz, Selectivity studies on liquid membrane, ion-selective electrodes, *Anal. Chem*. 41 (1969) 1203–1208.

[26] A.J. Schow, R.T. Peterson, J.D. Lamb, Polymer inclusion membranes containing macrocyclic carriers for use in cation separations, *J. Memb. Sci*. 111 (1996) 291–295.

[27] M. Baczyńska, M. Regel-Rosocka, M. Nowicki, M. Wiśniewski, Effect of the structure of polymer inclusion membranes on zn(II) transport from chloride aqueous solutions, *J. Appl. Polym. Sci*. 132 (2015) 42319.

[28] M. Regel-Rosocka, M. Rzelewska, M. Baczynska, M. Janus, M. Wisniewski, Removal of palladium(II) from aqueous chloride solutions with cyphos phosphonium ionic liquids as metal ion carriers for liquid-liquid extraction and transport across polymer inclusion membranes, *Physicochem. Probl. Miner. Process*. 51 (2015) 621–631.

[29] M. Regel-Rosocka, Ł. Nowak, M. Wiśniewski, Removal of zinc(II) and iron ions from chloride solutions with phosphonium ionic liquids, *Sep. Purif. Technol*. 97 (2012) 158–163.

[30] B. Pospiech, Separation of cadmium(II), cobalt(II) and nickel(II) by transport through polymer inclusion membranes with phosphonium ionic liquid as ion carrier, *Arch. Metall. Mater*. 60 (2015) 2933–2938.

[31] B. Pospiech, Application of Phosphonium Ionic Liquids as Ion Carriers in Polymer Inclusion Membranes (PIMs) for Separation of Cadmium(II) and Copper(II) from Aqueous Solutions, *J.*

Solution Chem. 44 (2015) 2431–2447.

[32] B. Pospiech, Facilitated transport of palladium(II) across polymer inclusion membrane with ammonium ionic liquid as effective carrier, *Chem. Pap*. 72 (2018) 301–308.

[33] A.T.N. Fajar, F. Kubota, M.L. Firmansyah, M. Goto, Separation of Palladium(II) and Rhodium(III) Using a Polymer Inclusion Membrane Containing a Phosphonium-Based Ionic Liquid Carrier, *Ind. Eng. Chem. Res*. 58 (2019) 22334–22342.

[34] A.T.N. Fajar, T. Hanada, M.L. Firmansyah, F. Kubota, M. Goto, Selective Separation of Platinum Group Metals via Sequential Transport through Polymer Inclusion Membranes Containing an Ionic Liquid Carrier, *ACS Sustain. Chem. Eng*. 8 (2020) 11283–11291.

[35] A.T.N. Fajar, T. Hanada, M. Goto, Recovery of platinum group metals from a spent automotive catalyst using polymer inclusion membranes containing an ionic liquid carrier, *J. Memb. Sci*. 629 (2021) 119296.

CHAPTER 2. SEPARATION OF PALLADIUM(II) AND RHODIUM(III) USING A POLYMER INCLUSION MEMBRANE CONTAINING A PHOSPHONIUM-BASED IONIC LIQUID CARRIER

Abstract:

In this study, we report the separation of Pd(II) and Rh(III) in a chloride solution using a polymer inclusion membrane (PIM). We designed trioctyl(dodecyl) phosphonium chloride ($P_{88812}Cl$) ionic liquid as a metal carrier for the PIM separation system. The effects of PIM composition and experimental conditions were systematically investigated. The concentration of hydrochloric acid in the feed solution and thiourea in the receiving solution were found to play a crucial role in the success of selective separation. Under the optimized conditions, Pd(II) could be effectively separated from Rh(III) with 98% recovery yield and 99% purity. We also compared the performance of our designed carrier, $P_{88812}Cl$, to that of a commercially available ionic liquid trihexyl(tetradecyl) phosphonium chloride ($P_{66614}Cl$) using a 7 cycle reusability test. The $P_{88812}Cl$ showed more stable performance and better durability compared with those of the commercial ionic liquid carrier.

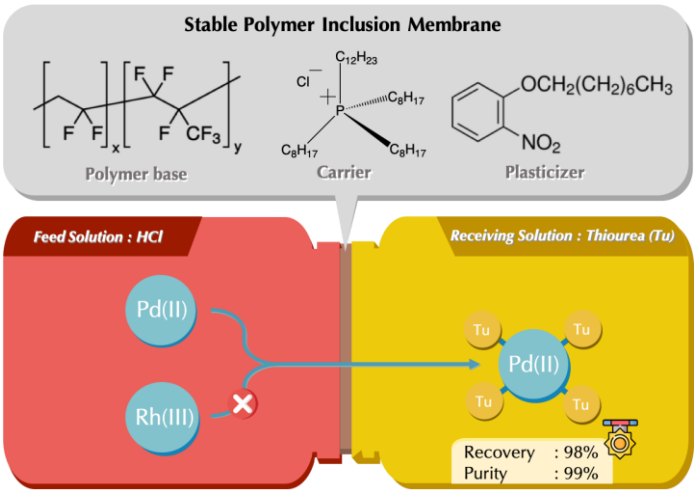

Remark:

This chapter was published in *Industrial & Engineering Chemistry Research*, 2019, 58, 22334–22342. Reproduced with permission. Copyright 2019 American Chemical Society.

2.1 Introduction

Platinum group metals (PGMs), which include platinum (Pt), palladium (Pd), rhodium (Rh), ruthenium (Ru), iridium (Ir), and osmium (Os), are essential in the manufacture of many advanced products used around the world. PGMs show unique properties in their catalytic activity [1–3], stability [4], conductivity [5], and even in their visual appearance [6]. Currently, PGMs are commonly used as the main component of automotive catalytic converters and in electrical circuits and jewelry [7]. The global demand for PGMs is increasing year by year, and in 2017 the total gross demand for Pd and Rh was 10,079,000 oz and 1,061,000 oz, respectively [8]. However, PGM supply is quite limited, in fact, it is below the global demand [8,9]. The concentration of PGMs in their ores is generally less than 0.001 wt%, and the major mines are located in specific geographical areas, for example, Russia and South Africa [10]. In addition, Nuss and Eckelman reported that the global warming potential of PGM mining processes was much higher than that of other metals [11]. For example, the CO_2 production of the Pd (3,880 kg CO_2-eq/kg) and Rh (35,100 kg CO_2-eq/kg) mining processes is much higher than that of Fe mining (1.5 kg CO_2-eq/kg). These findings show that the challenges facing PGM supply are not limited to their low abundance but also environmental considerations.

Recycling has been carried out in PGM industries to address the gap between supply and demand. Approximately 30% of Pt, Pd, and Rh demand is now fulfilled by recycling [8]. Automotive and electronic wastes are the main resources for recycling owing to their PGM-rich content. The concentration of Pd in automotive catalytic converters (2,000 g/tonne), mobile phones (350 g/tonne), and computer motherboards (80 g/tonne) is much higher than those in PGM primary ores (<10 g/tonne) [12]. In light of this, the recycling process should attract significant attention in order to make PGM industries more economically feasible and environmentally benign. PGM recycling is commonly carried out using a hydrometallurgical process, which involves a solvent extraction technique in the separation and the purification

step [13]. Recently, several novel extractants for use in solvent extraction of PGMs have been developed, such as thiodiglycolamides [14], thioamide-modified calix[4]arene [15], and tetrahexylammonium bis(trifluoromethanesulfonyl)imide [16]. These novel extractants have shown high performances in the extraction and back-extraction of PGMs. However, large-scale implementation of solvent extraction can result in serious environmental burdens. Moreover, the solvent extraction process requires a large amount of extractant and organic solvent and therefore has economic limitations. The use of extractants can be significantly reduced by using a polymer inclusion membrane (PIM) system.

PIM technology is based on the supported-liquid membrane (SLM) concept that first emerged in the 1950s [17–19], although the term "polymer inclusion membrane" was first used by Schow et al. in 1996 [20]. Subsequently, Kolev and co-workers carried out extensive research on PIM development and extended the application to various fields [21–27]. PIMs exhibit several interesting features; they significantly reduce the amount of extractants, eliminate the use of organic solvents, and are more stable than conventional SLMs [28]. Nevertheless, reports of PGM recovery using PIM transport systems are limited. Only a few reports showing successful Pd(II) transport are available, which were conducted by Regel-Rosocka et al. [29] and Pospiech [30,31]. The main focus of these reports was Pd(II) transport, and they do not address the separation of PGMs. In the latest report by Pospiech [31], the selective transport of Pd(II) over other transition metal ions such as Fe(III), Ni(III), and Mn(II) was briefly described. However, mutual separation among PGMs has not yet been demonstrated, and furthermore, the important issues of membrane stability and recovery efficiency remain unaddressed. Hence, a membrane transport system with sufficient durability to withstand a practical use is required for PGM separation.

Recently, we reported the successful separation and recovery of PGMs from an automotive catalyst leach liquor using the solvent extraction technique with a synthesized ionic liquid,

namely trioctyl(dodecyl) phosphonium chloride ($P_{88812}Cl$) [32]. The automotive catalyst leach liquor contained a relatively high concentration of the PGMs Pd (367.6 mg L^{-1}) and Rh (32.5 mg L^{-1}). By carefully adjusting the experimental conditions, high purity Pd(II) and Rh(III) were successfully recovered after a series of hydrometallurgical processes. On the basis of this insight, we aimed to develop an effective membrane transport system for Pd and Rh separation. Herein, we report successful separation of Pd(II) from Rh(III) in a chloride solution using a PIM transport system including the ionic liquid as the PGM carrier. The effects of membrane composition and experimental conditions were systematically investigated to optimize the performance. We also examined the reusability of the membrane and its stability in a multiple use recycle test and compared the performance of $P_{88812}Cl$ to a commercially available ionic liquid trihexyl(tetradecyl) phosphonium chloride ($P_{66614}Cl$). To the best of our knowledge, this is the first report of Pd(II) and Rh(III) separation employing a membrane transport system.

2.2 Experimental

2.2.1 Materials

We designed the trioctyl(dodecyl) phosphonium chloride ($P_{88812}Cl$) ionic liquid, which was then made by Nippon Chemical Industrial Co., Ltd. The palladium standard solution (1,000 ppm), thiourea (powder, 98%), and tetrahydrofuran (THF, 99.5%) were purchased from Wako Pure Chemical Ltd. The rhodium standard solution (1,000 ppm) and the phosphorous standard solution (1,000 ppm) were purchased from Kanto Chemical Co., Inc. Trihexyl(tetradecyl) phosphonium chloride ($P_{66614}Cl$) ionic liquid was obtained from Ionic Liquids Technologies GmbH. The poly(vinylidene fluoride-*co*-hexafluoropropylene) (PVDF-*co*-HFP) pellets were purchased from Sigma Aldrich. 2-Nitrophenyloctyl ether (2NPOE, 99.0%) was purchased from Dojindo Laboratories (Kumamoto, Japan). The hydrochloric acid solution (10 M) was purchased from Kishida Co., Ltd. All of the aqueous solutions were prepared in Milli-Q

deionized water (Merck Millipore). The chemical structures of PVDF-*co*-HFP, $P_{88812}Cl$, 2NPOE, and $P_{66614}Cl$ can be seen in Figure S2.1 (Appendix A).

2.2.2 Preparation of polymer inclusion membranes

Polymer inclusion membranes (PIMs) consisting of 40–70 wt% base-polymer (PVDF-*co*-HFP), 20–40 wt% metal ion carrier ($P_{88812}Cl$), and 0–20 wt% plasticizer (2NPOE) were prepared as described in the previous reports [33–35]. In a typical preparation, PIM components with a total mass of 400 mg were dissolved in 10 mL of THF at 40 °C with vigorous stirring. After a clear and homogenous solution was observed, it was poured into a glass ring (diameter of 7.5 cm) sitting on a flat glass plate. Subsequently, the top of the glass ring was covered with a filter paper and a watch glass to allow slow evaporation of the THF overnight. After the THF had completely evaporated, the remaining slightly cloudy membrane, which had a smooth surface was carefully peeled from the glass plate (Figure S2.2, Appendix A).

2.2.3 Membrane transport experiments

Membrane transport experiments were carried out in a transport apparatus consisting of two water-jacketed glass compartments. A circular sample of PIM was sandwiched between the rim of the two transport cells to separate the feed and receiving solutions. The feed and receiving cells were filled with 50 mL of the corresponding solutions. The effective surface area of the membrane that was exposed to each solution was 4.9×10^{-4} m^2 (diameter of 25.0 mm). During the transport experiments, the solution in each cell was stirred using a double cross-head type magnetic stirrer bar. The temperature in both the feed and receiving solutions was kept constant at 25 ± 0.5 °C by continuously circulating water to the jacket of each compartment from a thermoregulated water bath, NCB-1200 (EYELA). 0.5 mL samples were taken regularly from both of the solutions at designated time intervals, and the metal

concentrations were analyzed using an inductively coupled plasma optical emission spectrometer (ICP-OES) Optima 8300 (Perkin Elmer Co., MA USA). The solution removed for analysis was then replaced with the same volume of fresh corresponding solution.

Assuming the membrane transport kinetics is a first-order reaction, the rate constant (k, h^{-1}), permeability coefficient (P, m h^{-1}), and initial flux (J_0, mmol m^{-2} h^{-1}) for the Pd(II) transport were calculated using equations (2.1) – (2.3), respectively.

$$ln\left(\frac{C_{Pd,t}^{F}}{C_{Pd,i}^{F}}\right) = -kt \qquad (2.1)$$

$$P = \left(\frac{V}{A}\right)k \qquad (2.2)$$

$$J_0 = PC_{Pd,i}^{F} \qquad (2.3)$$

where $C_{Pd,t}^{F}$ (mol m^{-3}) is the concentration of Pd(II) in the feed solution at time t, $C_{Pd,i}^{F}$ (mol m^{-3}) is the initial concentration of Pd(II) in the feed solution, V (m^3) is the volume of the feed solution, and A (m^2) is the membrane surface area that was exposed to both the feed and receiving solutions. The k values were calculated with a correlation coefficient (R) value of ≥0.98.

In addition, other parameters i.e. the recovery factor (RF, %), separation factor (SF, –), and purity (PR, %) of Pd(II) transport were calculated using equations (2.4) – (2.6), respectively.

$$RF = \frac{C_{Pd,t}^{R}}{C_{Pd,i}^{F}} \times 100\% \qquad (2.4)$$

$$SF = \frac{C_{Pd,i}^{F} - C_{Pd,t}^{F}}{C_{Pd,t}^{F}} \times \frac{C_{Rh,t}^{F}}{C_{Rh,i}^{F} - C_{Rh,t}^{F}} \qquad (2.5)$$

$$PR = \frac{C_{Pd,t}^{R}}{C_{Pd,t}^{R} + C_{Rh,t}^{R}} \times 100\% \qquad (2.6)$$

where $C_{Pd,t}^{R}$ (mol m^{-3}) is the concentration of Pd(II) in the receiving solution at time t, $C_{Rh,i}^{F}$ (mol m^{-3}) is the initial concentration of Rh(III) in the feed solution, $C_{Rh,t}^{F}$ (mol m^{-3}) is the concentration of Rh(III) in the feed solution at time t, and $C_{Rh,t}^{R}$ (mol m^{-3}) is the concentration

of Rh(III) in the receiving solution at time *t*. The *RF*, *SF*, and *PR* values were calculated after 48 h of transport, unless stated otherwise.

2.2.4 Analysis of receiving solution after transport

After membrane transport experiments were carried out, the receiving solution was collected for analysis. Ultraviolet-visible (UV-Vis) spectra were measured using a V-670 UV-Vis spectrophotometer (JASCO) with 1 nm spectral resolution. Fourier transform infrared (FTIR) spectra were measured using an FTIR spectrometer (Perkin Elmer) with 32 scans and spectral resolution of 1 cm^{-1}. Since the concentration in the receiving solution was quite low, the solution was concentrated by evaporation at 100 °C prior to the FTIR measurement. The concentrated solution was then homogeneously mixed with KBr powder. Subsequently, the mixture was heated at 100 °C for 3 h to remove water, resulting in a yellow solid KBr powder. The powder was then analyzed using the FTIR spectrometer.

2.2.5 Reusability test

In order to confirm the stability of the PIM with $P_{88812}Cl$ ionic liquid as a carrier (PIM-P8), a membrane reusability test was performed. After finishing the first transport experiment, the solutions were removed from each cell, then 50 mL water was poured into the cells, stirred for 30 min, and quickly removed through the sampling windows to wash the inside of the device without removing the membrane. Subsequently, the fresh feed and receiving solutions were poured into the corresponding cells, and the second experiment was carried out in the same manner as the first. The operation was repeated seven times. Each transport experiment in the reusability test was carried out within 24 h. As a comparison, the reusability test was also performed for a PIM with $P_{66614}Cl$ ionic liquid as the carrier (PIM-P6).

To further examine the stability of the membranes in terms of carrier leakage, both PIM-P8 and PIM-P6 were subjected to an acid treatment. Small pieces of the PIMs (100 mg) were

soaked in 20 mL of 10 M HCl in glass bottles. The bottles were then continuously shaken at 120 rpm for 7 days on a thermostated shaker (NTS-4000BH, EYELA) at 25 ± 0.5 °C. The leakage of the carriers into the HCl solution was monitored by analyzing the P concentration using ICP-OES. The mass of the PIMs before and after the acid treatment was monitored using an analytical balance (Sartorius CPA225D).

2.2.6 Membrane characterization

To evaluate the PIM stability, infrared spectra of $P_{88812}Cl$, PVDF-*co*-HFP, and PIMs before use, after 7 uses, and after being soaked in 10 M HCl for 1 week were analyzed using an FTIR spectrometer. The spectra were measured using an attenuated total reflectance (ATR) accessory with 8 scans and a spectral resolution of 2 cm^{-1}. To observe the membrane thickness and P element mapping across the membrane, scanning electron microscopy with energy dispersive X-ray (SEM-EDX) measurement were performed on an SEM instrument (Hitachi TM4000). The SEM mapping images were recorded at 1000 times magnification with an accelerating voltage of 15 kV.

2.3 Results and Discussion

2.3.1 Effect of PIM compositions

The composition of the membrane is an important factor that determines the membrane separation performance. Therefore, the effect of the PIM composition on the transport behavior of Pd(II) and Rh(III) in a chloride solution was investigated. Several PIMs with different amounts of $P_{88812}Cl$ (20–40 wt%) and 2NPOE (0–20 wt%) were prepared as listed in Table 2.1. The PIMs with $P_{88812}Cl$ more than 40 wt% and 2NPOE more than 20 wt% were physically weak and too sticky, and thus were not investigated further. Pd(II) and Rh(III) transport behavior for the different PIM compositions under the same operating conditions is shown in Figure 2.1.

Table 2.1. Effect of PIM composition on Pd(II) transport.

	PIM composition (wt%)			J_0 (mmol m^{-2} h^{-1})	*RF* (%)
	PVDF-*co*-HFP	$P_{88812}Cl$	2NPOE		
(a)	70	20	10	0.46	61.1
(b)	60	30	10	1.27	63.5
(c)	50	40	10	2.26	64.8
(d)	60	40	0	0.83	63.3
(e)	40	40	20	2.00	50.3

Feed solution: 50 ppm Pd(II) and 50 ppm Rh(III) in 1 M HCl, receiving solution: 1 mM thiourea in 1 M HCl, transport operation: 48 h.

As shown in Figure 2.1 (a, b, and c), after 48 h of operation, the amounts of Pd(II) left in the feed solutions were 16%, 5%, and 0.5% for PIMs with $P_{88812}Cl$ composition of 20 wt%, 30 wt%, and 40 wt%, respectively. The initial flux (J_0) of the PIM with 40 wt% $P_{88812}Cl$ was twice that of the PIM with 30 wt% $P_{88812}Cl$, and five times that of the PIM with 20 wt% $P_{88812}Cl$ (Table 2.1 (a,b,c)). Therefore, as the amount of $P_{88812}Cl$ increased, the amount of Pd(II) extracted into the membrane and its initial flux were enhanced. However, no significant difference was observed in the recovery factor (*RF*) of Pd(II), which was ~60%. The degree of Rh(III) left in the feed solution was 99% for the PIM with 20 wt% $P_{88812}Cl$, showing that complete separation of Pd(II) and Rh(III) occurred, although the recovery efficiency requires improvement. Nevertheless, with the PIM containing 40 wt% $P_{88812}Cl$, the degree of Rh(III) left in the feed solution decreased to 85%. This result suggests that increasing the concentration of $P_{88812}Cl$ contributes to the extraction of metal ions into the membrane.

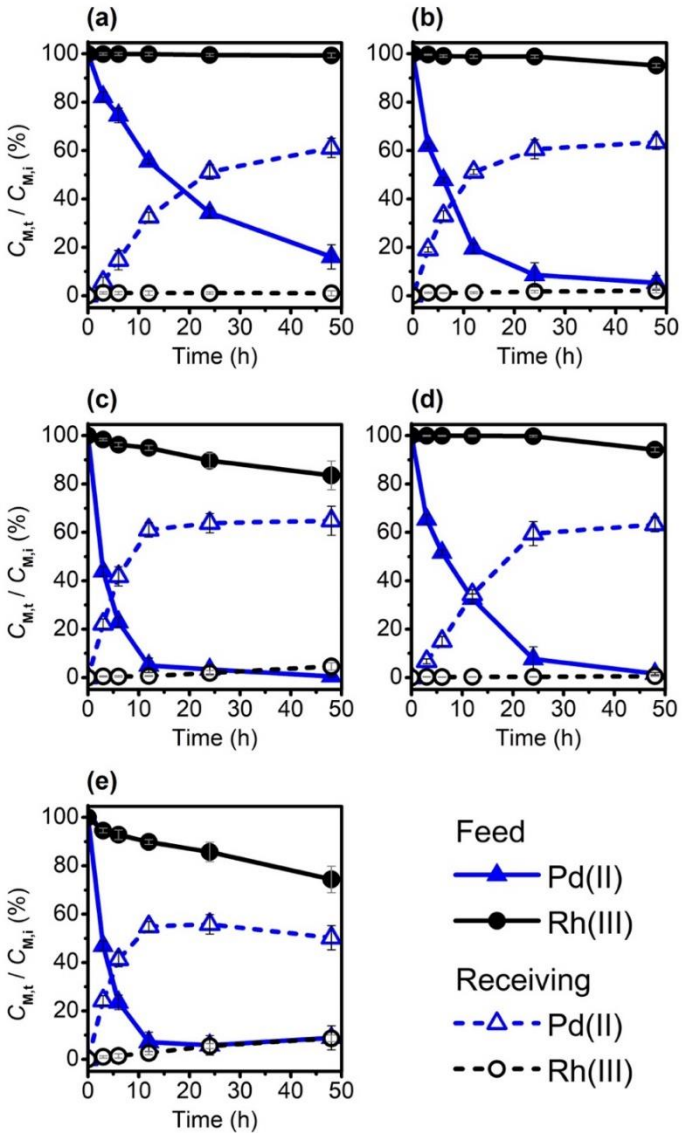

Figure 2.1. Pd(II) and Rh(III) transport behavior in different PIM compositions, (a) $P_{88812}Cl$ 20 wt%, (b) $P_{88812}Cl$ 30 wt%, (c) $P_{88812}Cl$ 40 wt%, (d) 2NPOE 0 wt% (e) 2NPOE 20 wt%. Feed solution: 50 ppm Pd(II) and 50 ppm Rh(III) in 1 M HCl, receiving solution: 1 mM thiourea in 1 M HCl. $C_{M,t}$ and $C_{M,i}$ are the metal ion concentration at time *t* and initial time, respectively.

In our previous PGM solvent extraction study using $P_{88812}Cl$ as an extractant [32], the stoichiometric equations for Pd(II) and Rh(III) extraction were considered as follows:

$$[PdCl_4]^{2-}(aq) + \overline{2[P_{88812}{}^{+}Cl^{-}]} \rightleftharpoons \overline{[P_{88812}{}^{+}]_2[PdCl_4{}^{2-}]} + 2Cl^{-}(aq) \quad (2.7)$$

$$[RhCl_5(H_2O)]^{2-}(aq) + \overline{2[P_{88812}{}^{+}Cl^{-}]} \rightleftharpoons \overline{[P_{88812}{}^{+}]_2[RhCl_5(H_2O)^{2-}]} + 2Cl^{-}(aq) \quad (2.8)$$

where the horizontal bars indicate the organic phase. Since we used the same carrier, it was assumed that equations (2.7) and (2.8) could be used to describe the extraction mechanism of

Pd(II) and Rh(III) into the PIMs although the extraction rate was slower than that in solvent extraction. As shown in Figure S2.3 and Table S2.1 (Appendix A), the rate constants of Pd(II) and Rh(III) for solvent extraction, k_{Pd} and k_{Rh}, were 8.52×10^{-4} s^{-1} and 1.49×10^{-4} s^{-1}, respectively, whereas the constants for extraction into membrane tips were 5.97×10^{-5} s^{-1} and 5.83×10^{-7} s^{-1}, respectively. This can be attributed to the slow diffusion of the extractants and complexes within the membrane. Fortunately, this feature improved the separation factor from 1.3 in solvent extraction to 38.3 in extraction into membrane tips at 5 h. Based on the results, the PIM with 40 wt% $P_{88812}Cl$ was further investigated.

The effect of 2NPOE was studied at a constant $P_{88812}Cl$ concentration since the carrier also contributes to the membrane transport as a plasticizer. The initial flux of Pd(II) using the PIM with 10 wt% 2NPOE improved significantly compared with that using the PIM without 2NPOE as shown in Table 2.1 (c, d). The plasticizer was found to be essential for efficient transport in the membrane system. For the PIM with 20 wt% 2NPOE, the Pd(II) concentration in the receiving solution decreased slowly after reaching a maximum value at 12 h, followed by an increase in the Pd(II) concentration in the feed solution (Figure 2.1 (e)). Pd(II) in the receiving solution appears to be back-transported to the feed solution after 12 h. Too much plasticizer was thought to make the membrane unstable. Moreover, the amount of Rh(III) transported into the receiving solution increased as the concentration of plasticizer increased (Figure 2.1 (d, c, e)). Increase of the plasticizer concentration might expand the network spaces in the polymer and increased the fluidity of the membrane to facilitate the movement of the bulky Rh(III) complex, which has a slow transfer rate. Based on the results, the PIM with composition PVDF-*co*-HFP 50 wt%, $P_{88812}Cl$ 40 wt%, and 2NPOE 10 wt% was used for further studies.

2.3.2 Effect of HCl concentration in the feed solution

Figure 2.2 shows the Pd(II) and Rh(III) separation as a function of HCl concentration in the feed solution in terms of the separation factor (*SF*) and the purity (*PR*). As the HCl

concentration increased from 0.5 M to 3 M, the *SF* value was significantly enhanced. Further increase in the HCl concentration to 5 M increased the *SF* values to a small extent. Similarly, the Pd(II) purity in the receiving solution improved significantly as the HCl concentration in the feed solution increased and reached 99% purity at 3 M HCl. The results show that Rh(III) transport could be effectively suppressed by increasing the HCl concentration in the feed solution. This finding was similar to that observed in the previous solvent extraction studies [32,36,37]. A spectroscopic study showed that Rh(III) predominantly exists as an $[RhCl_6]^{3-}$ species at high HCl concentration (≥3 M) [38]. A higher energy is required to break the water solvation to the trivalent Rh(III) chlorocomplex than that of the divalent one. This means that extraction of $[RhCl_6]^{3-}$ species from the aqueous solution is more difficult than that of $[RhCl_5]^{2-}$ owing to the charge density and the hydration energy [39]. Very small extraction of the trivalent Rh(III) anion can be attributed to this behavior. On the PIM, the features are amplified by the slow diffusion of the extractants and complexes within the membrane, thus allowing more effective Pd(II) and Rh(III) separation.

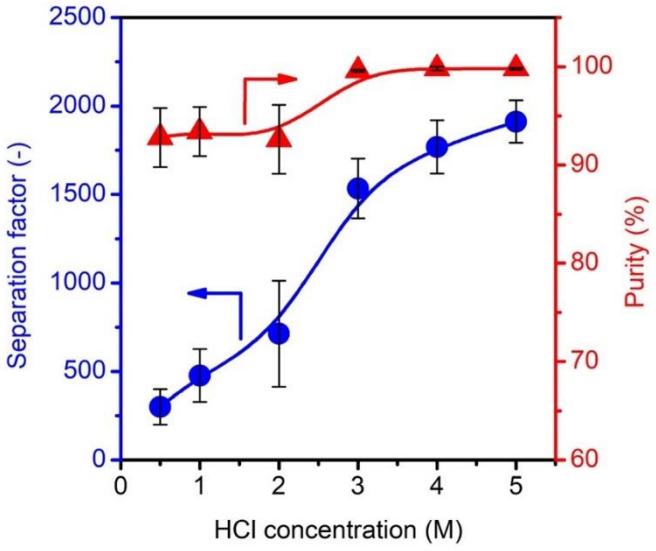

Figure 2.2. Effect of HCl concentration in the feed solution on the separation factor (*SF*) of Pd(II) from Rh(III) and the Pd(II) purity (*PR*) in the receiving solution. Membrane composition: 50 wt% PVDF-*co*-HFP, 40 wt% $P_{88812}Cl$, 10 wt% 2NPOE. Feed solution: 50 ppm Pd and 50 ppm Rh in 0.5–5 M HCl, receiving solution: 1 mM thiourea in 1 M HCl.

Table 2.2. Effect of HCl concentration on Pd(II) initial flux (J_0) and recovery factor (*RF*).

HCl conc. (M)	J_0 (mmol m^{-2} h^{-1})	*RF* (%)
0.5	2.52	65.4
1	2.26	64.8
2	1.93	65.3
3	1.93	64.2
4	1.33	63.8
5	0.99	65.3

Membrane composition: 50 wt% PVDF-*co*-HFP, 40 wt% $P_{88812}Cl$, 10 wt% 2NPOE. Feed solution: 50 ppm Pd(II) and 50 ppm Rh(III) in 0.5–5 M HCl, receiving solution: 1 mM thiourea in 1 M HCl, transport operation: 48 h.

The Pd(II) initial flux was slightly reduced as the HCl concentration increased, although the *RF* values were relatively constant at ~60% (Table 2.2). In solvent extraction, an increase in the HCl concentration did not affect the Pd(II) extraction behavior [32]. A spectroscopic study showed that Pd(II) predominantly exists as $[PdCl_4]^{2-}$ species in HCl concentrations of ≥1 M [40], therefore equation (2.7) could also describe the Pd(II) extraction behavior in a high HCl concentration. The decrease in the Pd(II) initial flux might correspond to the concentration of the carriers. In solvent extraction, the $P_{88812}Cl$ was presented in excess, therefore the addition of HCl did not change the reaction equilibrium. The amount of $P_{88812}Cl$ in the PIMs was relatively low, therefore, according to equation (2.7), adding a significant amount of HCl could shift the equilibrium to the left hand side. Based on the results, 3 M HCl in the feed solution was chosen for further investigation.

2.3.3 The effect of thiourea concentration

Thiourea was found to be an effective stripping agent for extracted Pd(II) in a liquid surfactant membrane, as demonstrated by Kakoi et al. [41], therefore we applied thiourea in the present study. Figure 2.3 shows the effect of thiourea concentration in the receiving solution on Pd(II) and Rh(III) transport behavior. At thiourea concentrations of 0.5 mM, 1 mM, and 2

mM, Pd(II) transported into the receiving solution after 48 h was 28.6%, 64.3%, and 98.2%, respectively. It was clearly demonstrated that the Pd(II) transport is governed by the thiourea concentration in the receiving solution. The effect of the thiourea concentration on the permeability of Pd(II) was also observed visually (Figure S2.4, Appendix A). The orange-yellow appearance of the used membranes, which is the color of extracted Pd(II), gradually diminished as the thiourea concentration increased and was no longer observed at 2 mM. Insufficient thiourea in the receiving solution leads to a low Pd(II) transport, therefore the thiourea concentration should be adjusted to an appropriate ratio to the Pd(II) concentration, which was found to be 2 mM to 50 ppm of Pd(II). Under the optimum conditions, the feed solution that was yellowish-red before running turned pale red due to the remaining Rh(III) over time, while the colorless receiving solution gradually became deep yellow after the transport operation, which visually indicated successful separation (Figure S2.5, Appendix A).

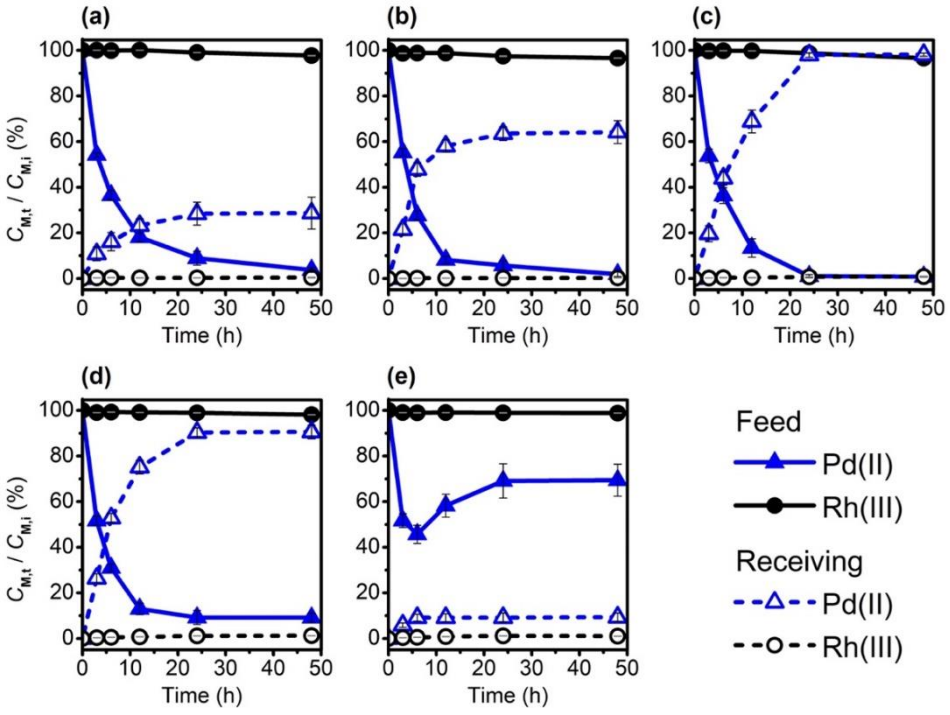

Figure 2.3. Effect of thiourea (Tu) concentration in the receiving solution on Pd(II) and Rh(III) transport behavior, (a) 0.5 mM, (b) 1 mM, (c) 2 mM, (d) 10 mM, and (e) 100 mM in 1 M HCl. Membrane composition: 50 wt% PVDF-*co*-HFP, 40 wt% $P_{88812}Cl$, 10 wt% 2NPOE. Feed solution: 50 ppm Pd(II) and 50 ppm Rh(III) in 3 M HCl. $C_{M,t}$ and $C_{M,i}$ are the metal ion concentration at time *t* and initial time, respectively.

However, further increase in the thiourea concentration reduced the Pd(II) transport efficiency to 90.6% at 10 mM thiourea and 9.4% at 100 mM thiourea. The Pd(II) transport behavior at 100 mM thiourea was quite unexpected, the Pd(II) concentration in the feed solution decreased rapidly to 45.7% in the first 6 h, then gradually increased. In the receiving solution, the Pd(II) concentration rose to around 9%. It was thought that the permeation of thiourea from the receiving to the feed solution resulted in the reverse transport of Pd(II) through the membrane. The concentration of thiourea in the feed solution after 24 h was then evaluated using ICP-OES by measuring the sulfur (S) concentration. As shown in Figure 2.4, thiourea was leaked into the feed solution to give a concentration of 7.3 mM when 100 mM thiourea was used as the receiving solution, while thiourea was hardly detected in all the cases where its initial concentration in the receiving solution was less than 10 mM. When thiourea was present in the feed solution, its strong interaction with Pd(II) interfered with the Pd(II) transport to the membrane. The role of HCl added to the receiving solution is to prevent the permeation of thiourea into the feed solution by its protonation as described in the previous reports [42,43], however it was found that the permeation of thiourea could not be prevented under the high concentration gradient between the solutions.

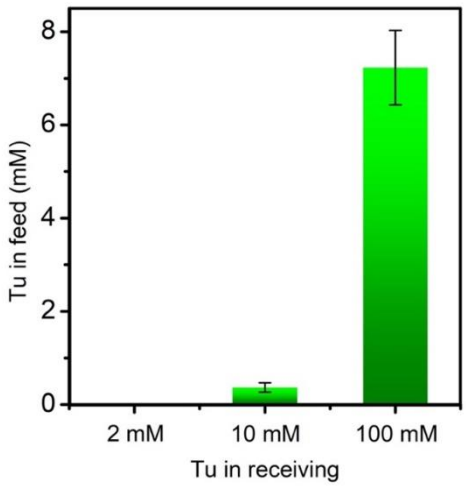

Figure 2.4. Concentration of thiourea (Tu) transferred into the feed solution after 24 h of operation.

2.3.4 Pd(II)–thiourea complex in the receiving solution

At a Pd(II) concentration of 50 ppm (0.5 mM), the *RF* values were around 25% for 0.5 mM thiourea (molar ratio = 1 : 1), around 60% for 1 mM thiourea (molar ratio = 1 : 2), and around 100% for 2 mM thiourea (molar ratio = 1 : 4) in the receiving solution (Figure 2.3 (a, b, and c)). These results indicate that one Pd(II) ion reacts with 4 molecules of thiourea, i.e. the formation of $[Pd(Tu)_4]^{2+}$ species, for the stripping of Pd(II) from the membrane. A previous crystallographic study on Pd(II)–thiourea complexes also showed that the formation of the cationic complex $[Pd(Tu)_4]^{2+}$ was more favorable than formation of the neutral complex $[Pd(Tu)_2Cl_2]$ [44]. To obtain more insight into the Pd(II) and thiourea interaction, the receiving solution after the transport operation was characterized using UV-Vis and FTIR spectroscopies.

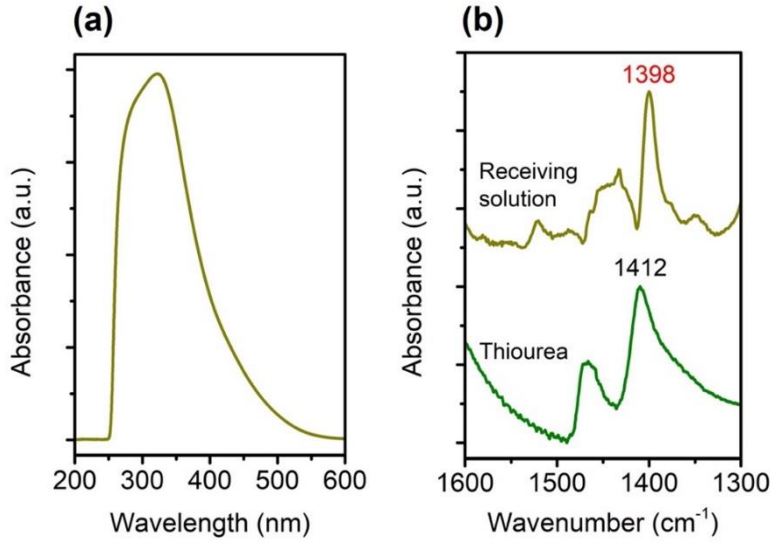

Figure 2.5. (a) UV-Vis and (b) FTIR spectra of the receiving solution. Membrane composition: 50 wt% PVDF-*co*-HFP, 40 wt% $P_{88812}Cl$, 10 wt% 2NPOE. Feed solution: 50 ppm Pd(II) and 50 ppm Rh(III) in 3 M HCl, receiving solution: 2 mM thiourea in 1 M HCl.

As shown in Figure 2.5 (a), a broad energy absorption at 250–500 nm was clearly observed. This absorption profile is a typical UV-Vis spectrum for the Pd(II)-thiourea complex as demonstrated in a previous report [45]. The maximum absorption (λ_{max}) that appeared at 325 nm can be attributed to the metal to ligand charge transfer (MLCT) since the Pd(II) is an electron-rich metal (d^8) and the thiourea ligand provided an empty π^* orbital. In the FTIR

spectrum (Figure 2.5 (b)) for the initial receiving solution, the asymmetric stretching vibration for the S=C< bond of free thiourea appeared at 1412 cm^{-1}. For the receiving solution after operation, a red-shift of this peak to 1398 cm^{-1} was observed, showing a reduction of S=C< bond strength. This shift can be attributed to the formation of coordination bonds between the S atom on thiourea and Pd(II), which reduced the electron density of the S=C< bond.

2.3.5 The effect of metal concentration in the feed solution

The effect of metal concentration in the feed solution on the transport behavior was investigated. As the optimum molar ratio of Pd(II) to thiourea was known, the investigation was carried out by increasing and reducing the Pd(II) and Rh(III) concentrations while maintaining the molar ratio of Pd(II) to thiourea at 1 : 4 (Table 2.3). As can be seen, when the metal concentration was reduced to 25 ppm or increased to 100 ppm, the Pd(II) recovery (*RF*) was maintained at ~98% with 99% purity (*PR*) in the receiving solution. This result suggests that PIM transport is applicable for various feed metal concentrations. The initial flux increased as the Pd(II) concentration increased, giving 0.849, 1.551, and 1.804 mmol m^{-2} h^{-1} for Pd(II) concentrations of 25, 50, and 100 ppm, respectively. Higher metal concentration in the feed solution, which provides a higher concentration gradient, leads to faster metal ion permeation.

Table 2.3. Effect of metal ion concentration in the feed solution on the transport behavior.

Pd(II) (ppm)	Rh(III) (ppm)	Tu (mM)	J_0 (mmol m^{-2} h^{-1})	*RF* (%)	*PR* (%)
25	25	1	0.85	98.3	99.5
50	50	2	1.55	98.2	99.2
100	100	4	1.80	97.5	99.3

Membrane composition: 50 wt% PVDF-*co*-HFP, 40 wt% $P_{88812}Cl$, 10 wt% 2NPOE. Feed solution: 25–100 ppm Pd(II) and 25–100 ppm Rh(III) in 3 M HCl, receiving solution: 1–4 mM thiourea (Tu) in 1 M HCl, transport operation: 48 h.

According to the results described above, the selective recovery of Pd(II) through the PIM is thought to have occurred as follows: $[PdCl_4]^{2-}$ species were effectively extracted as $[P_{88812}^{+}]_2[PdCl_4]^{2-}$ with $P_{88812}Cl$ via the ion exchange mechanism represented by equation (2.7) at the membrane surface on the feed side and reacted with thiourea at the opposite surface of the membrane as described in equation (2.9). As a result, Pd(II) can be recovered to the receiving solution as $[Pd(Tu)_4]^{2+}$, and the ionic liquids are regenerated.

$$\overline{\left[P_{88812}{}^{+}\right]_2\left[PdCl_4{}^{2-}\right]} + 4SC(NH_2)_2(aq) \rightleftharpoons \overline{2[P_{88812}{}^{+}Cl^{-}]} + [Pd(SC(NH_2)_2)_4]^{2+}(aq) + 2Cl^{-}(aq) \quad (2.9)$$

2.3.6 Reusability of the membrane

Another important factor in the membrane transport system is the reusability of the membrane. In the reusability test, the performance of $P_{88812}Cl$ as a carrier in a PIM was compared with that of a commercially available ionic liquid, $P_{66614}Cl$. As shown in Figure 2.6, the performance of the PIM with $P_{88812}Cl$ as the carrier (PIM-P8) was quite stable throughout 7 operation cycles. The Pd(II) recovery remained ~96% at the 7th cycle. In contrast, the performance of PIM with $P_{66614}Cl$ as the carrier (PIM-P6) gradually decreased. The Pd(II) recovery had reduced by ~30% at the 7th cycle. On each cycle of the reusability test, the leakage of the carrier from the PIM into the feed and receiving solutions was monitored. Carrier leakage from PIM-P8 to the feed and receiving solutions was not detected, while ~0.2–0.4 ppm of P from PIM-P6 was detected in both solutions at each cycle (Table S2.2, Appendix A). These results suggest that the membrane stability relates to the performance of the PIMs. PIM-P8 showed a more stable performance as the carrier did not leak, while PIM-P6 was less stable owing to the carrier leakage.

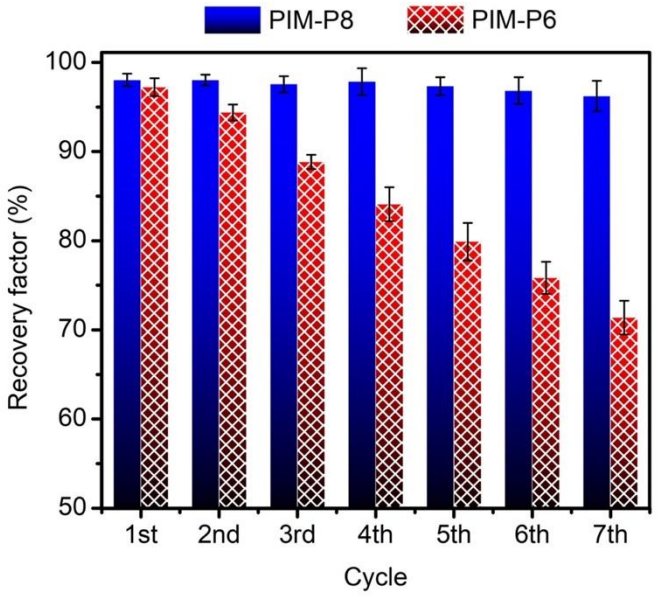

Figure 2.6. Recovery factor (*RF*) of Pd(II) transport throughout 7 operation cycles using PIM-P8 and PIM-P6; each cycle was performed within 24 h. Membrane composition: 50 wt% PVDF-*co*-HFP, 40 wt% $P_{88812}Cl$ (PIM-P8) or 40 wt% $P_{66614}Cl$ (PIM-P6), 10 wt% 2NPOE. Feed solution: 50 ppm Pd(II) and 50 ppm Rh(III) in 3 M HCl, receiving solution: 2 mM thiourea in 1 M HCl.

To obtain deeper insight into the carrier leakage behavior, the PIMs were subjected to a harsh acid environment i.e. soaked in 10 M HCl for 7 days with shaking. After the treatment, the mass of the PIM-P8 had decreased slightly (± 5%) while that of the PIM-P6 had significantly decreased (± 20%) (Figure S2.6, Appendix A). The P concentrations in the acid solutions for PIM-P8 and PIM-P6 after the treatment were 0.013 and 5.714 ppm, respectively (Table S2.3, Appendix A). These results demonstrate that leakage of the carrier (PIM-P8) was indeed inhibited compared with that of PIM-P6. The results are also in good agreement with our previous stability study, which compared $P_{88812}Cl$ and $P_{66614}Cl$ ionic liquids as extractants in the solvent extraction of PGMs [36]. It was shown that the water content in the ionic liquid and the concentration of P—i.e. the concentration of the ionic liquid—released into the water, at the equilibrium state of each ionic liquid, were as follows: 4.30 wt% and 0.301 mg L^{-1} for $P_{88812}Cl$, and 6.26 wt% and 6.887 mg L^{-1} for $P_{66614}Cl$. The hydrophobicity of $P_{88812}Cl$, which

is higher than that of $P_{66614}Cl$ as indicated by the above water content and P release, are thought to contribute to the higher stability of the membranes.

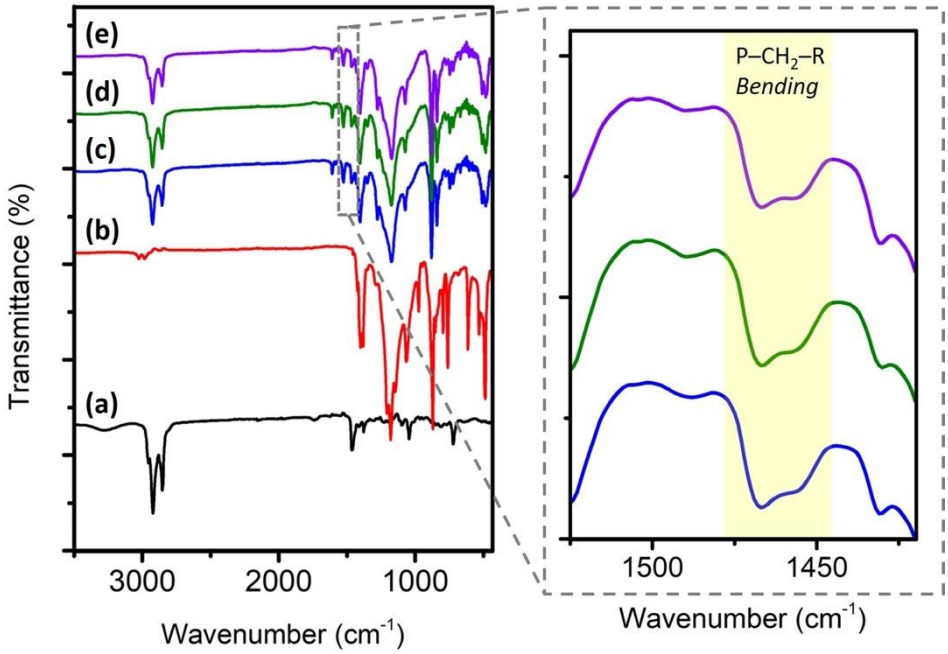

Figure 2.7. FTIR spectra of (a) $P_{88812}Cl$, (b) PVDF-*co*-HFP, (c) PIM unused, (d) PIM after 7 uses, (e) PIM after being soaked in 10 M HCl for 7 days.

2.3.7 Membrane characterization

The membrane stability was further confirmed by examining its structural change using FTIR spectroscopy. The spectra of the PIMs before use, after 7 uses, and after being soaked in 10 M HCl for 7 days are shown in Figure 2.7, along with that of $P_{88812}Cl$ and PVDF-*co*-HFP. In the $P_{88812}Cl$ spectra, vibrations of P–C stretching, C–C stretching, P–CH_2–R bending, and C–H stretching were exhibited at 722 cm^{-1}, 1045 cm^{-1}, 1468 cm^{-1}, and around 2900 cm^{-1}, respectively. PVDF-*co*-HFP exhibited a strong fingerprint in the 500–1500 cm^{-1} region and therefore predominates the infrared spectra of the PIM. Nevertheless, it was clearly observed that the spectra of the PIM after 7 uses and the PIM soaked in 10 M HCl for 7 days were similar to that of the PIM before use, showing that no significant structural changes occurred. Indeed, the block copolymer PVDF-*co*-HFP exhibits good physical and chemical endurance even under

various harsh conditions [46–48], therefore it can maintain the stability of the PIMs. In addition, the strong C–H stretching band of the $P_{88812}Cl$ was clearly observed around 2900 cm^{-1} with preserved intensity, showing that the carrier was maintained inside the PIM after membrane operations or contact with HCl. Moreover, by enlarging the spectra around 1500 cm^{-1}, it can be seen that the P–CH_2–R bending band from $P_{88812}Cl$ was also preserved for PIMs after 7 uses as well as after being soaked in 10 HCl for 7 days, showing that the carrier had not deteriorated. The results demonstrated that the chemical structure of both the polymer base and carrier in the PIMs was stable over the multiple transport cycles and even in a harsh acid environment.

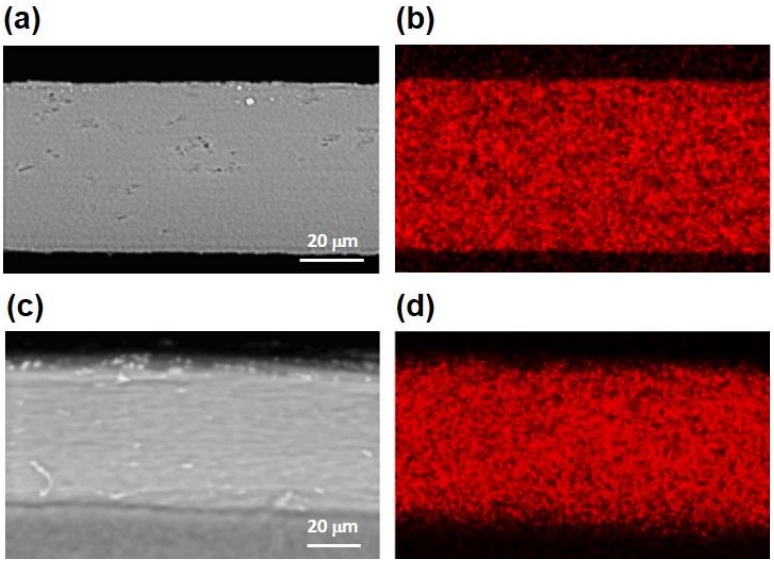

Figure 2.8. SEM and P element EDX mapping images of the PIMs (a and b) before use and (c and d) after 7 uses. Membrane composition: 50 wt% PVDF-*co*-HFP, 40 wt% $P_{88812}Cl$, 10 wt% 2NPOE with total mass of 400 mg.

The PIMs were also characterized using SEM and EDX elemental mapping. An SEM image of the cross-section of the membrane is shown in Figure S2.7 (Appendix A). It can be seen that the PIM has a thickness of 56.7 μm and a dense structure. The SEM-EDX elemental mapping images along cross-section regions of the PIMs are shown in Figure 2.8. The P was finely distributed across the membrane for the PIM before use (Figure 2.8 (b)), showing a homogenous dispersion between the $P_{88812}Cl$ ionic liquid and the polymer base. After 7 uses (Figure 2.8 (d)), the P species remained finely distributed inside the PIM, showing the stability

of the PIM over multiple uses. This result is also in good agreement with those demonstrated in the reusability test, the monitoring of carrier leakage, and the infrared spectroscopy.

2.4 Conclusions

The separation of Pd(II) from Rh(III) using a PIM transport system with the ionic liquid $P_{88812}Cl$ as the metal carrier was demonstrated. The optimum PIM composition investigated in this study was 50 wt% PVDF-*co*-HFP (base-polymer), 40 wt% $P_{88812}Cl$ (carrier), and 10 wt% 2NPOE (plasticizer). Selective transport of Pd(III) could be achieved by adjusting the HCl concentration in the feed solution to ≥3 M to suppress the transport of Rh(III) species. To obtain quantitative recovery of Pd(II), a 1 : 4 molar ratio of Pd(II) to thiourea in the receiving solution should be maintained. Insufficient thiourea leads to a low Pd(II) recovery yield, while an excess leads to permeation of thiourea from the receiving solution to the feed solution. The stoichiometry of the Pd(II) transport and spectroscopic data suggested that $[Pd(Tu)_4]^{2+}$ species were formed in the receiving solution. PIMs with $P_{88812}Cl$ ionic liquid as a carrier showed a stable performance over 7 reusability test cycles, with the recovery of Pd(II) still reaching 96% for the 7^{th} cycle. In contrast, PIMs with commercial $P_{66614}Cl$ as a carrier showed a less stable performance with ~30% depletion of the Pd(II) recovery at the 7^{th} cycle. Membrane characterization using infrared spectroscopy, and SEM-EDX mapping demonstrated that the chemical structure and composition of PIMs with $P_{88812}Cl$ were well preserved over multiple uses. This study demonstrated that the application of our designed ionic liquid $P_{88812}Cl$ as a carrier in PIMs results in remarkably good performances for the separation of Pd(II) and Rh(III) with high stability. This study suggests that PIMs can be applied to more complex separation systems for platinum group metals.

References

[1] J. Liu, M. Jiao, L. Lu, H.M. Barkholtz, Y. Li, L. Jiang, Z. Wu, D.J. Liu, L. Zhuang, C. Ma, J. Zeng, B. Zhang, D. Su, P. Song, W. Xing, W. Xu, Y. Wang, Z. Jiang, G. Sun, High performance platinum single atom electrocatalyst for oxygen reduction reaction, *Nat. Commun.* 8 (2017) 1–9.

[2] M. Page, D.R. Dekel, H.A. Miller, F. D'Acapito, Y. Paska, A. Lavacchi, F. Di Benedetto, F. Vizza, M. Marelli, A Pd/C-CeO_2 Anode Catalyst for High-Performance Platinum-Free Anion Exchange Membrane Fuel Cells, *Angew. Chemie Int. Ed.* 55 (2016) 6004–6007.

[3] Y. Zhang, J. Bi, Q. Wang, Y. Wang, D. Gao, C. Xu, M. Hu, G. Fan, Hyper-cross-linked polymer supported rhodium: an effective catalyst for hydrogen evolution from ammonia borane, *Dalt. Trans.* 47 (2018) 2561–2567.

[4] D. Victor, J. Leape, Materials science: Share corrosion data, *Nature*. 527 (2015) 441–442.

[5] E.K. Goharshadi, H. Azizi-Toupkanloo, M. Karimi, Electrical conductivity of water-based palladium nanofluids, *Microfluid. Nanofluidics*. 18 (2015) 667–672.

[6] V. Fernandez, Some facts on the platinum-group elements, *Int. Rev. Financ. Anal.* 52 (2017) 333–347.

[7] World Platinum Investment Council, *Platinum quarterly Q3*, 2018.

[8] A. Cowley, Johnson Matthey PGM Market Report May 2018, 2018.

[9] H. Dong, J. Zhao, J. Chen, Y. Wu, B. Li, Recovery of platinum group metals from spent catalysts: A review, *Int. J. Miner. Process.* 145 (2015) 108–113.

[10] F.K. Crundwell, M.S. Moats, G. Robinson, G. William, Metallurgy of Nickel , Cobalt and Platinum-Group Metals, *Elsevier*, Oxford, 2011.

[11] P. Nuss, M.J. Eckelman, Life cycle assessment of metals: A scientific synthesis, *PLoS One*. 9 (2014) 1–12.

[12] C. Hagelüken, Recycling the Platinum Group Metals : A European Perspective, *Platin. Met. Rev.* 56 (2012) 29–35.

[13] A. Tuncuk, V. Stazi, A. Akcil, E.Y. Yazici, H. Deveci, Aqueous metal recovery techniques from e-scrap: Hydrometallurgy in recycling, *Miner. Eng.* 25 (2012) 28–37.

[14] E.A. Mowafy, D. Mohamed, A. Alshammari, Extraction and Separation of Selected Platinum-Group and Base Metal Ions from Nitric Acid Solutions Using Thiodiglycolamides (TDGA) as Novel Extractants, *Sep. Sci. Technol.* 50 (2015) 2352–2359.

[15] M. Yamada, M. Rajiv Gandhi, A. Shibayama, Rapid and selective recovery of palladium from platinum group metals and base metals using a thioamide-modified calix[4]arene extractant in environmentally friendly hydrocarbon fluids, *Sci. Rep.* 8 (2018) 16909.

[16] B. Marin, L. Dupont, S. Boudesocque, A. Mohamadou, A. Conreux, The recovery and selective extraction of gold and platinum by novel ionic liquids, *Sep. Purif. Technol.* 210 (2018) 824–834.

[17] V.W. Sidel, J.F. Hoffman, Apparent "solvent drag" across a liquid membrane, in: *Biophys. Soc.*

Abstr. Chicago Meet., 1963.

[18] R.E. Kesting, W.J. Subcasky, J.D. Paton, Liquid membranes at the cellulose acetate membrane/saline solution interface in reverse osmosis, *J. Colloid Interface Sci*. 28 (1968) 156–160.

[19] K. Srinivasan, G.A. Rechnitz, Selectivity studies on liquid membrane, ion-selective electrodes, *Anal. Chem*. 41 (1969) 1203–1208.

[20] A.J. Schow, R.T. Peterson, J.D. Lamb, Polymer inclusion membranes containing macrocyclic carriers for use in cation separations, *J. Memb. Sci*. 111 (1996) 291–295.

[21] L.D. Nghiem, P. Mornane, I.D. Potter, J.M. Perera, R.W. Cattrall, S.D. Kolev, Extraction and transport of metal ions and small organic compounds using polymer inclusion membranes (PIMs), *J. Memb. Sci*. 281 (2006) 7–41.

[22] N. Pereira, A. St John, R.W. Cattrall, J.M. Perera, S.D. Kolev, Influence of the composition of polymer inclusion membranes on their homogeneity and flexibility, *Desalination*. 236 (2009) 327–333.

[23] Y. Sakai, K. Kadota, T. Hayashita, R.W. Cattrall, S.D. Kolev, The effect of the counter anion on the transport of thiourea in a PVC-based polymer inclusion membrane using Capriquat as carrier, *J. Memb. Sci*. 346 (2010) 250–255.

[24] A.M. St John, R.W. Cattrall, S.D. Kolev, Transport and separation of uranium(VI) by a polymer inclusion membrane based on di-(2-ethylhexyl) phosphoric acid, *J. Memb. Sci*. 409–410 (2012) 242–250.

[25] B.M. Jayawardane, L. dlC. Coo, R.W. Cattrall, S.D. Kolev, The use of a polymer inclusion membrane in a paper-based sensor for the selective determination of Cu(II), *Anal. Chim. Acta*. 803 (2013) 106–112.

[26] Y. O'Bryan, R.W. Cattrall, Y.B. Truong, I.L. Kyratzis, S.D. Kolev, The use of poly(vinylidenefluoride-*co*-hexafluoropropylene) for the preparation of polymer inclusion membranes. Application to the extraction of thiocyanate, *J. Memb. Sci*. 510 (2016) 481–488.

[27] D. Wang, R.W. Cattrall, J. Li, M.I.G.S. Almeida, G.W. Stevens, S.D. Kolev, A comparison of the use of commercial and diluent free LIX84I in poly(vinylidene fluoride-*co*-hexafluoropropylene) (PVDF-HFP)-based polymer inclusion membranes for the extraction and transport of Cu(II), *Sep. Purif. Technol*. 202 (2018) 59–66.

[28] M.I.G.S. Almeida, R.W. Cattrall, S.D. Kolev, Polymer inclusion membranes (PIMs) in chemical analysis - A review, *Anal. Chim. Acta*. 987 (2017) 1–14.

[29] M. Regel-Rosocka, M. Rzelewska, M. Baczynska, M. Janus, M. Wisniewski, Removal of palladium(II) from aqueous chloride solutions with cyphos phosphonium ionic liquids as metal ion carriers for liquid-liquid extraction and transport across polymer inclusion membranes, *Physicochem. Probl. Miner. Process*. 51 (2015) 621–631.

[30] B. Pospiech, Highly efficient facilitated membrane transport of palladium(II) ions from

hydrochloric acid solutions through plasticizer membranes with cyanex 471X, *Physicochem. Probl. Miner. Process*. 51 (2015) 281–291.

[31] B. Pospiech, Facilitated transport of palladium(II) across polymer inclusion membrane with ammonium ionic liquid as effective carrier, *Chem. Pap*. 72 (2018) 301–308.

[32] M.L. Firmansyah, F. Kubota, W. Yoshida, M. Goto, Application of a Novel Phosphonium-Based Ionic Liquid to the Separation of Platinum Group Metals from Automobile Catalyst Leach Liquor, *Ind. Eng. Chem. Res*. 58 (2019) 3845–3852.

[33] F. Kubota, R. Kono, W. Yoshida, M. Sharaf, S.D. Kolev, M. Goto, Recovery of gold ions from discarded mobile phone leachate by solvent extraction and polymer inclusion membrane (PIM) based separation using an amic acid extractant, *Sep. Purif. Technol*. 214 (2019) 156–161.

[34] M. Sharaf, W. Yoshida, F. Kubota, S.D. Kolev, M. Goto, A polymer inclusion membrane composed of the binary carrier PC-88A and Versatic 10 for the selective separation and recovery of Sc, *RSC Adv*. 8 (2018) 8631–8637.

[35] W. Yoshida, Y. Baba, F. Kubota, S.D. Kolev, M. Goto, Selective transport of scandium(III) across polymer inclusion membranes with improved stability which contain an amic acid carrier, *J. Memb. Sci*. 572 (2019) 291–299.

[36] M.L. Firmansyah, F. Kubota, M. Goto, Solvent extraction of Pt (IV), Pd (II), and Rh (III) with the ionic liquid trioctyl (dodecyl) phosphonium chloride, *J. Chem. Technol. Biotechnol*. 93 (2018) 1714–1721.

[37] L. Svecova, N. Papaiconomou, I. Billard, Quantitative extraction of Rh(III) using ionic liquids and its simple separation from Pd(II), *Dalt. Trans*. 45 (2016) 15162–15169.

[38] W.C. Wolsey, C.A. Reynolds, J. Kleinberg, Complexes in the rhodium (III)-chloride system in acid solution, *Inorg. Chem*. 2 (1963) 463–468.

[39] A. Majavu, Z.R. Tshentu, Separation of rhodium(III) and iridium(IV) chlorido species by quaternary diammonium centres hosted on silica microparticles, South African *J. Chem. Eng*. 24 (2017) 82–94.

[40] C.J. le Roux, R.J. Kriek, A detailed spectrophotometric investigation of the complexation of palladium(II) with chloride and bromide, *Hydrometallurgy*. 169 (2017) 447–455.

[41] T. Kakoi, M. Goto, K. Kondo, F. Nakashio, Extraction of palladium by liquid surfactant membranes using new surfactants, *J. Memb. Sci*. 84 (1993) 249–258.

[42] T. Kakoi, N. Horinouchi, M. Goto, F. Nakashio, Recovery of Palladium from an Industrial Wastewater Using Liquid Surfactant Membranes, *Sep. Sci. Technol*. 31 (1996) 381–399.

[43] T. Kakoi, N. Horinouchi, M. Goto, F. Nakashio, Selective recovery of palladium from a simulated industrial waste water by liquid surfactant membrane process, *J. Memb. Sci*. 118 (1996) 63–71.

[44] S. Nadeem, M.K. Rauf, S. Ahmad, M. Ebihara, S.A. Tirmizi, S.A. Bashir, A. Badshah, Synthesis and characterization of palladium(II) complexes of thioureas. X-ray structures of [Pd(N,N'-dimethylthiourea)$_4$]Cl$_2$• 2H$_2$O and [Pd(tetramethylthiourea)$_4$]Cl$_2$, *Transit. Met. Chem*. 34 (2009)

197–202.

[45] A. Dakshinamoorthy, P.S. Dhami, P.W. Naik, N.L. Dudwadkar, S.K. Munshi, P.K. Dey, V. Venugopal, Separation of palladium from high level liquid waste of PUREX origin by solvent extraction and precipitation methods using oximes, *Desalination*. 232 (2008) 26–36.

[46] G. Kang, Y. Cao, Application and modification of poly(vinylidene fluoride) (PVDF) membranes – A review, *J. Memb. Sci*. 463 (2014) 145–165.

[47] M. Kamberi, D. Pinson, S. Pacetti, L.E.L. Perkins, S. Hossainy, H. Mori, R.J. Rapoza, F. Kolodgie, R. Virmani, Evaluation of chemical stability of polymers of XIENCE everolimus-eluting coronary stents in vivo by pyrolysis-gas chromatography/mass spectrometry, *J. Biomed. Mater. Res. Part B Appl. Biomater*. 106 (2018) 1721–1729.

[48] C. Ribeiro, C.M. Costa, D.M. Correia, J. Nunes-Pereira, J. Oliveira, P. Martins, R. Gonçalves, V.F. Cardoso, S. Lanceros-Méndez, Electroactive poly(vinylidene fluoride)-based structures for advanced applications, *Nat. Protoc*. 13 (2018) 681.

Appendix A. Supporting Information

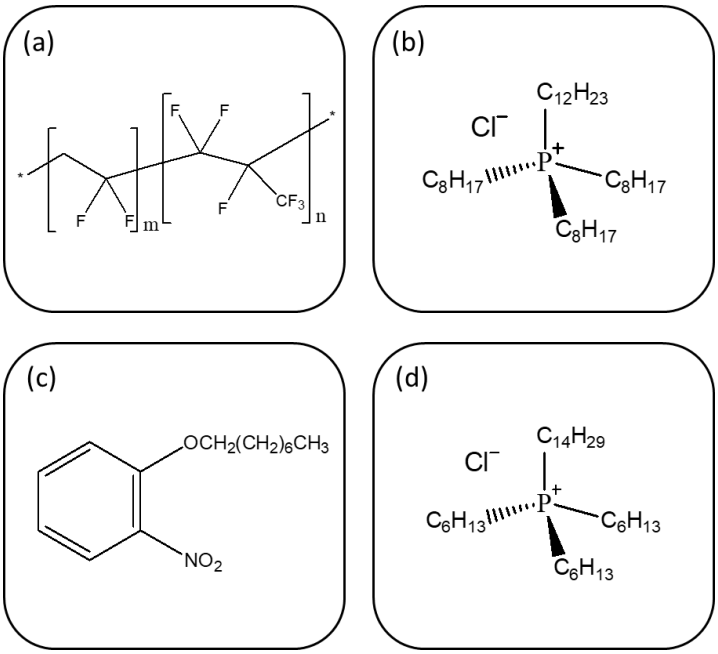

Figure S2.1. Chemical structure of (a) PVDF-*co*-HFP, (b) $P_{88812}Cl$, (c) 2NPOE, and (d) $P_{66614}Cl$.

Figure S2.2. PIM with the composition of 50 wt% PVDF-*co*-HFP, 40 wt% $P_{88812}Cl$, 10 wt% 2NPOE with total mass of 400 mg.

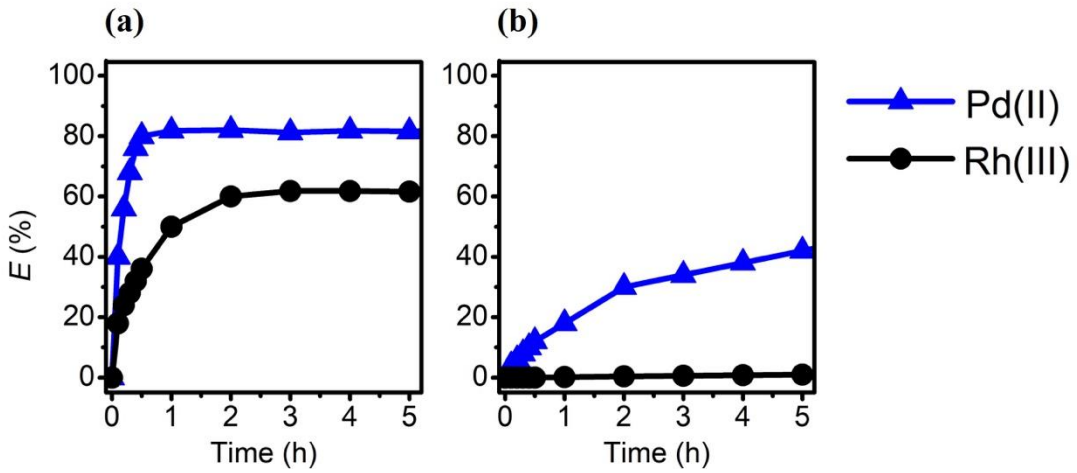

Figure S2.3. The extraction behavior of Pd(II) and Rh(III) in (a) solvent extraction using undiluted $P_{88812}Cl$ and (b) extraction into membrane tips. Membrane composition: 50 wt% PVDF-*co*-HFP, 40 wt% $P_{88812}Cl$, 10 wt% 2NPOE.

Table S2.1. The rate constant (*k*) and separation factor (*SF*) of Pd(II) and Rh(III) extraction in solvent extraction and extraction into membrane tips.

Extraction	***k*** **(s^{-1})**		***SF*** **(–)**
	Pd(II)	**Rh(III)**	
Solvent	8.52×10^{-4}	1.49×10^{-4}	1.3
Membrane	5.97×10^{-5}	5.83×10^{-7}	38.3

Aqueous solution: 50 ppm Pd(II) and 50 ppm Rh(III) in 1 M HCl. Solvent extraction was conducted in volume ratio of aqueous/organic phase = 4 with total volume of 5 mL. Extraction into membrane tips was conducted using 50 mL of the aqueous solution and 100 mg of the membrane. Both of solvent and membrane extraction were performed in a mechanical shaker (120 rpm) for 5 h at 25 °C.

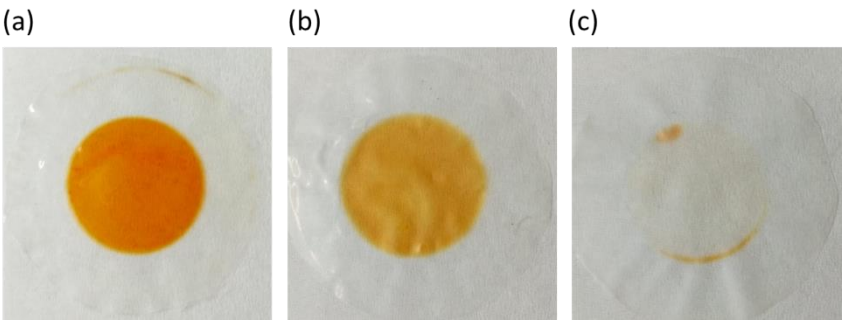

Figure S2.4. Membrane colors after use in transport operations with different concentrations of thiourea (Tu) in the receiving solution, (a) 0.5 mM, (b) 1 mM, and (c) 2 mM in 1 M HCl. Membrane composition: 50 wt% PVDF-*co*-HFP, 40 wt% $P_{88812}Cl$, 10 wt% 2NPOE. Feed solution: 50 ppm Pd(II) and 50 ppm Rh(III) in 3 M HCl.

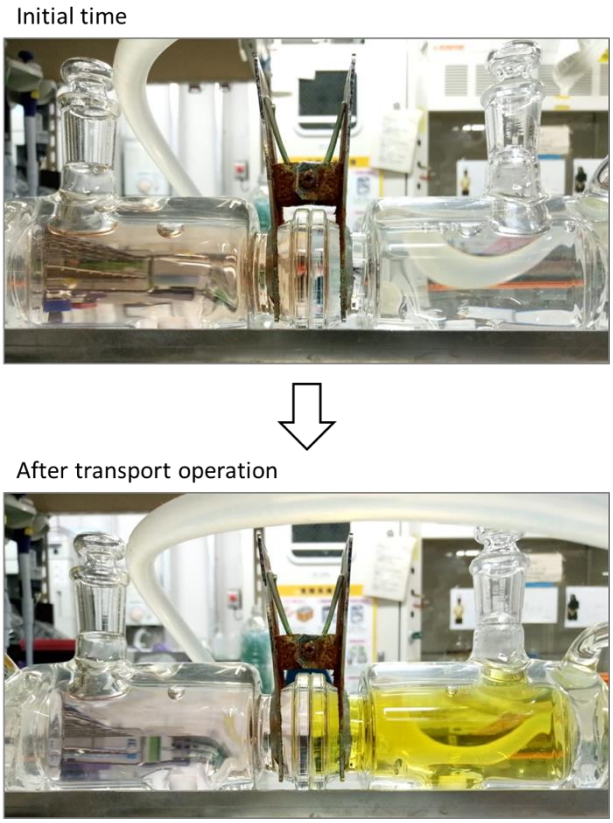

Figure S2.5. Visual observation of the membrane transport operation at initial time (top) and after operation (bottom). The left hand side is the feed solution and the right hand side is the receiving solution. Feed solution: 50 ppm Pd(II) and 50 ppm Rh(III) in 3 M HCl, receiving solution: 2 mM thiourea in 1 M HCl. Membrane composition: 50 wt% PVDF-*co*-HFP, 40 wt% $P_{88812}Cl$, 10 wt% 2NPOE.

Table S2.2. P concentration in feed and receiving solutions during 7 cycles of transport operation using PIM-P6. Membrane composition: 50 wt% PVDF-*co*-HFP, 40 wt% $P_{66614}Cl$, 10 wt% 2NPOE. Feed solution: 50 ppm Pd(II) and 50 ppm Rh(III) in 3 M HCl, receiving solution: 2 mM thiourea in 1 M HCl

Cycle	P concentration (ppm)	
	Feed solution	Receiving solution
1	0.422	0.432
2	0.299	0.302
3	0.281	0.295
4	0.260	0.297
5	0.263	0.313
6	0.255	0.302
7	0.259	0.297

For transport operation using PIM-P8, the P concentration in feed or receiving solutions was not detected on ICP-OES.

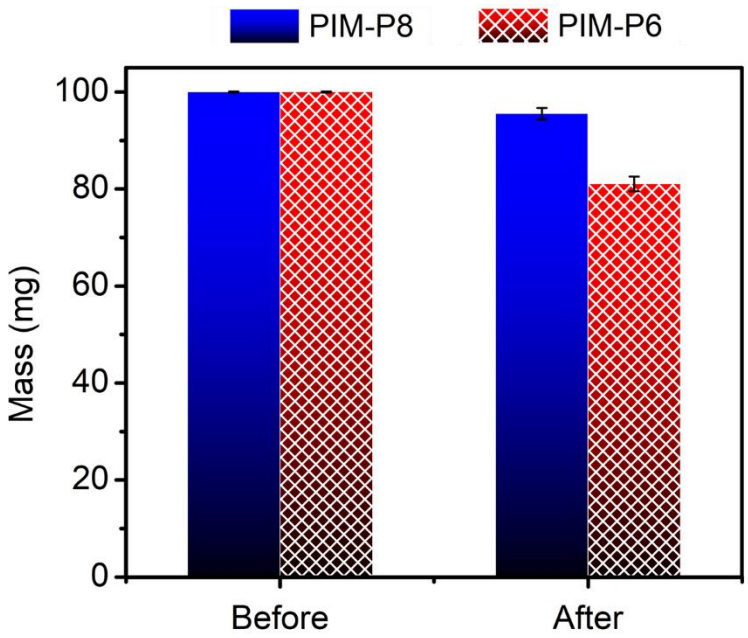

Figure S2.6. The mass change of PIM-P8 and PIM-P6 after soaked in 10 M HCl for 7 days under shaking.

Table S2.3. P concentration in aqueous phase after the PIMs were soaked in 10 M HCl for 7 days under shaking.

Membrane	P concentration (ppm)
PIM-P8	0.013
PIM-P6	5.714

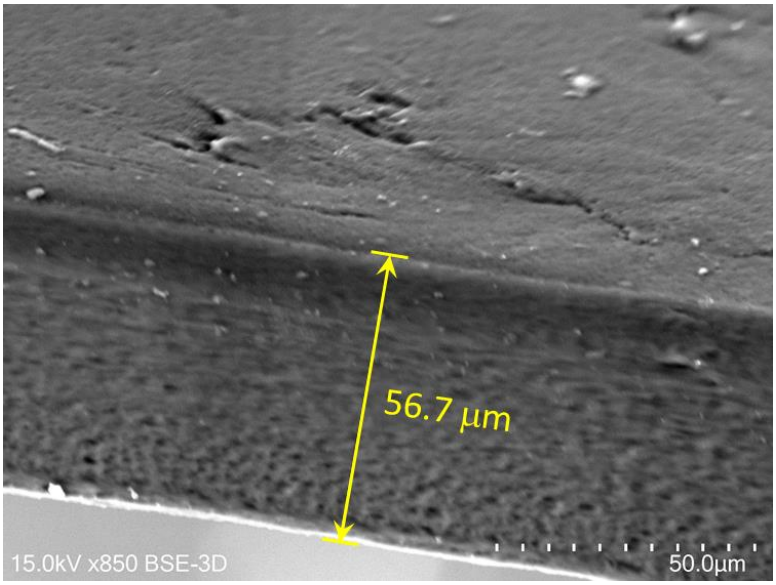

Figure S2.7. SEM image of the cross-section of the PIM. The PIM composition is 50 wt% PVDF-*co*-HFP, 40 wt% $P_{88812}Cl$, 10 wt% 2NPOE with total mass of 400 mg.

~ End of Chapter 2 ~

CHAPTER 3. SELECTIVE SEPARATION OF PLATINUM GROUP METALS VIA SEQUENTIAL TRANSPORT THROUGH POLYMER INCLUSION MEMBRANES CONTAINING AN IONIC LIQUID CARRIER

Abstract:

Mutual separation of platinum group metals (PGMs) is a particularly challenging issue in metal recovery technology. In this study, we report the successful separation of Pt(IV), Pd(II), and Rh(III) by sequential transport through polymer inclusion membranes (PIMs) containing the ionic liquid trioctyl(dodecyl) phosphonium chloride ($P_{88812}Cl$) as a metal carrier. This study describes the screening of suitable receiving solutions, optimization of the operating conditions, establishing a possible transport mechanism, and evaluation of the membrane stability. In the first transport sequence, Pt(IV) was selectively transported into the receiving solution with a recovery of >95%, while Pd(II) and Rh(III) remained in the feed solution. In the second transport sequence, high purity Pd(II) was transported into the receiving solution with a recovery of >95%, while Rh(III) remained completely in the feed solution. Furthermore, the PIM exhibited a stable performance with multiple uses over a 4 week period during which 4 Pt(IV) and Pd(II) sequential transport cycles were continuously carried out.

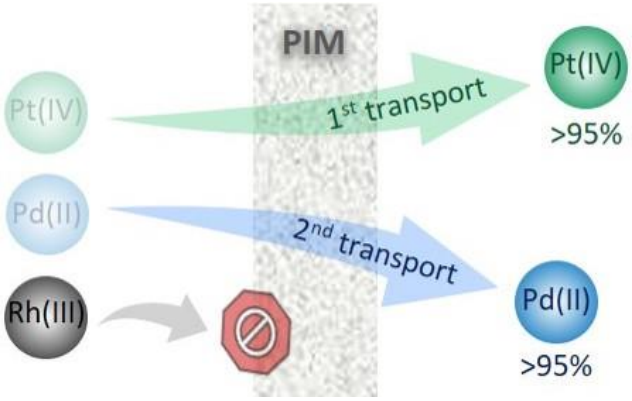

Remark:

This chapter was published in *ACS Sustainable Chemistry & Engineering*, 2020, 8, 11283–11291. Reproduced with permission. Copyright 2020 American Chemical Society.

3.1 Introduction

The demand for platinum group metals (PGMs)—e.g. platinum (Pt), palladium (Pd), and rhodium (Rh)—for the manufacture of various products has been steadily rising over the years [1]. The total world demand for Pt, Pd, and Rh in 2019 was 8,484,000 oz, 11,502,000 oz, and 1,144,000 oz, respectively [2]. PGMs are essential constituents of automobile catalytic converters, computers, smartphones, fuel cells, and catalysts for the oil-refining and fine chemical industries [3,4]. PGMs exhibit stable electrical properties [5], are resistant to high-temperature corrosion and oxidation [6,7], and improve the properties of other transition metals by forming alloys [8]. Owing to the unique characteristics of PGMs, they are rarely substituted with different elements or compounds in applications. However, PGM resources in the earth's crust are limited. In the past decade, PGM demand has consistently exceeded the supply by approximately 30% [2,9].

The use of secondary resources, for example recycling waste materials, could address the issue of PGM scarcity. Several technologies have been developed to optimize metal recycling processes, including bio-recycling [10], precipitation [11,12], ion-exchange resins [13,14], liquid-liquid extraction [15–17], and membrane technology [18]. From an economic point of view, membrane technology would be advantageous for industrial purposes as it would provide a simple one-step metal recovery process, which would reduce the operation cost. Polymer inclusion membranes (PIMs)—a type of carrier-mediated membrane—have demonstrated promising results for various metal separation and recovery processes [19–22]. PIMs exhibit several advantages including durability, high selectivity, and facile tunability [23]. Furthermore, PIMs are considered more eco-friendly than their liquid-liquid extraction counterparts owing to markedly less extractant being required.

There have been some reports of the application of PIM technology for PGM recovery [24–28]. However, the core problem, which is the mutual separation of PGMs, is rarely

addressed in detail. PGMs are extremely difficult to separate from each other because of the similarity of their physical and chemical properties. PGMs are transition metals in the *d*-block of the periodic table that have valence shells of $6s^1 5d^9$, $4d^{10}$, and $5s^1 4d^8$ for Pt, Pd, and Rh, respectively. Consequently, they exhibit similar paramagnetic properties and a strong tendency to form similar kinds of complexes [29]. According to the hard-soft acid-base (HSAB) theory, these metals show soft-acid characteristics; thus, they prefer to coordinate with soft-base ligands e.g. cyanide, amine, ammonia, and sulfur ligands, as well as halides. Moreover, the atomic sizes of Pt (1.75 Å), Pd (1.63 Å), and Rh (2.00 Å) show only very small differences, obviating the possibility of size exclusion-based separation.

To address the challenges of PGM recycling, our group designed a novel extractant; trioctyl(dodecyl) phosphonium chloride ($P_{88812}Cl$) ionic liquid. This ionic liquid has performed remarkably well for PGM recovery from an automotive catalytic converter leach liquor in a liquid-liquid extraction [30,31]. $P_{88812}Cl$ was able to rapidly extract Pt(IV), Pd(II), and Rh(III) from an aqueous chloride solution through the ion-exchange mechanism [32]. Subsequently, we expanded the application of the ionic liquid to PIM technology with the aim of creating a simpler, cheaper, and more environmentally friendly process. As recently reported, a stable PIM for selective separation of Pd(II) and Rh(III) was successfully fabricated by incorporating the $P_{88812}Cl$ ionic liquid carrier into a poly(vinylidene fluoride-*co*-hexafluoropropyle) (PVDF-*co*-HFP) polymer base with a small amount of 2-nitrophenyloctyl ether (2NPOE) as a plasticizer [33]. In the current study, we aimed to demonstrate a complete process for PGM mutual separation using the PIM transport system.

Herein, we report the successful separation of Pt(IV), Pd(II), and Rh(III) with high recovery and purity from a mixture solution via sequential transport through a PIM containing a $P_{88812}Cl$ carrier. The sequential transport was carried out in a one-pot system using suitable receiving solutions for each transport sequence without replacing the membrane. In addition,

the PIM stability was examined for multiple transport cycles over a continuous 4-week period. To the best of our knowledge, this is the first report of the complete mutual separation of Pt, Pd, and Rh in a membrane transport system.

3.2 Experimental

3.2.1 Materials

The ionic liquid trioctyl(dodecyl) phosphonium chloride ($P_{88812}Cl$, assay 98%) was supplied by Nippon Chemical Industrial Co., Ltd. (Tokyo, Japan). The poly(vinylidene fluoride-*co*-hexafluoropropyle) (PVDF-*co*-HFP) pellets were purchased from Sigma-Aldrich. The 2-nitrophenyloctyl ether (2NPOE, 99%) was purchased from Dojindo Laboratories. The tetrahydrofuran (THF, 99.5%), standard solution of platinum (H_2PtCl_6 in 1 M HCl, 1000 ppm), standard solution of palladium ($PdCl_2$ in 1 M HCl, 1000 ppm), thiourea powder ($SC(NH_2)_2$, 98%), and ammonia solution (NH_3, 28%) were purchased from Wako Pure Chemical Ltd. The standard solution of phosphorous (KH_2PO_4 in H_2O, 1000 ppm) and the standard solution of rhodium (Rh(III) in 1 M HCl, 1000 ppm) were purchased from Kanto Chemical Co., Inc. The hydrochloric acid solution (HCl, 10 M), nitric acid solution (HNO_3, 5 M), sodium perchlorate powder ($NaClO_4$, 98%), ammonium chloride powder (NH_4Cl, 99%), and potassium thiocyanate powder (KSCN, 99.5%) were purchased from Kishida Co., Ltd. Deionized water (Milli-Q, Merck Millipore) was used to prepare all of the aqueous solutions.

3.2.2 Preparation of the polymer inclusion membranes

The polymer inclusion membranes (PIMs) were fabricated based on the findings of our previous report [33]. The PIM components—$P_{88812}Cl$ (carrier, 40 wt%), PVDF-*co*-HFP (polymer base, 50 wt%), and 2NPOE (plasticizer, 10 wt%) with a total mass of 400 mg—were dissolved in 10 mL of THF. The mixture was stirred vigorously at 40 °C until a homogenous solution was obtained. The solution was then poured into a 7.5 cm diameter glass ring on top

of a glass plate. A filter paper and a watch glass were positioned on the top of the glass ring to enable the THF to slowly evaporate for one day. The PIMs were then carefully separated from the cast when they were completely dry. The PIM thickness was 55 μm (see Figure S3.1(a), Appendix B).

3.2.3 Membrane batch extraction and stripping experiments

The membrane batch extraction experiment was carried out by immersing a segment of the PIM with a mass of 100 mg in 50 mL of the feed solution in a glass jar. The jar was shaken at 90 rpm in a water bath shaker (EYELA NTS-4000BH) at 25 ± 0.5 °C for 24 h. At the end of the extraction experiment, the metal loaded PIM segment was taken from the feed solution and gently dried. The PIM segment was then subjected to a stripping experiment by immersing it in 50 mL of the stripping solution in a glass jar. The jar was treated in the same manner as for the extraction experiment for 24 h. The metal concentration in the feed and stripping solutions after each treatment was measured using an inductively coupled plasma optical emission spectrometer (ICP-OES) Optima 8300 (PerkinElmer). The extraction (E, %) and stripping (S, %) efficiencies were calculated using equations (3.1) and (3.2), respectively.

$$E = \frac{\left(C_{M,i}^{F} - C_{M,f}^{F}\right)}{C_{M,i}^{F}} \times 100\% \qquad (3.1)$$

$$S = \frac{C_{M,f}^{S}}{\left(C_{M,i}^{F} - C_{M,f}^{F}\right)} \times 100\% \qquad (3.2)$$

where $C_{M,i}^{F}$ is the initial metal M concentration in the feed solution (mol m^{-3}), $C_{M,f}^{F}$ is the final metal M concentration in the feed solution (mol m^{-3}), and $C_{M,f}^{S}$ is the final metal M concentration in the stripping solution (mol m^{-3}).

3.2.4 Membrane transport experiments

The transport operations were performed in a membrane transport system comprising paired glass chambers surrounded by a circulating water-jacket. A circular PIM sample with a

mass of 121 ± 1 mg was clamped between the flange of the feed and receiving chambers. The feed and receiving solutions (volume of 50 mL, respectively) were added to the corresponding chambers. The diameter of the membrane in contact with each solution was 25.0 mm (effective surface area of 4.9×10^{-4} m^2). The solution in each chamber was stirred using a magnetic stirrer bar during the transport operations. A water bath (EYELA NCB-1200) was used to maintain the temperature of the feed and receiving solutions at 25 ± 0.5 °C by constantly flowing water into the jacket of each chamber. At designated time intervals, 0.5 mL solutions were sampled systematically from both chambers. The metal concentrations were monitored using an ICP-OES. When solution samples were taken for analysis, corresponding volumes of fresh solution were added to the chambers.

The kinetics of the membrane transport were assumed to follow a first-order reaction, thus the rate constant (k, h^{-1}), permeability coefficient (P, m h^{-1}), initial flux (J_0, mmol m^{-2} h^{-1}), recovery factor (RF, %), and product purity (PR, %) of the transported metals were determined using equations (3.3) – (3.7), respectively.

$$ln\left(\frac{C_{M,t}^{F}}{C_{M,i}^{F}}\right) = -kt \qquad (3.3)$$

$$P = \left(\frac{V}{A}\right)k \qquad (3.4)$$

$$J_0 = PC_{M,i}^{F} \qquad (3.5)$$

$$RF = \frac{C_{M,t}^{R}}{C_{M,i}^{F}} \times 100\% \qquad (3.6)$$

$$PR = \frac{C_{M,t}^{R}}{C_{Mtot,t}^{R}} \times 100\% \qquad (3.7)$$

where $C_{M,t}^{F}$ is the metal M concentration in the feed solution at time t (mol m^{-3}), $C_{M,i}^{F}$ is the initial metal M concentration in the feed solution (mol m^{-3}), t is the time of the transport operation (h), V is the feed solution volume (m^3), and A is the area of the membrane surface in contact with both the feed and receiving solutions (m^2), $C_{M,t}^{R}$ is the metal M concentration

transported into the receiving solution at time t (mol m^{-3}), and $C^{R}_{Mtot,t}$ is the total metal concentration in the receiving solution (mol m^{-3}).

The sequential transport of Pt(IV) and Pd(II) was carried out without replacing the PIM. After finishing the Pt(IV) transport (1st sequence), the receiving solution was removed from the chamber. The inner side of the receiving chamber was then washed three times using deionized water. Fresh receiving solution was then added to the receiving chamber for the Pd(II) transport (2nd sequence). The metal concentration in feed solution was measured prior to each sequence and designated the initial concentration.

3.2.5 Membrane stability test

The stability of the PIM was evaluated for a continuous transport operation over a 4-week period performing 4 cycles of sequential Pt(IV) and Pd(II) transport. After completing the first cycle of sequential Pt(IV) and Pd(II) transport, both the feed and receiving solutions were removed from the chambers. The inner side of the chambers was washed three times using deionized water while the membrane was kept in position. The fresh feed and receiving solutions were then added to the corresponding chambers, and the second cycle was conducted, and so on. Each sequential transport cycle required 7 days for completion; 4 days for Pt(IV) transport and 3 days for Pd(II) transport. To monitor the leakage of carrier from the membrane, the phosphorous concentration in the feed and receiving solutions was analyzed periodically using ICP-OES. The weight of the PIM before and after the stability test was recorded using a digital balance (Sartorius CPA225D). The PIM was also examined using several characterization techniques.

3.2.6 Characterization

The infrared spectra of the PIMs were acquired using a Fourier transform infrared (FTIR) spectrometer equipped with an attenuated total reflectance (ATR) accessory (PerkinElmer).

The spectra were scanned 8 times with a resolution of 2 cm^{-1}. The membrane morphology and elemental mapping were observed using a scanning electron microscope with energy dispersive X-ray (SEM-EDX) instrument (Hitachi TM4000) with a voltage acceleration of 15 kV and magnification of 1000×. The characteristics of the PIM surface were analyzed using a scanning probe microscope (SPM) instrument (Hitachi Nanocute) in dynamic force mode with a microcantilever SI-DF3P2. To establish a plausible transport mechanism, the complex compound species that were formed during transport were analyzed using an ultraviolet-visible (UV-Vis) spectrometer (JASCO V-670) at 25 °C with a 1 nm spectral resolution. To measure the UV-Vis spectra of the metal complex formed inside the PIM, the metal loaded PIM obtained following the transport operation was dissolved into 20 mL of THF and vigorously stirred at 40 °C until a homogenous solution was observed.

3.3 Results and Discussion

3.3.1 Screening of suitable receiving solutions

In the liquid-liquid extraction experiment the $P_{88812}Cl$ ionic liquid rapidly extracted Pt(IV), Pd(II), and Rh(III) from the appropriate aqueous solution as described in equations (3.8) – (3.10) [32]. Thus, a selective stripping solution is required to achieve mutual PGM separation. Since the separation of Pd(II) and Rh(III) was demonstrated in our previous study [33], the first target in the current study was the selective separation of Pt(IV) from Pd(II) and Rh(III). Prior to the membrane transport operations, membrane batch extraction and stripping experiments were carried out to find a selective stripping solution for Pt(IV). Six stripping agents were proposed; $NaClO_4$, NH_3, NH_4Cl, $SC(NH_2)_2$, HNO_3, and KSCN.

$$[PtCl_6]^{2-}{}_{(aq)} + 2\left(P_{88812}{}^{+}Cl^{-}\right)_{(org)} \rightleftharpoons \left(P_{88812}{}^{+}\right)_2[PtCl_6]^{2-}{}_{(org)} + 2Cl^{-}{}_{(aq)} \quad (3.8)$$

$$[PdCl_4]^{2-}{}_{(aq)} + 2\left(P_{88812}{}^{+}Cl^{-}\right)_{(org)} \rightleftharpoons \left(P_{88812}{}^{+}\right)_2[PdCl_4]^{2-}{}_{(org)} + 2Cl^{-}{}_{(aq)} \quad (3.9)$$

$$[RhCl_5(H_2O)]^{2-}{}_{(aq)} + 2\left(P_{88812}{}^{+}Cl^{-}\right)_{(org)} \rightleftharpoons \left(P_{88812}{}^{+}\right)_2[RhCl_5(H_2O)]^{2-}{}_{(org)} + 2Cl^{-}{}_{(aq)} \quad (3.10)$$

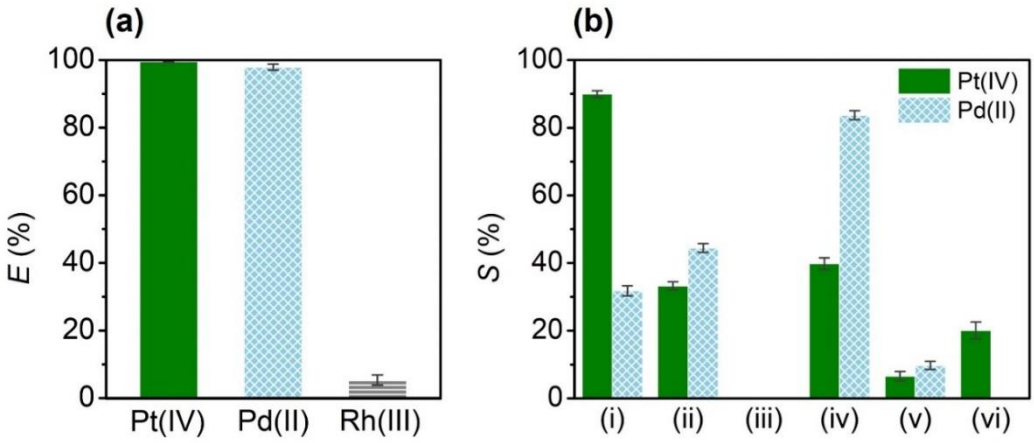

Figure 3.1. (a) Extraction efficiency (*E*) of PGMs into PIM segments and (b) stripping efficiency (*S*) from metal loaded PIM segments into stripping solutions. Feed solution: Pt(IV), Pd(II), Rh(III) 20 ppm in HCl 3 M. Stripping solutions: (i) $NaClO_4$, (ii) NH_3, (iii) NH_4Cl, (iv) $SC(NH_2)_2$, (v) HNO_3, or (vi) KSCN 0.1 M.

Figure 3.1(a) shows the extraction of Pt(IV), Pd(II), and Rh(III) from the feed solution into the PIM segments. Under a high concentration of HCl (3 M), the Pt(IV) and Pd(II) were easily extracted into the membrane, while the Rh(III) stayed in the feed solution. This result is in line with previous literature, which showed that Rh(III) was hardly extracted under a high concentration of Cl^- ions [34–36], although the extracted species were different [37]. The result also implied that the separation of Pt(IV) and Pd(II) would be a significant challenge. The stripping efficiency of Pt(IV) and Pd(II) from the PIM segments into several stripping agents is shown in Figure 3.1(b). Encouraging results for Pt(IV) stripping were exhibited for $NaClO_4$ and KSCN solutions. The Pt(IV) stripping into $NaClO_4$ solution was high (≈90%), although a small amount (≈30%) of Pd(II) was also stripped. The KSCN solution was able to selectively strip Pt(IV), although the efficiency was relatively low (<25%). Of the other solutions NH_3, $SC(NH_2)_2$, and HNO_3 exhibited higher selectivity for Pd(II), while the NH_4Cl solution was unable to strip either Pt(IV) or Pd(II). Based on the findings, the $NaClO_4$ solution was selected as the receiving solution for the membrane transport experiments.

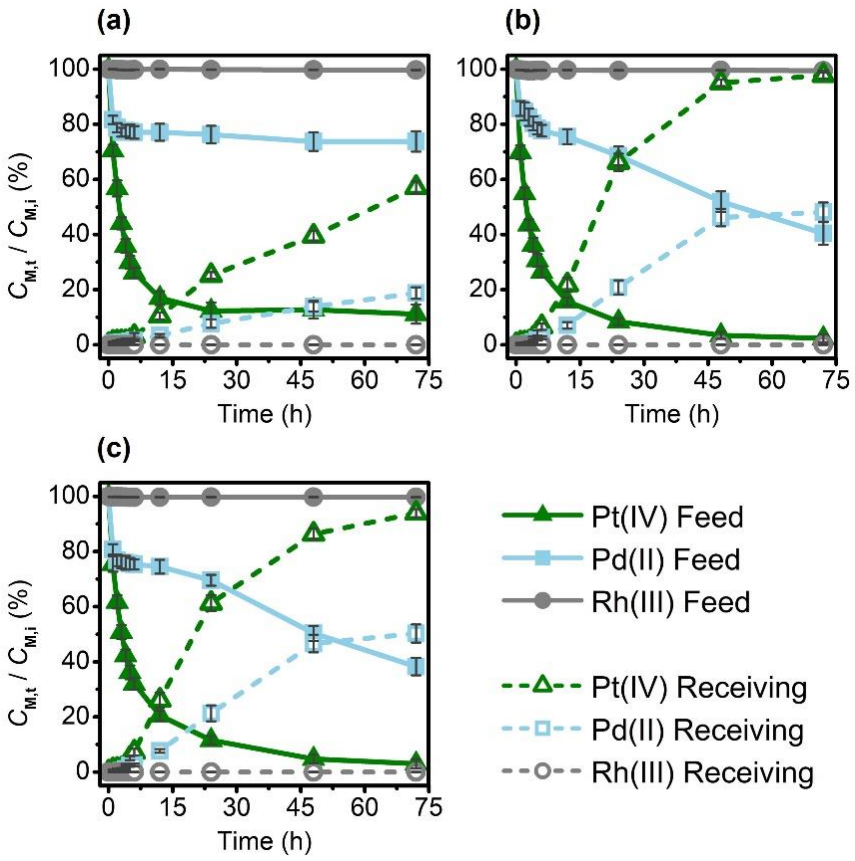

Figure 3.2. Effect of receiving solution concentration on the transport behavior of Pt(IV), Pd(II), and Rh(III): (a) 0.01 M, (b) 0.1 M, (c) 1 M $NaClO_4$. Feed solution: Pt(IV), Pd(II), Rh(III) 20 ppm in HCl 3 M.

3.3.2 Optimization of the membrane transport operations

First, the effect of the $NaClO_4$ receiving solution concentration on metal ion transport was investigated. As can be seen in Figure 3.2, the amount of Pt(IV) transported into receiving solutions of 0.01 M, 0.1 M, and 1 M $NaClO_4$ after 3 days was 57%, 98%, and 94%, respectively. The 0.1 M $NaClO_4$ receiving solution was therefore selected for subsequent experiments since it demonstrated the highest Pt(IV) recovery. However, although the recovery was satisfactory, the transport selectivity required improvement. Along with Pt(IV), 48% of the Pd(II) was also transported into the receiving solution, reducing the product purity.

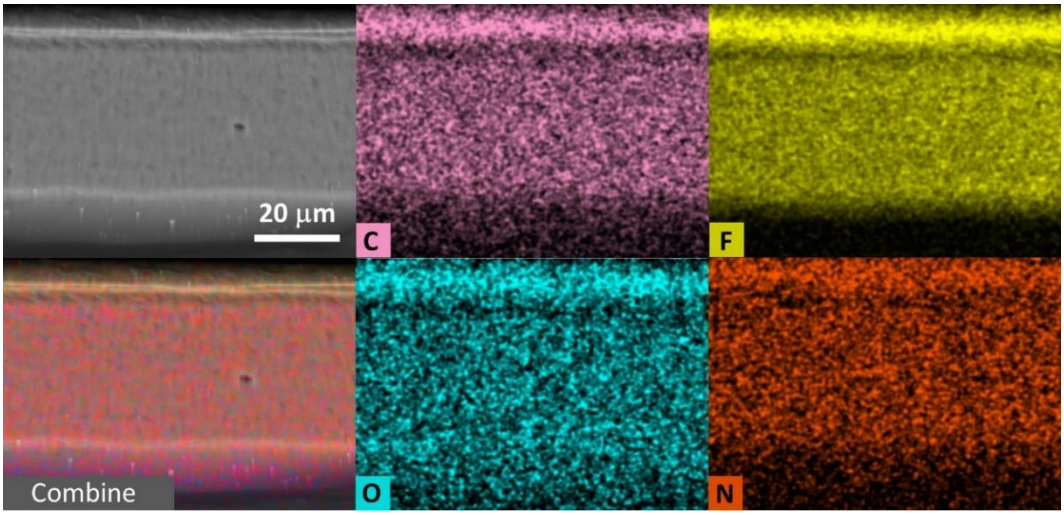

Figure 3.3. Membrane cross-section SEM-EDX images of the PIM after the transport operation with a 0.1 M $NaClO_4$ receiving solution. EDX elemental mapping: carbon (C), fluorine (F), oxygen (O), and nitrogen (N). The upper side is the side of the membrane that contacted the receiving solution.

An unexpected observation was made for the PIM after the transport operation. A white precipitation-like layer was observed on the membrane surface that contacted the receiving solution (Figure S3.1(b), Appendix B). To investigate what happened on the membrane surface, an SEM-EDX measurement was conducted. Figure 3.3 shows the membrane cross-section SEM image with EDX elemental mapping for carbon (C), fluorine (F), oxygen (O), and nitrogen (N). On the upper side of the mapping images, which was the receiving solution side, a small line gap was clearly observed for C and F and was visible but blurry for O and N. This result indicates that the precipitation-like layer was a damaged part of the membrane, in particular the polymer base. PVDF-*co*-HFP is a stable polymer that can endure severe environments [38–40], however, it appeared that prolonged contact with the $NaClO_4$ solution resulted in surface damage. A nucleophilic attack by oxygen species from the ClO_4^- ion on the fluoride moieties in the PVDF polymer block might be the reason for the damage, as suggested in several studies [41–43].

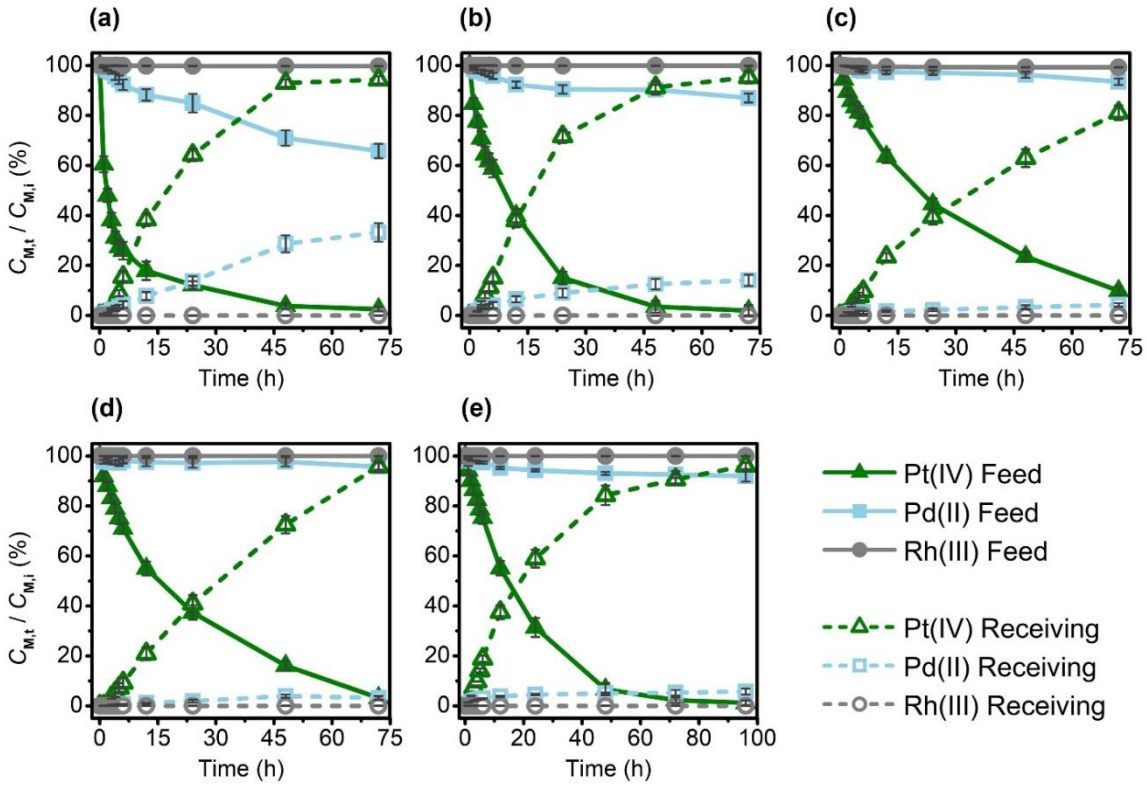

Figure 3.4. Effect of feed solution concentration on the transport behavior of Pt(IV), Pd(II), and Rh(III): (a) Pt(IV), Pd(II), Rh(III) 20 ppm, (b) Pt(IV), Pd(II), Rh(III) 50 ppm, (c) Pt(IV), Pd(II), Rh(III) 100 ppm, (d) Pt(IV) and Pd(II) 80 ppm, Rh(III) 30 ppm, (e) Pt(IV) 80 ppm, Pd(II) 160 ppm, Rh(III) 30 ppm in HCl 3 M. Receiving solution: $NaClO_4$ 0.1 M in HCl 1 M.

To prevent damage of the PIM surface, hydrochloric acid was added to the receiving solution. The presence of hydronium ions (H_3O^+), a strong electrophile, prevented the oxygen species from attacking the polymer. Adding HCl 1 M to the $NaClO_4$ 0.1 M receiving solution had little effect on the transport behavior (Figure 3.4(a)), however it prevented membrane damage during the transport operation (Figure S3.1(c), Appendix B). Thus, the mixture of $NaClO_4$ and HCl was used for subsequent experiments.

The effect of the concentration of the metals in the feed solution was also studied. Five different concentrations and ratios were used as listed in Table 3.1. Increasing the concentration of each ion in the feed solution from 20 ppm to 50 ppm, did not affect the Pt(IV) transport behavior, however the Pd(II) transport was significantly reduced from ≈40% to ≈15% (Figure 4(a,b)) after 3 days of operation. Further increasing the feed concentration to 100 ppm reduced

the Pd(II) transport to less than 5%, however the Pt(IV) transport was only slightly reduced (Figure 3.4(c)). Thus, increasing the feed concentration gradually reduced the Pt(IV) recovery factor (*RF*) but increased the product purity (*PR*) (Table 3.1, a–c). The results suggest that the PIM exhibited some kind of maximum transport capacity: at the lower feed concentration, the capacity could accommodate both Pt(IV) and Pd(II), while at the higher feed concentration, it could only accommodate Pt(IV), resulting in a higher transport selectivity. This insight was also supported by the initial flux (J_0) data that showed a gradual decrease as the feed concentration was increased (Table 3.1, a–c), which indicated the presence of a capacity barrier. Often, as implied by Fick's law of diffusion, increasing the feed concentration increases the initial flux since the gradient concentration between the feed and receiving solutions is increased.

Table 3.1. Effect of the feed solution concentration on the membrane transport behavior.

No.	Metal concentration (ppm)			$J_{0,Pt(IV)}$ (mmol m^{-2} h^{-1})	$RF_{Pt(IV)}$ (%)	$PR_{Pt(IV)}$ (%)
	Pt(IV)	Pd(II)	Rh(III)			
(a)	20	20	20	2.29	94	74.3
(b)	50	50	50	2.07	95	87.0
(c)	100	100	100	1.92	81	95.1
(d)	80	80	30	2.14	96	96.7
(e)*	80	160	30	1.76	96	89.6

*Transport operation: 4 days.

An optimum Pt(IV) transport performance was exhibited for a feed concentration of 80 ppm (Figure 3.4(d)) with *RF* and *PR* values of 96% and 97%, respectively (Table 3.1, d). It should be noted that the concentration of Rh(III) was kept low (30 ppm) since the Rh(III) always remained on the feed side regardless of its concentration. Unfortunately, the optimum feed concentration was not similar to the PGM concentration in real waste leach liquor. The transport behavior when the feed concentration models the PGM concentration in an

automotive catalytic leach liquor is shown in Figure 3.4(e). When the Pd(II) concentration (160 ppm) was twice as high as that of Pt(IV) (80 ppm), the Pt(IV) transport kinetics were slowed and required 4 days to reach an *RF* of 96%. The Pt(IV) purity in the receiving solution decreased slightly to 89.6% as a result of ≈5% Pd(II) transport (Table 3.1, e). Pt(IV) and Pd(II) were competing to be extracted by the $P_{88812}Cl$ inside the PIM, thus increasing the Pd(II) concentration reduced Pt(IV) transport kinetics. Nevertheless, the recovery and purity obtained for Pt(IV) transport in this study was satisfactory and could potentially be applied on an industrial scale.

3.3.3 Sequential transport of Pt(IV) and Pd(II)

This study was aimed at providing a complete solution for PGM separation. Thus, after the selective Pt(IV) transport (1st transport sequence) was achieved, the raffinate of the feed solution was subjected to a subsequent treatment for Pd(II) and Rh(III) separation (2nd transport sequence). On the first attempt to transport Pd(II) from the raffinate feed solution, thiourea 5 mM in HCl 1 M was used as the receiving solution, based on findings from a previous report [33]. However, very little Pd(II) was transported into the receiving solution even after 3 days of operation, as shown in Figure 3.5(a). This result was unexpected since the high affinity of thiourea for Pd(II) has been well documented in the literature [28,30–32,44–46]. Therefore, a series experiments to investigate what happened to the raffinate feed solution and to obtain a high transport recovery was carried out.

The transport of ClO_4^- ions from the receiving to the feed solution during the 1st transport sequence was suspected to have hindered Pd(II) transport. Therefore, Pd(II) transport into thiourea receiving solution was carried out with a small amount of $NaClO_4$ added to the feed solution. As shown in Figure S3.2(a) (Appendix B), very little Pd(II) was transported under these conditions, indicating that ClO_4^- ions acted as an inhibitor for Pd(II) transport into the thiourea receiving solution. When another receiving solution, KSCN 0.1 M, was used, unusual

transport behavior was observed (see Figure S3.2(b), Appendix B). Almost 100% of the Pd(II) was extracted into the PIM but not transported into the receiving solution, resulting in an accumulation of Pd inside the PIM as shown by its intense orange appearance (Figure S2(d), Appendix B). Analysis of the PIM surface using EDX showed the presence of Pd and S in relatively high quantities (Figure S3.3, Appendix B), suggesting the formation of Pd(II)-SCN complexes inside the membrane. Complexation of Pd(II) and SCN^- ligands resulted in complex species that could be easily absorbed into a polymer material as demonstrated by Al-Bazi and Chow [47].

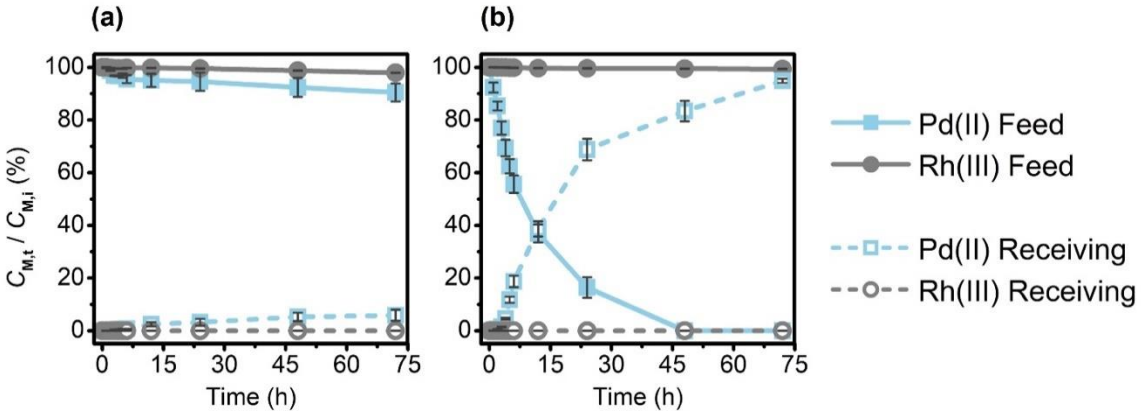

Figure 3.5. Transport of Pd(II) and Rh(III) from the raffinate feed solution into (a) thiourea 5 mM in HCl 1 M and (b) a mix of thiourea 10 mM and KSCN 0.1 M in HCl 1 M. Feed solution: raffinate solution from the 1st transport sequence.

Interestingly, when a mixture of thiourea 10 mM and KSCN 0.1 M in HCl 1 M was used as the receiving solution, effective Pd(II) transport and a colorless membrane were observed after the transport operation (Figure S3.2(c,e), Appendix B). The mixture was then applied as the receiving solution for Pd(II) transport from the raffinate feed solution. As can be seen in Figure 3.5(b), ≈95% of the Pd(II) was effectively recovered into the receiving solution after 3 days of operation, while the Rh(III) remained completely in the feed solution. The addition of KSCN into the thiourea receiving solution overcame the inhibition of Pd(II) transport by the ClO_4^- ions.

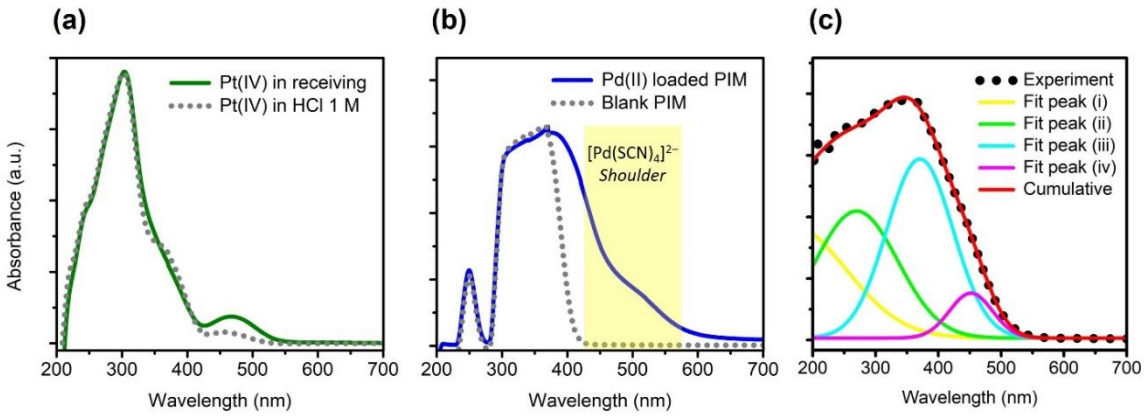

Figure 3.6. UV-Vis spectra of (a) the receiving solution after Pt(IV) transport, (b) the PIM with Pd(II) accumulation inside the membrane, and (c) the receiving solution after Pd(II) transport. The spectrum (c) was deconvolved using a Gaussian function.

3.3.4 Plausible transport mechanism

The complex species of Pt(IV) and Pd(II) formed during the transport operation were studied using UV-Vis spectroscopy. Figure 3.6 shows the UV-Vis spectra for the Pt(IV) and Pd(II) species obtained during the transport operations. The UV-Vis spectrum of Pt(IV) transported into the $NaClO_4$ receiving solution was similar to that of Pt(IV) in HCl 1 M (Figure 3.6(a)). A small difference in intensity at around 475 nm was observed, while the peak of the predominant species i.e. the $[PtCl_6]^{2-}$ complex, which was observed as a band at 250–350 nm, remained unchanged [48,49]. The results indicated that the Pt(IV) did not undergo a complex species alteration during the transport process. For Pd(II), the complex species formed inside the PIM and transported into the receiving solution were analyzed. The PIM loaded with Pd when KSCN was used as the receiving solution (Figure S3.2(d), Appendix B), was dissolved in THF for UV-Vis measurement. Figure 3.6(b) shows the UV-Vis spectrum of Pd(II) loaded PIM compared with that of an as-prepared (blank) PIM. The maximum absorption (λ_{max}) of the $[Pd(SCN)_4]^{2-}$ complex should be observed at around 315 nm [50], however it was hardly observed owing to overlap with the broad absorption of the PIM components. Nevertheless, the $[Pd(SCN)_4]^{2-}$ complex absorption shoulder at around 450–500 nm was clearly observed

owing to its intense orange color [51,52]. In the receiving solution following Pd(II) transport, a broad UV-Vis spectrum from 200 nm to 500 nm was observed (Figure 3.6(c)). For easier interpretation, the spectrum was deconvolved using a Gaussian function, resulting in four fit peaks. Fit peaks (i) and (ii) were attributed to the absorbance of excess thiourea and KSCN in the receiving solution as shown in Figure S3.4 (Appendix B). Fit peaks (iii) and (iv) were attributed to the Pd-thiourea complex i.e. $Pd(SC(NH_2)_2)_4$ [33,46].

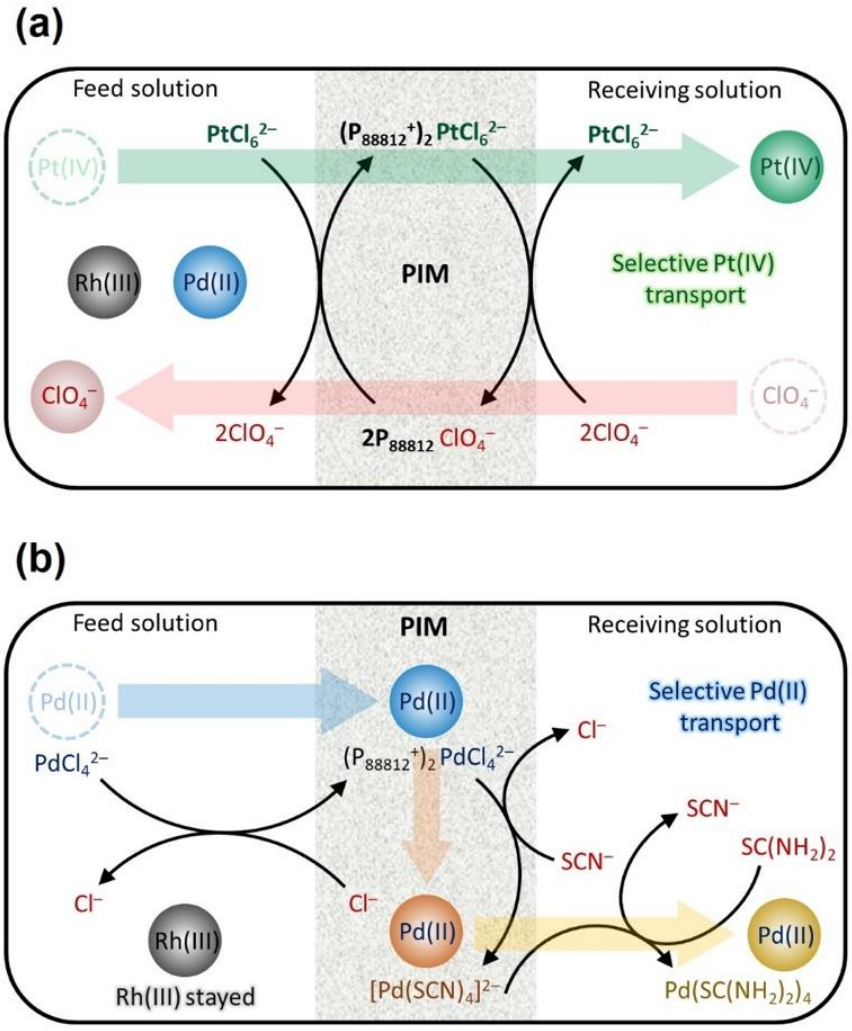

Figure 3.7. Plausible mechanisms for (a) Pt(IV) and (b) Pd(II) transport in this study.

Plausible mechanisms for Pt(IV) and Pd(II) transport were proposed based on the spectroscopic analysis and the transport behavior. Figure 3.7(a) depicts the Pt(IV) transport mechanism. The $[PtCl_6]^{2-}$ species in the feed solution were extracted into the membrane by ion

exchange with the Cl^- ion of the $P_{88812}Cl$ ionic liquid, yielding a $(P_{88812}^+)_2PtCl_6^{2-}$ complex inside the PIM. Subsequently, the $[PtCl_6]^{2-}$ exchanged with ClO_4^- in the receiving solution. Therefore, coupled transport occurred between the $[PtCl_6]^{2-}$ complex in the feed solution and the ClO_4^- ion in the receiving solution, resulting in selective Pt(IV) transport, while Pd(II) and Rh(III) remained in the feed solution. This interpretation is in agreement with that of Pt(IV) extraction [31,32] and the previously reported transport mechanism [24]. Figure 3.7(b) depicts the Pd(II) transport mechanism. The $[PdCl_4]^{2-}$ species in the feed solution were extracted into the membrane via ion exchange with Cl^- ions of the $P_{88812}Cl$ ionic liquid and subsequently underwent a ligand substitution with SCN^- ions, yielding the $[Pd(SCN)_4]^{2-}$ complex inside the PIM, as indicated by the intense orange appearance and the UV-Vis spectra. Subsequently, the Pd(II) was withdrawn into the receiving solution through the ligand substitution of thiourea driven by the concentration gradient and high affinity of Pd(II) for thiourea, yielding the $Pd(SC(NH_2)_2)_4$ complex as indicated by UV-Vis analysis. The Rh(III) species remained in the feed solution in both the 1st and 2nd transport sequences. Hence, effective separation of Pt(IV), Pd(II), and Rh(III) was achieved using the sequential transport strategy.

3.3.5 Membrane stability

Membrane stability is a crucial factor in the implementation of PIM technology on an industrial scale. In this study, the PIM stability was examined for a continuous transport operation over the course of 4 weeks, during which 4 cycles of sequential Pt(IV) and Pd(II) transport were conducted. As shown in Figure 3.8, the transport performance was quite stable as demonstrated by the steady recovery factor (*RF*) values over 4 operation cycles. The *RF* value of Pt(IV) transport only decreased slightly from 96% initially to 89% at the 4th cycle, while that of Pd(II) transport remained constant at ≈95%. The initial flux (J_0) of both Pt(IV) and Pd(II) transport gradually decreased over time (Table 3.2) showing a decline in transport kinetics. The purity of Pt(IV) in the receiving solution (*PR*) decreased from 89.6% initially to

83.2% at the 4th cycle, while that of Pd(II) decreased slightly from 99.9% to 98.6%. The results demonstrated that the PIM was relatively stable as it was able to maintain fairly stable *RF* and *PR* values over 4 sequential cycles. Notwithstanding, the reduction in the J_0 values indicated a nanostructure alteration.

Table 3.2. Membrane transport initial flux (J_0) and product purity (*PR*) during the stability test.

Cycle	Pt(IV): 1st sequence		Pd(II): 2nd sequence	
	$J_{0,Pt(IV)}$ (mmol m^{-2} h^{-1})	$PR_{Pt(IV)}$ (%)	$J_{0,Pd(II)}$ (mmol m^{-2} h^{-1})	$PR_{Pd(II)}$ (%)
I	1.76	89.6	13.31	99.9
II	1.65	87.1	12.33	99.8
III	1.61	85.7	10.81	99.4
IV	1.56	83.2	9.33	98.6

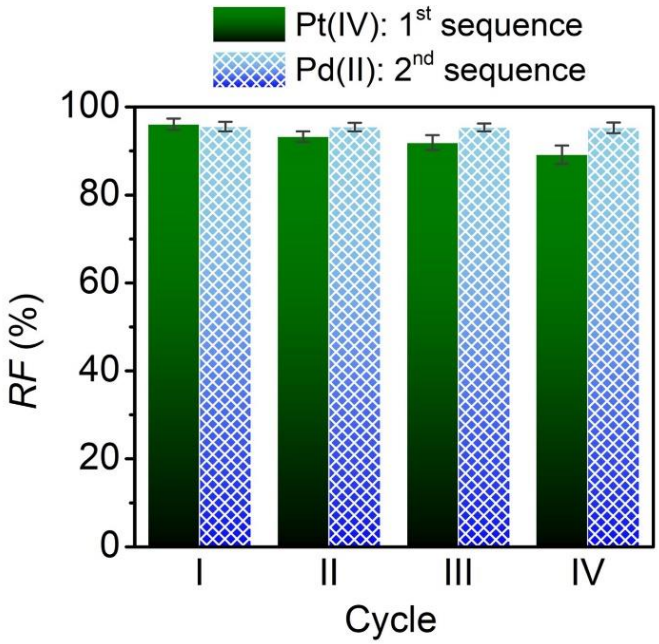

Figure 3.8. Recovery factor (*RF*) for Pt(IV) and Pd(II) sequential transport over 4 cycles of continuous operation.

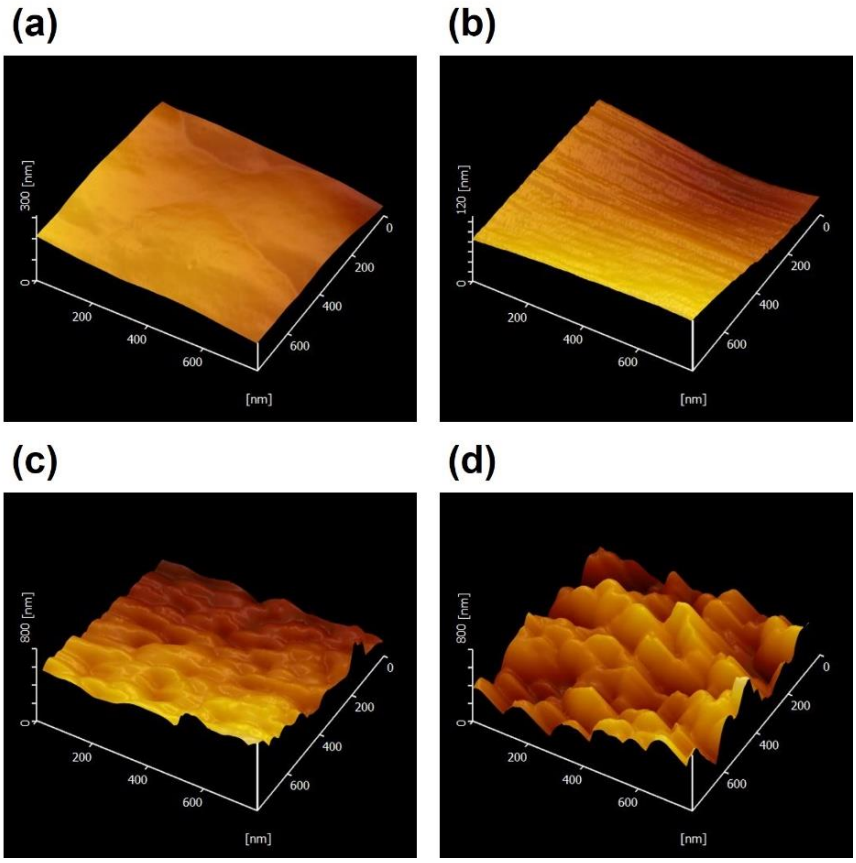

Figure 3.9. SPM images of the PIM on the (a) feed and (b) receiving side before the transport operation and (c) feed and (d) receiving side after 4 cycles of Pt(IV) and Pd(II) sequential transport.

To evaluate the structural changes of the PIM, the membrane was characterized using SPM and FTIR. Figure 3.9 shows SPM images of the PIM surfaces measured in dynamic force mode. The as-prepared PIM showed a relatively smooth surface on both the feed and receiving sides with only small differences in the morphology (Figure 3.9(a,b)). Note that the feed side and receiving side were the PIM sides that contacted the glass plate and were exposed to air during preparation, respectively; thus, they exhibited slightly different morphology. After being used in 4 sequential transport cycles, the surface roughness was moderately and significantly increased on the feed and receiving sides, respectively (Figure 3.9(c,d)). Etching of the PIM surface or removal of thin viscous liquid membrane film occurred during the multiple transport operations, particularly on the receiving side. The prolonged alternate use of $NaClO_4$ and the mixture of thiourea and KSCN as receiving solutions may have caused the etching of the PIM

surface. Nevertheless, the membrane was sufficiently strong to prevent serious damage as observed in Figure S3.5 (Appendix B). Moreover, the PIM only exhibited a small mass loss (6.2 ± 0.5 mg from 121 ± 1 mg) and no phosphorous leakage into the aqueous feed and receiving solutions was detected by ICP-OES measurements.

Figure 3.10 shows the FTIR analysis of the PIM before and after use in the stability test. The complex peaks in the range 500–1500 cm^{-1} are attributed to the strong fingerprint of the PVDF-*co*-HFP. Characteristic peaks of $P_{88812}Cl$ can be observed at 1468 cm^{-1} and 2900 cm^{-1}, which correspond to P−CH_2−R bending and C−H stretching vibrations, respectively. As can be seen, neither the PVDF-*co*-HFP nor $P_{88812}Cl$ signals underwent significant deformation, indicating that the PIM was stable at the chemical structure level. In addition, a new peak at 2109 cm^{-1} emerged for the PIM after use. This peak is attributed to the S−C≡N stretching vibration of the thiocyanate anion that was ion-exchanged into the PIM, replacing the Cl^- ion of the $P_{88812}Cl$ during the Pd(II) transport operation. The increase of roughness on the PIM surface and the ion-exchange between SCN^- and Cl^- ions inside the PIM, may correspond to the reduction of the initial flux (J_0) value.

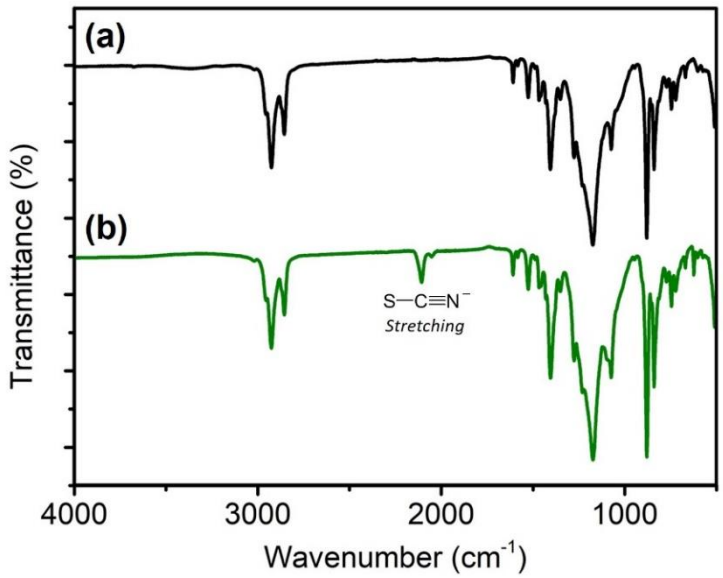

Figure 3.10. FTIR spectra of the PIM (a) before and (b) after use in 4 cycles of Pt(IV) and Pd(II) sequential transport.

3.4 Conclusions

This work demonstrated the successful separation of PGMs—Pt(IV), Pd(II), and Rh(III)—using a sequential transport operation through a PIM containing $P_{88812}Cl$ ionic liquid carrier. For the Pt(IV) transport (1st sequence), $NaClO_4$ 0.1 in HCl 1 M was found to be a suitable receiving solution. Under the optimized conditions, selective Pt(IV) transport with a recovery of 96% and purity of 89.9% was achieved, while Pd(II) and Rh(III) remained in the feed solution. For the Pd(II) transport (2nd sequence), a mixture of thiourea 10 mM and KSCN 0.1 M in HCl 1 M was found to be a suitable receiving solution. The presence of KSCN was able to overcome Pd(II) transport inhibition by ClO_4^- ions that permeated into the feed solution during the 1st transport sequence. Pd(II) was transported into the receiving solution with a recovery of 96% and purity of 99.9%, while the Rh(III) remained completely in the feed solution. A membrane stability test demonstrated that the PIM exhibited a stable performance over 4 cycles of Pt(IV) and Pd(II) sequential transport throughout a total operation time of 4 weeks. The results obtained in this study show that using a PIM containing an ionic liquid carrier could successfully address the issue of PGM mutual separation. The PIM transport system could be further developed to effectively recover PGMs from real waste materials such as a spent automobile catalytic converter.

References

[1] World Platinum Investment Council, *Platinum Quarterly Q*3, 2019.

[2] A. Cowley, Johnson Matthey PGM Market Report February 2020, 2020.

[3] Y. Ding, S. Zhang, B. Liu, H. Zheng, C. chi Chang, C. Ekberg, Recovery of precious metals from electronic waste and spent catalysts: A review, *Resour. Conserv. Recycl*. 141 (2019) 284–298.

[4] H. Dong, J. Zhao, J. Chen, Y. Wu, B. Li, Recovery of platinum group metals from spent catalysts: A review, *Int. J. Miner. Process*. 145 (2015) 108–113.

[5] C. Simonnet, A. Grandjean, J. Phalippou, Electrical behavior of platinum-group metals in glass-forming oxide melts, *J. Nucl. Mater*. 336 (2005) 243–250.

[6] B. Fischer, a. Behrends, D. Freund, D.F. Lupton, J. Merker, High-temperature mechanical properties of the platinum group metals, *Platin. Met. Rev*. 43 (1999) 18–20.

[7] C.A. Krier, R.I. Jaffee, Oxidation of the platinum-group metals, *J. Less-Common Met*. 5 (1963) 411–431.

[8] K. Kusada, D. Wu, H. Kitagawa, New Aspects of Platinum Group Metal-Based Solid-Solution Alloy Nanoparticles: Binary to High-Entropy Alloys, *Chem.–A Eur. J*. (2019).

[9] L. Bloxham, S. Brown, L. Cole, A. Cowley, P. Duncan, M. Fujita, J. Jiang, J. Li, O. Meara, R. Raithatha, E. Zadoff, Platinum 2013 Interim Review, *Platin. Met. Rev*. 57 (2013) 215–216.

[10] K. Pollmann, S. Kutschke, S. Matys, J. Raff, G. Hlawacek, F.L. Lederer, Bio-recycling of metals: Recycling of technical products using biological applications, *Biotechnol. Adv*. 36 (2018) 1048–1062.

[11] T. Makino, S. Nagai, F. Iskandar, K. Okuyama, T. Ogi, Recovery and Recycling of Tungsten by Alkaline Leaching of Scrap and Charged Amino Group Assisted Precipitation, *ACS Sustain. Chem. Eng*. 6 (2018) 4246–4252.

[12] A. Porvali, B.P. Wilson, M. Lundström, Lanthanide-alkali double sulfate precipitation from strong sulfuric acid NiMH battery waste leachate, *Waste Manag*. 71 (2018) 381–389.

[13] S. Gámez, K. Garcés, E. de la Torre, A. Guevara, Precious metals recovery from waste printed circuit boards using thiosulfate leaching and ion exchange resin, *Hydrometallurgy*. 186 (2019) 1–11.

[14] B. Padh, P.C. Rout, G.K. Mishra, K.R. Suresh, B. Ramachandra Reddy, Recovery of nickel and molybdate from ammoniacal leach liquors of spent HDS catalysts using chelating ion exchange resin, *Hydrometallurgy*. 184 (2019) 88–94.

[15] Z. Li, Z. Zhang, S. Smolders, X. Li, S. Raiguel, E. Nies, D.E. De Vos, K. Binnemans, Enhancing Metal Separations by Liquid–Liquid Extraction Using Polar Solvents, *Chem. - A Eur. J*. 25 (2019) 9197–9201.

[16] Z. Li, B. Onghena, X. Li, Z. Zhang, K. Binnemans, Enhancing Metal Separations Using Hydrophilic Ionic Liquids and Analogues as Complexing Agents in the More Polar Phase of

Liquid-Liquid Extraction Systems, *Ind. Eng. Chem. Res*. 58 (2019) 15628–15636.

[17] S. Sobekova Foltova, T. Vander Hoogerstraete, D. Banerjee, K. Binnemans, Samarium/cobalt separation by solvent extraction with undiluted quaternary ammonium ionic liquids, *Sep. Purif. Technol*. 210 (2019) 209–218.

[18] X. Li, Y. Mo, W. Qing, S. Shao, C.Y. Tang, J. Li, Membrane-based technologies for lithium recovery from water lithium resources: A review, *J. Memb. Sci*. 591 (2019) 117317.

[19] W. Yoshida, Y. Baba, F. Kubota, S.D. Kolev, M. Goto, Selective transport of scandium(III) across polymer inclusion membranes with improved stability which contain an amic acid carrier, *J. Memb. Sci*. 572 (2019) 291–299.

[20] F. Kubota, R. Kono, W. Yoshida, M. Sharaf, S.D. Kolev, M. Goto, Recovery of gold ions from discarded mobile phone leachate by solvent extraction and polymer inclusion membrane (PIM) based separation using an amic acid extractant, *Sep. Purif. Technol*. 214 (2019) 156–161.

[21] C.F. Croft, M.I.G.S. Almeida, R.W. Cattrall, S.D. Kolev, Separation of lanthanum(III), gadolinium(III) and ytterbium(III) from sulfuric acid solutions by using a polymer inclusion membrane, *J. Memb. Sci*. 545 (2018) 259–265.

[22] M.R. Yaftian, M.I.G.S. Almeida, R.W. Cattrall, S.D. Kolev, Selective extraction of vanadium(V) from sulfate solutions into a polymer inclusion membrane composed of poly(vinylidenefluoride-co-hexafluoropropylene) and Cyphos® IL 101, *J. Memb. Sci*. 545 (2018) 57–65.

[23] M.I.G.S. Almeida, R.W. Cattrall, S.D. Kolev, Polymer inclusion membranes (PIMs) in chemical analysis - A review, *Anal. Chim. Acta*. 987 (2017) 1–14.

[24] C. Fontàs, R. Tayeb, S. Tingry, M. Hidalgo, P. Seta, Transport of platinum(IV) through supported liquid membrane (SLM) and polymeric plasticized membrane (PPM), *J. Memb. Sci*. 263 (2005) 96–102.

[25] C. Fontàs, R. Tayeb, M. Dhahbi, E. Gaudichet, F. Thominette, P. Roy, K. Steenkeste, M.P. Fontaine-Aupart, S. Tingry, E. Tronel-Peyroz, P. Seta, Polymer inclusion membranes: The concept of fixed sites membrane revised, *J. Memb. Sci*. 290 (2007) 62–72.

[26] B. Pospiech, Highly efficient facilitated membrane transport of palladium(II) ions from hydrochloric acid solutions through plasticizer membranes with cyanex 471X, P*hysicochem. Probl. Miner. Process*. 51 (2015) 281–291.

[27] M. Regel-Rosocka, M. Rzelewska, M. Baczynska, M. Janus, M. Wisniewski, Removal of palladium(II) from aqueous chloride solutions with cyphos phosphonium ionic liquids as metal ion carriers for liquid-liquid extraction and transport across polymer inclusion membranes, *Physicochem. Probl. Miner. Process*. 51 (2015) 621–631.

[28] B. Pospiech, Facilitated transport of palladium(II) across polymer inclusion membrane with ammonium ionic liquid as effective carrier, *Chem. Pap*. 72 (2018) 301–308.

[29] H. Renner, G. Schlamp, I. Kleinwächter, E. Drost, H.M. Lüschow, P. Tews, P. Panster, M. Diehl, J. Lang, T. Kreuzer, A. Knödler, K.A. Starz, K. Dermann, J. Rothaut, R. Drieselmann, C. Peter, R.

Schiele, J. Coombes, M. Hosford, D.F. Lupton, Platinum Group Metals and Compounds, *Ullmann's Encycl. Ind. Chem*. (2018) 1–73.

[30] M.L. Firmansyah, F. Kubota, W. Yoshida, M. Goto, Application of a Novel Phosphonium-Based Ionic Liquid to the Separation of Platinum Group Metals from Automobile Catalyst Leach Liquor, *Ind. Eng. Chem. Res*. 58 (2019) 3845–3852.

[31] M.L. Firmansyah, F. Kubota, M. Goto, Selective recovery of platinum group metals from spent automotive catalysts by leaching and solvent extraction, *J. Chem. Eng. Japan*. 52 (2019) 835–842.

[32] M.L. Firmansyah, F. Kubota, M. Goto, Solvent extraction of Pt(IV), Pd(II), and Rh(III) with the ionic liquid trioctyl(dodecyl) phosphonium chloride, *J. Chem. Technol. Biotechnol*. 93 (2018) 1714–1721.

[33] A.T.N. Fajar, F. Kubota, M.L. Firmansyah, M. Goto, Separation of Pallaium(II) an Rhoium(III) Using a Polymer Inclusion Membrane Containing a Phosphonium-Base Ionic Liqui Carrier, *Ind. Eng. Chem. Res*. 58 (2019) 22334–22342.

[34] G. Levitin, G. Schmuckler, Solvent extraction of rhodium chloride from aqueous solutions and its separation from palladium and platinum, *React. Funct. Polym*. 54 (2003) 149–154.

[35] L. Svecova, N. Papaiconomou, I. Billard, Quantitative extraction of Rh(III) using ionic liquids and its simple separation from Pd(II), *Dalt. Trans*. 45 (2016) 15162–15169.

[36] A. Majavu, Z.R. Tshentu, Separation of rhodium(III) and iridium(IV) chlorido species by quaternary diammonium centres hosted on silica microparticles, *South African J. Chem. Eng*. 24 (2017) 82–94.

[37] L. Svecova, N. Papaïconomou, I. Billard, Rh(III) aqueous speciation with chloride as a driver for its extraction by phosphonium based ionic liquids, *Molecules*. 24 (2019).

[38] G. Kang, Y. Cao, Application and modification of poly(vinylidene fluoride) (PVDF) membranes – A review, *J. Memb. Sci*. 463 (2014) 145–165.

[39] C. Ribeiro, C.M. Costa, D.M. Correia, J. Nunes-Pereira, J. Oliveira, P. Martins, R. Gonçalves, V.F. Cardoso, S. Lanceros-Méndez, Electroactive poly(vinylidene fluoride)-based structures for advanced applications, Nat. Protoc. 13 (2018) 681. doi:10.1038/nprot.2017.157.

[40] M. Kamberi, D. Pinson, S. Pacetti, L.E.L. Perkins, S. Hossainy, H. Mori, R.J. Rapoza, F. Kolodgie, R. Virmani, Evaluation of chemical stability of polymers of XIENCE everolimus-eluting coronary stents in vivo by pyrolysis-gas chromatography/mass spectrometry, *J. Biomed. Mater. Res. Part B Appl. Biomater*. 106 (2018) 1721–1729.

[41] G.J. Ross, J.F. Watts, M.P. Hill, P. Morrissey, Surface modification of poly(vinylidene fluoride) by alkaline treatment: 1. The degradation mechanism, *Polymer*. 41 (2000) 1685–1696.

[42] S. Zhang, J. Shen, X. Qiu, D. Weng, W. Zhu, ESR and vibrational spectroscopy study on poly(vinylidene fluoride) membranes with alkaline treatment, *J. Power Sources*. 153 (2006) 234–238.

[43] X. Zhao, L. Song, J. Fu, P. Tang, F. Liu, Experimental and DFT investigation of surface

degradation of polyvinylidene fluoride membrane in alkaline solution, *Surf. Sci*. 605 (2011) 1005–1015.

[44] T. Kakoi, N. Horinouchi, M. Goto, F. Nakashio, Selective recovery of palladium from a simulated industrial waste water by liquid surfactant membrane process, *J. Memb. Sci*. 118 (1996) 63–71.

[45] T. Kakoi, M. Goto, F. Nakashio, Separation of platinum and palladium by liquid surfactant membranes utilizing a novel bi-functional surfactant, *J. Memb. Sci*. 120 (1996) 77–88.

[46] A. Dakshinamoorthy, P.S. Dhami, P.W. Naik, N.L. Dudwadkar, S.K. Munshi, P.K. Dey, V. Venugopal, Separation of palladium from high level liquid waste of PUREX origin by solvent extraction and precipitation methods using oximes, *Desalination*. 232 (2008) 26–36.

[47] S.J. Al-Bazi, A. Chow, Extraction of Platinum and Its Separation from Palladium by Polyurethane Foam, *Anal. Chem*. 55 (1983) 1094–1098.

[48] P.H. van Wyk, W.J. Gerber, K.R. Koch, A robust method for speciation, separation and photometric characterization of all [PtCl6-nBrn]2- (n=0-6) and [PtCl4-nBrn]2- (n=0-4) complex anions by means of ion-pairing RP-HPLC coupled to ICP-MS/OES, validated by high resolution 195Pt NMR spectroscopy, *Anal. Chim. Acta*. 704 (2011) 154–161.

[49] M. V. Tran, T.T. Doan, P.N. Duong, M.L.P. Le, T.P.T. Nguyen, Electrochemical Behavior and Morphology of Nano Catalyst for Fuel Cell: The effect of Ultrasonic and Microwave Techniques, *ECS Trans*. 50 (2013) 2001–2008.

[50] C.J. Le Roux, P. Gans, R.J. Kriek, Complexation of palladium(II) with thiocyanate - A spectrophotometric investigation, *J. Coord. Chem*. 67 (2014) 1520–1529.

[51] K. Ha, Refinement of crystal structure of potassium tetrakis-(thiocyanato-κS)palladate(II),K2Pd[SCN]4, *Zeitschrift Fur Krist. - New Cryst. Struct*. 225 (2010) 619–620.

[52] T.G. Roy, S.K.S. Hazari, K.K. Barua, D. Il Kim, Y.C. Park, E.R.T. Tiekink, Syntheses, characterization and anti-microbial activities of palladium(II) and palladium(IV) complexes of 3,10-C-meso-Me8[14]diene (L1) and its reduced isomeric anes (LA, LB and LC). Crystal and molecular structure of $[PdL_1][Pd(SCN)_4]$, *Appl. Organomet. Chem*. 22 (2008) 637–646.

Appendix B. Supporting Information

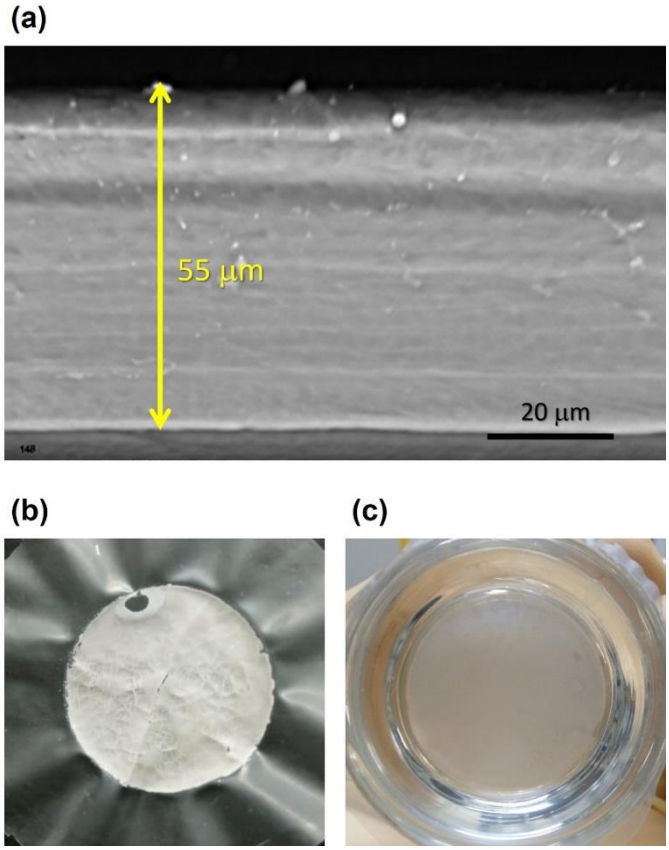

Figure S3.1. (a) SEM image of the membrane cross-section (PIM thickness: 55 µm); photograph of the PIMs after transport operations with different receiving solutions: (a) $NaClO_4$ 0.1 M and (b) $NaClO_4$ 0.1 M in HCl 1 M.

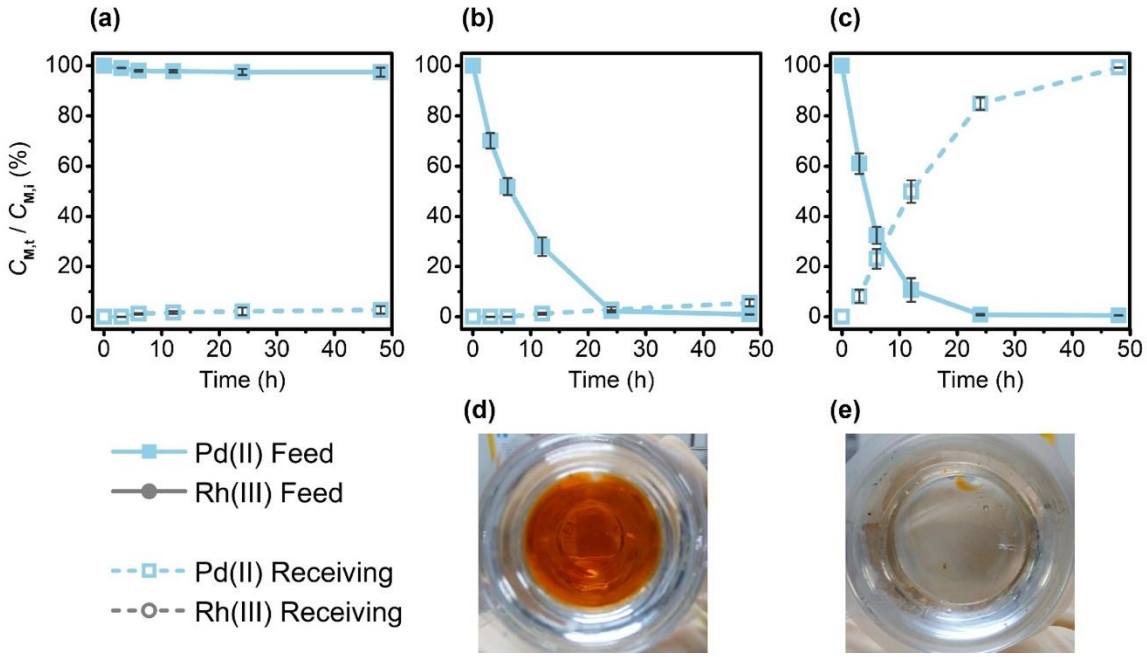

Figure S3.2. Transport behavior of Pd(II) with different receiving solutions: (a) thiourea 10 mM in HCl 1 M, (b) KSCN 0.1 M, (c) a mixture of thiourea 10 mM and KSCN 0.1 M in HCl 1 M; Photograph (d) and (e) were the membrane color after transport operation of the experiment (b) and (c), respectively. Prior to the transport operation, 0.5 mL of $NaClO_4$ 0.1 M was added to the Pd(II) 50 ppm feed solution.

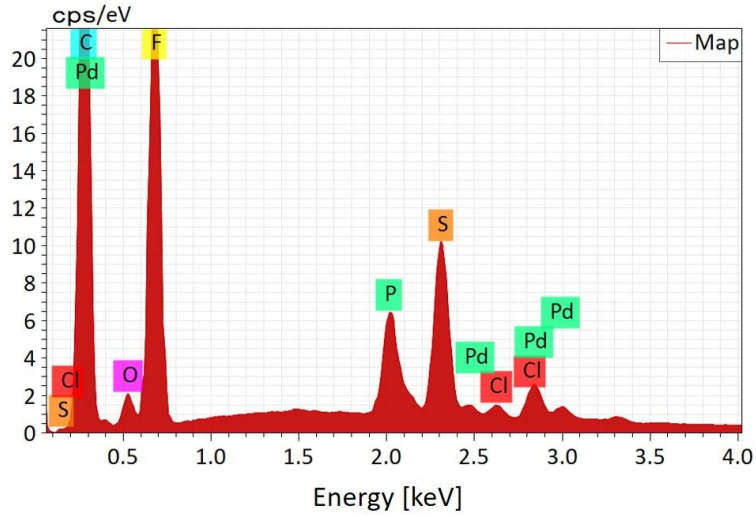

Figure S3.3. EDX elements analysis of the PIM after transport operation with receiving solution of KSCN 0.1 M (the photograph was shown in Figure S3.2(d)).

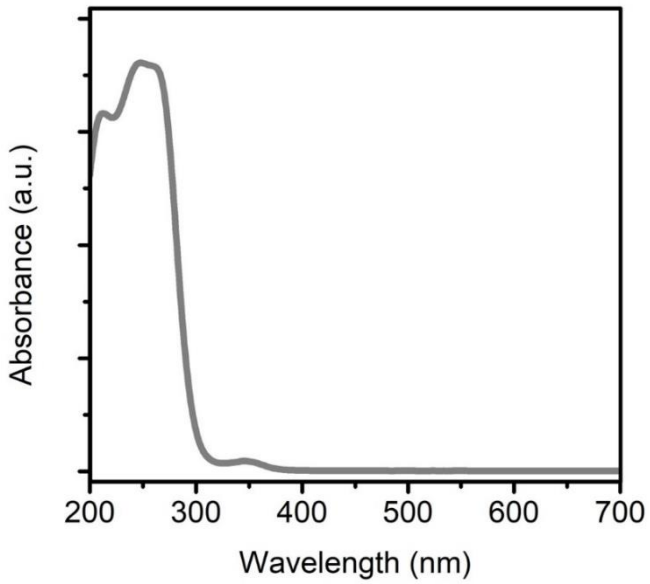

Figure S3.4. UV-Vis spectra of a mixture of thiourea 10 mM and KSCN 0.1 M in HCl 1 M.

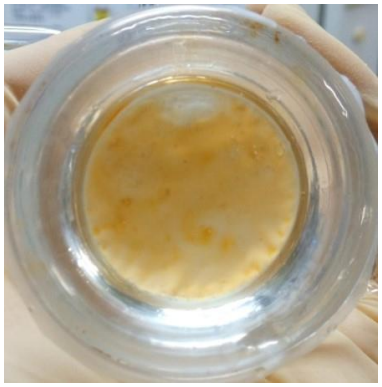

Figure S3.5. Photograph of the PIM after a continuous transport operation over a 4-week period. The PIM showed a mass loss of 6.2 ± 0.5 mg from a total mass of 121 ± 1 mg. Phosphorous leakage into aqueous phase was not detected in ICP-OES measurements.

~ End of Chapter 3 ~

CHAPTER 4. RECOVERY OF PLATINUM GROUP METALS FROM A SPENT AUTOMOTIVE CATALYST USING POLYMER INCLUSION MEMBRANES CONTAINING AN IONIC LIQUID CARRIER

Abstract:

Spent automotive catalysts (SACs) are the most abundant secondary source of platinum group metals (PGMs), but the recycling of these materials is quite challenging. In the present study, we assessed the recovery of Pt, Pd, and Rh from a SAC leachate solution using polymer inclusion membranes (PIMs) containing the ionic liquid trioctyl(dodecyl) phosphonium chloride ($P_{88812}Cl$). After pretreatment of the SAC using a reducing agent, metals could be extracted using relatively dilute acid solutions. The selective transport of PGMs from such solutions was demonstrated with two types of membranes having the same chemical composition: an isotropic dense membrane (ID-PIM) and an anisotropic porous membrane (AP-PIM). Using the ID-PIM, more than 90% of Pt and Pd in the SAC extraction solutions could be recovered with remarkably high purity. In contrast, the AP-PIM could recover Pt, Pd, and Rh in reasonable yields and purities with dramatically faster transport kinetics. Both membrane types demonstrated excellent durability with no loss of carrier molecules over a 10-day exposure to various harsh chemicals.

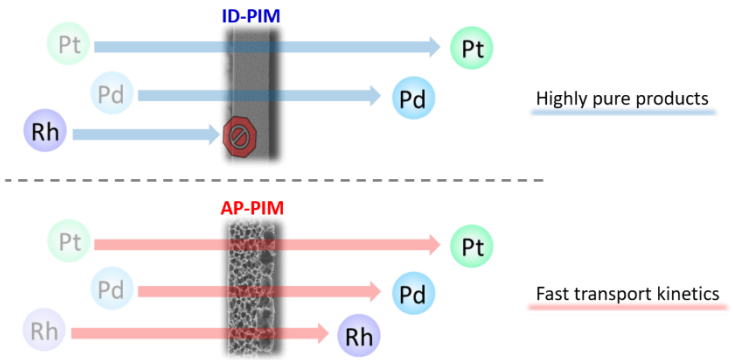

Remark:

This chapter was published in *Journal of Membrane Science*, 2021, 629, 119296. Reproduced with permission. Copyright 2021 Elsevier.

4.1 Introduction

The quantity of platinum group metals (PGMs) used by the automotive and electronic industries is predicted to continuously increase in the future [1]. However, the amounts of PGMs such as platinum (Pt), palladium (Pd), and rhodium (Rh) that are available in the Earth's crust are, of course, limited. The high demand for these metals is primarily the result of their use in automotive exhaust treatment catalysts. As an example, approximately 35% of the Pt and 80% of the Pd and Rh out of the annual gross demand for PGMs are allocated to the manufacture of automotive catalysts [2]. These catalysts have been continuously employed to reduce vehicle emissions since they were first introduced in the 1970s [3]. As such, spent automotive catalysts (SACs) are currently a plentiful secondary source of PGMs. In fact, the concentration of PGMs in SACs (approximately 0.5 wt%) [4] is much higher than that in the primary ores (approximately 0.001 wt%) [5]. Therefore, the recycling of PGMs from automotive catalyst waste could potentially address the scarcity of these metals and may also be economically feasible. Furthermore, the recovery of PGMs from SACs is beneficial from an environmental viewpoint, because it prevents the disposal of harmful materials in landfills and also decreases the necessity for exploring new mining sites.

The characteristics of a given waste material will affect the efficiency of the metal recycling process. Automotive catalysts are typically manufactured with a honeycomb structure that contains cordierite ($2MgO{\cdot}2Al_2O_3{\cdot}5SiO_2$) coated with gamma-alumina (γ-Al_2O_3), active metals (Pt, Pd or Rh), and certain additives (Ce, Zr, La, Ni, Fe, and various alkaline earth metals) [6]. In the as-prepared catalysts, the PGMs are presented in the metallic state, typically as a result of the hydrogen reduction of their chloro-complex precursors [7]. However, as the catalyst is exposed to exhaust gases, the surfaces of the metallic particles are gradually converted into oxides such as PtO_2, PdO, and Rh_2O_3 due to the high temperature of the gases [8]. Unfortunately, the extraction of PGMs (which are essentially inert elements) in their oxide

forms is quite challenging. Highly concentrated acids combined with oxidant additives are usually employed to leach PGMs along with the other metals from SACs, to obtain aqueous solutions [9]. Subsequently, the PGMs must be separated from the other metals and then into individual pure PGMs. The latter is also a challenging task because PGMs possess similar physical and chemical properties.

Previously, our group has attempted to address the challenges associated with PGM recycling by developing trioctyl(dodecyl) phosphonium chloride ($P_{88812}Cl$), a novel ionic liquid, as an effective extractant for Pt(IV), Pd(II), and Rh(III) from SAC leachates [4]. To develop greener, less-expensive systems for using this material, we have recently incorporated $P_{88812}Cl$ into polymer inclusion membranes (PIMs) by mixing the ionic liquid with a polymer base and plasticizer. The effects of the PIM composition and various experimental conditions on the separation of Pd(II) and Rh(III) chloride solutions were examined [10]. Subsequently, we applied an optimized membrane to the separation of PGMs into pure Pt(IV), Pd(II), and Rh(III) through sequential transport operations [11]. The excellent transport performance of this PIM is attributed to the ability of the $P_{88812}Cl$ ionic liquid to function as a metal carrier. In the present study, we employed this same PIM technology to recover PGMs from actual automotive catalyst waste. Studies concerning PIMs have often focused on the development of carriers, the selection of appropriate polymer bases, and the optimization of membrane compositions [12,13]. Admittedly, the carrier is an essential factor determining the performance of the PIM, because these membranes are based on a facilitated transport mechanism. Nevertheless, when a suitable carrier has been established, the effects of physical factors such as the membrane morphology must be investigated, as these can also play important roles in determining the surface properties, the possible location of the carrier, and stability.

Herein, we report the selective recovery of Pt(IV), Pd(II), and Rh(III) from a SAC leachate solution using PIMs containing $P_{88812}Cl$. This process was based on selecting the optimal PGM

leaching technique so as to provide solutions that promoted membrane transport. The separation of PGMs from other leached metals was carried out sequentially in a one-pot transport system to generate individual solutions for each target metal, without replacing the membrane. In addition, we also compared the transport behaviors of two different PIMs with the same composition but different morphologies: isotropic dense and anisotropic porous. To the best of our knowledge, this is the first report concerning the use of PIM technology to recover PGMs from a SAC as well as the first direct comparison of PIM morphologies.

4.2 Experimental

4.2.1 Materials

The SAC was supplied by the Seishin Enterprise Co., Ltd. from its Hibiki factory in Kitakyushu, Japan, in the form of a fine powder (Figure S4.1, Appendix C). The $P_{88812}Cl$ (98%) used as the extractant was provided by the Nippon Chemical Industrial Co., Ltd. (Tokyo, Japan). Nitric acid (HNO_3, 60%), thiourea ($SC(NH_2)_2$, 98%), and tetrahydrofuran (THF, 99.5%) were purchased from Wako Pure Chemical, Ltd., and 2-nitrophenyloctyl ether (2NPOE, 99%) was purchased from Dojindo Laboratories. Poly(vinylidene fluoride-*co*-hexafluoropropylene) (PVDF-*co*-HFP) was purchased from Sigma-Aldrich, and formic acid (HCOOH, 98%), hydrochloric acid (HCl, 32%), sodium perchlorate ($NaClO_4$, 98%), potassium thiocyanate (KSCN, 99.5%), ammonium chloride (NH_4Cl, 99%), sodium sulfite (Na_2SO_3, 97%), and *N*,*N*-dimethylacetamide (DMAc, 99%) were purchased from the Kishida Co., Ltd. All the aqueous solutions used in this work were prepared in deionized water (Milli-Q, Merck Millipore).

4.2.2 Leaching of spent automotive catalyst

The SAC powder was pre-treated before the leaching using a modified version of a procedure previously reported by Trinh et al. [8]. In this process, a quantity of the SAC (5 g) was dispersed in a 20 vol% HCOOH solution (100 mL) in a round-bottom flask followed by

vigorous stirring under reflux at 60 °C for 24 h. The liquid and solid were subsequently separated by centrifugation followed by decantation. The solid pre-treated SAC was then subjected to a leaching process.

Leaching was performed by dispersing the pre-treated SAC in a 2 M HCl solution (100 mL) in a round-bottom flask. This mixture was stirred under reflux at 70 °C for 48 h, after which the leachate solution and the solid SAC residue were separated by filtration. The metal concentration in the leachate was determined using inductively coupled plasma optical emission spectrometry (ICP-OES; Optima 8300, PerkinElmer). For comparison purposes, leaching trials following the same procedure but without the pre-treatment step were carried out, using 2 and 5 M HCl. The leaching efficiency was calculated by determining the initial PGM concentrations in the SAC sample following digestion in aqua regia (see Appendix C).

4.2.3 Preparation of polymer inclusion membranes

Two types of PIM were prepared in this study: isotropic dense (ID-PIM) and anisotropic porous (AP-PIM). The ID-PIMs were prepared using a procedure previously reported by our group [10,11]. In this process, the polymer base (PVDF-*co*-HFP, 40 wt%), plasticizer (2NPOE, 10 wt%), and carrier ($P_{88812}Cl$, 40 wt%) were combined to give a total mass of 400 mg and then dissolved in 10 mL of THF and stirred at 40 °C until a homogenous solution was obtained. This solution was poured into a glass ring with a diameter of 7.5 cm, positioned on top of a flat glass plate. The glass ring was covered with filter paper and a watch glass to enable the THF to slowly evaporate over the course of 1 day. After the THF had evaporated completely, the membrane was carefully separated from the glass plate.

The AP-PIMs were prepared using a combination of dual solvent casting and nonsolvent induced phase separation (NIPS). The PIM components were combined in the same ratio as used to produce the ID-PIMs to give a total mass of 200 mg, then dissolved in 2 mL of THF and stirred at 50 °C for 1 h. A 0.5 mL quantity of DMAc was then added to the solution with

further stirring at room temperature for 15 min. The solution was subsequently poured into the same type of glass ring as used to produce the ID-PIMs. A filter paper was positioned on top of the glass ring to allow moderately rapid evaporation of the solvents over a time span of 3 h. Following this, the newly formed membrane (still in the glass plate) was carefully immersed in a room temperature water bath adjusted to a pH of 4 using HCl and allowed to soak for 24 h. The membrane was separated from the glass plate and subsequently dried at room temperature for another 24 h.

4.2.4 Membrane transport trials

The transport assessments of each membrane were carried out in an apparatus comprising two water-jacketed glass chambers. Each PIM sample was cut into a circular shape and then clamped in a flange between the two glass chambers that separated the feed and receiving solutions, after which each chamber was filled with 50 mL of the corresponding solutions. The effective surface area of the membrane in contact with each solution was 4.9×10^{-4} m^2 (equivalent to a diameter of 2.5 cm). During each transport experiment, the solution in each chamber was stirred using a magnetic stir bar. The temperatures of the chambers were kept constant by continuously circulating water through the jackets using a water bath with a temperature controller (EYELA NCB- 1200). All trials were performed at 25 °C unless stated otherwise. At specific intervals, 0.5 mL aliquots were taken from both chambers for analysis of the metal concentrations by ICP-OES. Each time, the chambers were replenished with an equal amount of fresh solution.

Assuming that the transport kinetics corresponded to a first-order process, the rate constant (k, h^{-1}), permeability coefficient (P, m h^{-1}), and initial flux (J_0, mmol m^{-2} h^{-1}) were calculated using equations (4.1) – (4.3).

$$ln\left(\frac{C_{M,t}^{F}}{C_{M,i}^{F}}\right) = -kt \qquad (4.1)$$

$$P = \left(\frac{V}{A}\right) k \qquad (4.2)$$

$$J_0 = P C_{M,i}^F \qquad (4.3)$$

Where $C_{M,t}^F$ is the concentration of metal *M* (mol m^{-3}) in the feed solution at time *t*, $C_{M,i}^F$ is the initial concentration of metal *M* (mol m^{-3}) in the feed solution at the start of the trial, *t* is the time interval at which the sample is taken (h), *V* is the volume of the feed solution (m^3), and *A* is the effective surface area of the membrane (m^2). In addition, the recovery factor (*RF*, %) and purity (%) of the transported metals were calculated using equations (4.4) – (4.5).

$$RF = \left(\frac{C_{M,t}^R}{C_{M,i}^F}\right) \times 100\% \qquad (4.4)$$

$$Purity = \left(\frac{C_{M,t}^R}{C_{Mtot,t}^F}\right) \times 100\% \qquad (4.5)$$

where $C_{M,t}^R$ is the concentration of metal *M* (mol m^{-3}) transported into the receiving solution at time *t* and $C_{Mtot,t}^R$ is the total concentration of metals transported into the receiving solution (mol m^{-3}).

Recovery of PGMs from the leachate was carried out sequentially with one target metal per transport sequence. The feed solution was the SAC leachate solution in 2 M HCl. The target for the first transport sequence was Pt(IV) and the receiving solution was 0.1 M $NaClO_4$ in 1 M HCl. The target for the second transport sequence was Pd(II) and the receiving solution was 10 mM thiourea and 0.1 M KSCN in 1 M HCl. The target for the third transport sequence was Rh(III) and the receiving solution was 4.9 M NH_4Cl in 0.1 M HCl. These receiving solutions were determined in our previous reports using pure solutions [11,14]. After each sequence was complete, the receiving solution was drained, and the chamber was washed three times with deionized water. The receiving chamber was then filled with the corresponding fresh solution. Prior to each sequence, the feed solution was analyzed using ICP-OES to determine the initial metal concentrations.

4.2.5 Characterizations and membrane stability test

Scanning electron microscopy (SEM) in conjunction with energy dispersive X-ray spectroscopy (EDX) (Hitachi SU3500) was used to observe the SAC particles as well as the PIM morphologies. The membrane compositions and thermal stabilities were examined by thermogravimetric analysis (TGA) (Hitachi TG/DTA7300). These TGA assessments were carried out with a ramp temperature of 10 °C/min over the range of 30–550 °C under nitrogen. The contact angles of water droplets (±10 μL) on the membranes were determined using an optical tensiometer (KRÜSS DSA25S), employing the sessile drop method and repeating each measurement ten times.

The stability tests examined the resistance of each membrane to various chemicals i.e. 5 M HCl, 1 M $NaClO_4$, 1 M thiourea + 1 M KSCN, and 5 M NH_4Cl. In each experiment, a small portion of the PIM having a mass of 100 mg was immersed in 50 mL of each solution in a glass container that was subsequently agitated at 60 rpm in a water bath shaker (EYELA NTS-4000BH) at 25 °C for 10 days. The mass of the membrane before and after this treatment was determined using an analytical balance (Sartorius CPA225D), while any leaching out of the $P_{88812}Cl$ from the membrane was monitored by determining the phosphorous (P) concentration in the solution using ICP-OES. Attenuated total reflectance Fourier transform infrared spectroscopy (ATR-FTIR; PerkinElmer) was employed to acquire spectra from the membranes. Each spectrum was obtained by summing eight scans at a resolution of 2 cm^{-1}.

4.3 Results and Discussion

4.3.1 Preparation of leachate solution

Figure 4.1 presents an SEM image of the SAC particles together with representative elemental maps obtained via EDX. The particle size of this material was sufficiently small (≤ 20 μm) to allow for effective extraction of metals. The elemental mapping images indicate that

aluminum (Al) and oxygen (O) were present over the entire surfaces of the particles, which was expected because the main components of automotive catalysts are cordierite and gamma-alumina. The abundance of oxygen (O) also suggests that the metals in the SAC sample were mainly in their oxide forms. However, Pt could be observed only in certain particles, showing that the distribution of PGMs throughout the sample was not homogenous.

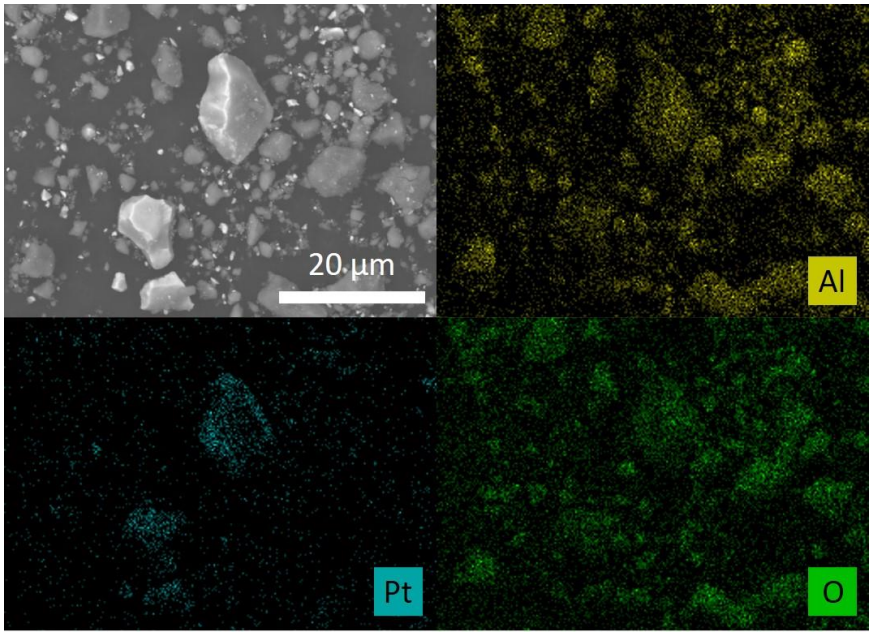

Figure 4.1. An SEM image and representative EDX elemental maps of SAC particles.

As noted, prior to the leaching process, the SAC specimens were pretreated with HCOOH to remove oxide layers on the PGMs, as described in equations (4.6) – (4.8) [8,15].

$$PtO_2 + 2HCOOH \longrightarrow Pt + 2H_2O + 2CO_2, \quad (4.6)$$

$$PdO + HCOOH \longrightarrow Pd + H_2O + CO_2 \quad (4.7)$$

$$Rh_2O_3 + 3HCOOH \longrightarrow 2Rh + 3H_2O + 3CO_2 \quad (4.8)$$

This pretreatment enabled effective extraction of the PGMs using relatively dilute HCl (2 M), which was preferable with regard to the subsequent membrane separation process. A comparison of PGM extractions from the SAC performed with and without this pretreatment as well as data providing the original PGM concentrations in the SAC are shown in Table S4.1 (Appendix C). The leaching efficiency of Pt, Pd, and Rh was 91, 96, and 93%, respectively.

The concentrations of all metals found in the leachate solution acquired using 2 M HCl with HCOOH pretreatment are summarized in Table 4.1. In addition to the PGMs, nine other metals were detected by ICP-OES with a wide range of concentrations, including rare earth metals (Ce and La), transition metals (Fe, Zn, Cu, Ni, and Zr), and main group metals (Mg and Al). This leachate solution was used as the feed solution in the membrane transport trials.

Table 4.1. Metal concentrations in the SAC leachate solution.

Metal	Pt	Pd	Rh	Fe	Zn	Cu	Ce	La	Ni	Zr	Mg	Al
C (ppm)	58.5	148	29.5	41.9	17.0	8.6	151	752	0.2	1.2	1668	6193

4.3.2 Preparation and characterizations of the PIMs

Both ID-PIMs and AP-PIMs were successfully prepared using a simple solvent casting method and a combination of dual solvent casting with the NIPS technique, respectively. Photographs of the as-prepared PIMs are presented in Figure S4.2 (Appendix C), and demonstrate that the visual appearances of the membranes were quite different. Specifically, the ID-PIMs were transparent whereas the AP-PIMs were white and opaque. Figure 4.2 shows cross-sectional SEM images of the membranes, from which it is evident that the two types had comparable thicknesses but very different morphologies. The ID-PIMs exhibited a dense, isotropic morphology with a thickness close to 63 μm, whereas the AP-PIMs showed an anisotropic, porous morphology with a thickness of approximately 72 μm. The polymer base used to make these membranes, PVDF-*co*-HFP, is a semi-crystalline polymer that can be precipitated via liquid-liquid demixing or solid-liquid demixing mechanisms during membrane preparation [16,17]. In the case of the ID-PIMs, the dense, isotropic structure indicated that the polymer precipitated evenly over the entire area of the membrane as a result of the solid-liquid demixing phenomenon associated with slow evaporation of the solvent. In this type of PIM, the carrier molecules were located in the amorphous regions or were phase-separated from the

polymer to form tortuous channels that facilitated metal extractions, as demonstrated by previous X-ray scattering analyses reported by Kolev and co-workers [18]. In contrast, the anisotropic and porous structure of the AP-PIMs suggested that the polymer had precipitated at different rates at the upper (the side in contact with air) and lower (the glass side) surfaces via liquid-liquid demixing. The exchange of the solvent and nonsolvent occurred more quickly at the top surface and more slowly at the lower surface [19], resulting in the formation of large pores and a surface skin with small pores, respectively (Figure S4.3, Appendix C). This type of porous membrane having an anisotropic morphology was studied by Chen and co-workers with regard to the rapid transport of Lu(III) [20,21]. In the present trials, the upper surface of the AP-PIM was positioned so as to be in contact with the receiving solution during each transport trial.

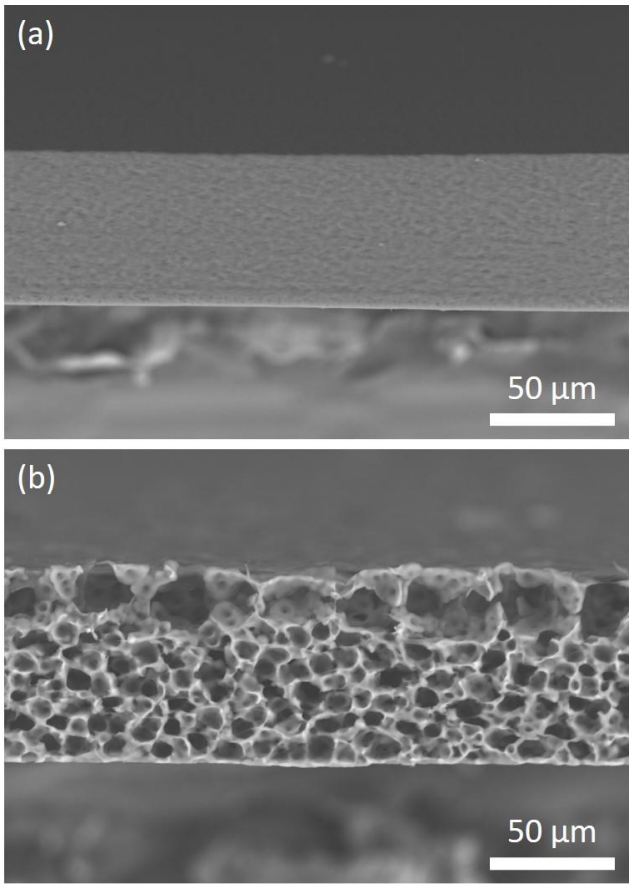

Figure 4.2. Cross-sectional SEM images of an (a) ID-PIM and (b) AP-PIM. The top and bottom surfaces in these images represent the air side and glass side during membrane preparation, respectively.

One of the main concerns in the preparation of PIMs using the NIPS method is the possibility of carrier loss during coagulation in the water bath. Thus, the compositions of the as-prepared membranes were investigated using TGA. Figure 4.3 provides the resulting thermal decomposition data obtained from the raw ingredients and from ID-PIM and AP-PIM specimens over the temperature range of 30–550 °C. The PVDF-*co*-HFP, $P_{88812}Cl$, and 2NPOE were found to begin to decompose at approximately 400, 320, and 175 °C, respectively. The TGA plots for the ID-PIM and AP-PIM specimens also reflect the thermal decomposition behavior of their components, as expected based on their PVDF-*co*-HFP:$P_{88812}Cl$:NPOE mass ratios of approximately 50:40:10. These results confirm that the ionic liquid carrier remained inside the AP-PIM during the coagulation step and that both types of membranes possessed the same chemical compositions.

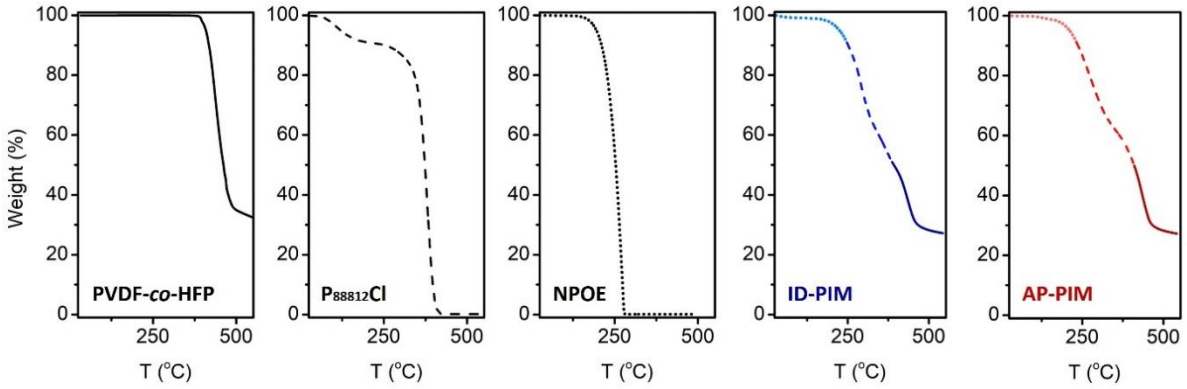

Figure 4.3. Thermal decomposition behaviors of the membrane components and of ID-PIM and AP-PIM specimens.

The effects of the different membrane morphologies on the surface properties of the membranes were studied by measuring water contact angles. As shown in Figure 4.4, the angles on the AP-PIM were higher than those on the ID-PIM. The wetting properties of PIM surfaces are directly related to the hydrophobicity of the membrane components [22]. However, in this case, the two types of membranes showed very different wetting properties despite having the same chemical compositions. Thus, the different wetting properties were attributed to the

varying morphologies, meaning that the rougher surface of the AP-PIM specimen was responsible for its higher water contact angles.

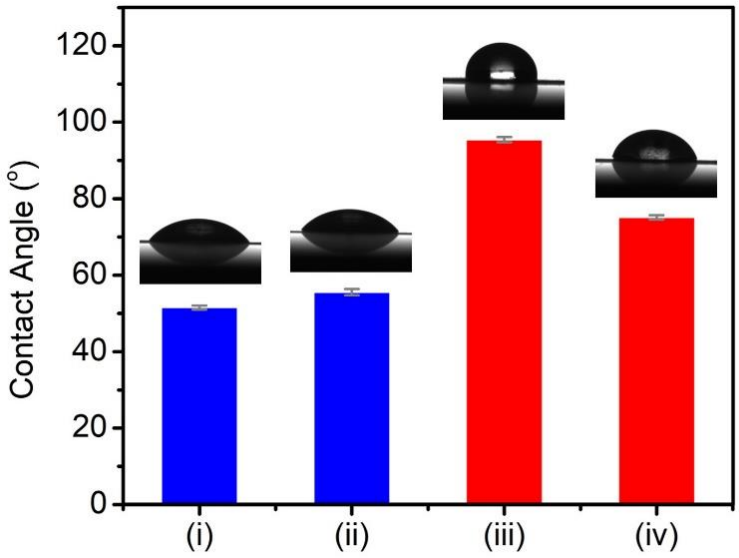

Figure 4.4. Water contact angles on the surfaces of the (i) ID-PIM top side, (ii) ID-PIM bottom side, (iii) AP-PIM top side, and (iv) AP-PIM bottom side.

4.3.3 Sequential membrane transport trials

In a previous solvent extraction study, it was found that $P_{88812}Cl$ was able to extract Pt(IV), Pd(II), and Rh(III) via an ion exchange mechanism, as described in equations (4.9) – (4.11) [23].

$$[PtCl_6]^{2-} + 2\left(P_{88812}{}^{+}Cl^{-}\right) \rightleftharpoons \left(P_{88812}{}^{+}\right)_2[PtCl_6]^{2-} + 2Cl^{-}, \quad (4.9)$$

$$[PdCl_4]^{2-} + 2\left(P_{88812}{}^{+}Cl^{-}\right) \rightleftharpoons \left(P_{88812}{}^{+}\right)_2[PdCl_4]^{2-} + 2Cl^{-} \quad (4.10)$$

$$[RhCl_5(H_2O)]^{2-} + 2\left(P_{88812}{}^{+}Cl^{-}\right) \rightleftharpoons \left(P_{88812}{}^{+}\right)_2[RhCl_5(H_2O)]^{2-} + 2Cl^{-} \quad (4.11)$$

When SAC leachate solutions were used as the feeds, PGMs and certain transition metals were extracted, while rare earth and main group metals were not [4,24]. The presence of transition metals, particularly Fe, in the leachate was expected to compete for uptake during recovery of the PGMs because this metal had an affinity for the receiving solutions. Therefore, Fe was removed before the transport trial through selective adsorption into the ID-PIM. The absorption

behavior and the metal concentrations after Fe removal are shown in Figure S4.4 and Table S4.2 (Appendix C). It should be noted that metals with concentrations of less than 1.5 ppm (in the present case: Fe, Ni, and Zr) were neglected when calculating the transport results for the sake of simplicity. The sequential migrations of Pt, Pd, and Rh were then carried out using the SAC leachate as the feed solution and appropriate receiving solutions for each target metal, based on the findings of our previous studies [10,11,14].

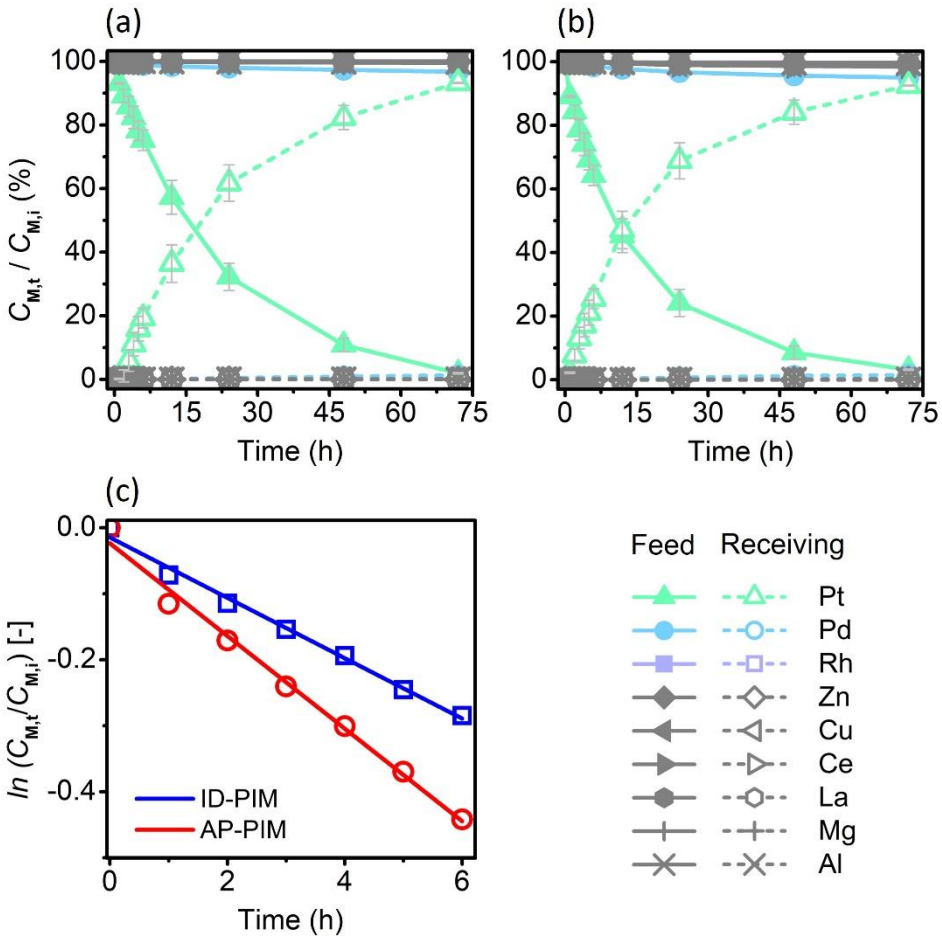

Figure 4.5. Data related to selective Pt(IV) transport from the SAC leachate solution through (a) ID-PIM and (b) AP-PIM specimens, and (c) kinetics plots for both processes. Receiving solution: 0.1 M $NaClO_4$ in 1 M HCl.

Selective Pt(IV) transport was carried out using 0.1 M $NaClO_4$ in 1 M HCl as the receiving solution for both the ID-PIMs and AP-PIMs. As shown in Figures 4.5(a) and (b), Pt(IV) was quantitatively transferred to the receiving solution after 3 days of operation using both types of

membrane. The associated kinetics plots (Figure 4.5 (c)) demonstrate that the AP-PIM data had a lower slope with a higher rate constant and initial flux compared with the ID-PIM (Table 4.2). However, the latter membrane generated a more pure product (93.2 %) relative to that obtained from the AP-PIM, with minimal levels of impurities in the receiving solution. Despite the similar *RF* values after 3 days, the Pt(IV) transport characteristics through the ID-PIM and AP-PIM were therefore somewhat different.

Table 4.2. Kinetics and other transport parameters for PGM recovery from the SAC leachate solution using ID-PIM and AP-PIM specimens.

Metal	Membrane	k (h^{-1})	J_0 (mmol m^{-2} h^{-1})	RF (%)	Purity (%)	Impurity (ppm)[1]
Pt	ID-PIM	0.046	1.34	93	93.2	n.a.
	AP-PIM	0.070	2.06	92	80.2	Pd (2), Mg (3), Al (7)
Pd	ID-PIM	0.079	10.52	93	99.7	n.a.
	AP-PIM	0.208	27.21	94	65.2	La (6), Mg (13), Al (47)
Rh	ID-PIM	n.a.	n.a.	n.a.	n.a.	n.a.
	AP-PIM	0.039	1.09	52	n.a.	Ce (2), Mg (3), Al (10)
	AP-PIM[2]	0.040	1.10	67	n.a.	Ce (2), Mg (3), Al (11)

n.a.: not available

[1]Impurities with concentrations of less than 1.5 ppm are not shown.

[2]This trial was performed at 35 °C.

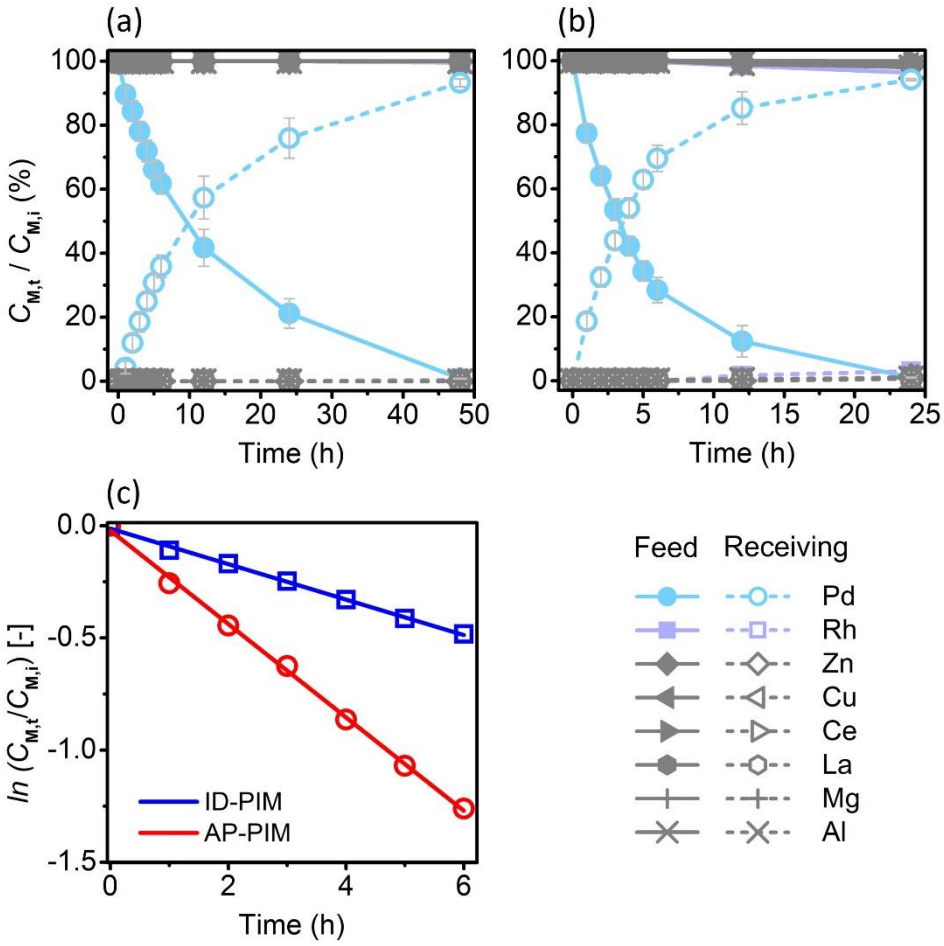

Figure 4.6. Data related to selective Pd(II) transport from the SAC leachate solution through (a) ID-PIM and (b) AP-PIM specimens, and (c) kinetics plots for both processes. Receiving solution: 10 mM thiourea and 0.1 M KSCN in 1 M HCl.

In the case of the Pd(II) transport data, the difference between the ID-PIM and AP-PIM could be observed more clearly. Using a receiving solution consisting of 10 mM thiourea and 0.1 M KSCN in 1 M HCl, quantitative transport of the Pd(II) in the original solution could be achieved after 2 days using the ID-PIM, whereas only 1 day was required with the AP-PIM (Figures 4.6(a) and (b)). The slope of the Pd(II) kinetics plot for the AP-PIM data was significantly lower than that of the ID-PIM data (Figure 4.6(c)), and the k and J_0 values for the former type of membrane were almost three times those for the latter (Table 4.2). However, the product purity obtained using the AP-PIM was lower and the receiving solution contained relatively high levels of La, Mg, and Al. These results showed that the performance of the AP-

PIM was better than that of the ID-PIM in terms of transport kinetics, which can possibly be attributed to the anisotropic, porous structure of the former. This porous morphology would increase the effective surface area in contact with the feed and receiving solutions and thus increase the probability that the metal species would reach carrier molecules on the membrane surface. This factor interplayed with the other driving forces such as concentration gradient and affinity to the carrier or the receiving solution would govern the rate constants. However, the ID-PIM demonstrated better performance in terms of product purity. Its dense structure likely tolerated a high concentration gradient between the feed and receiving solutions, resulting in higher transport selectivity.

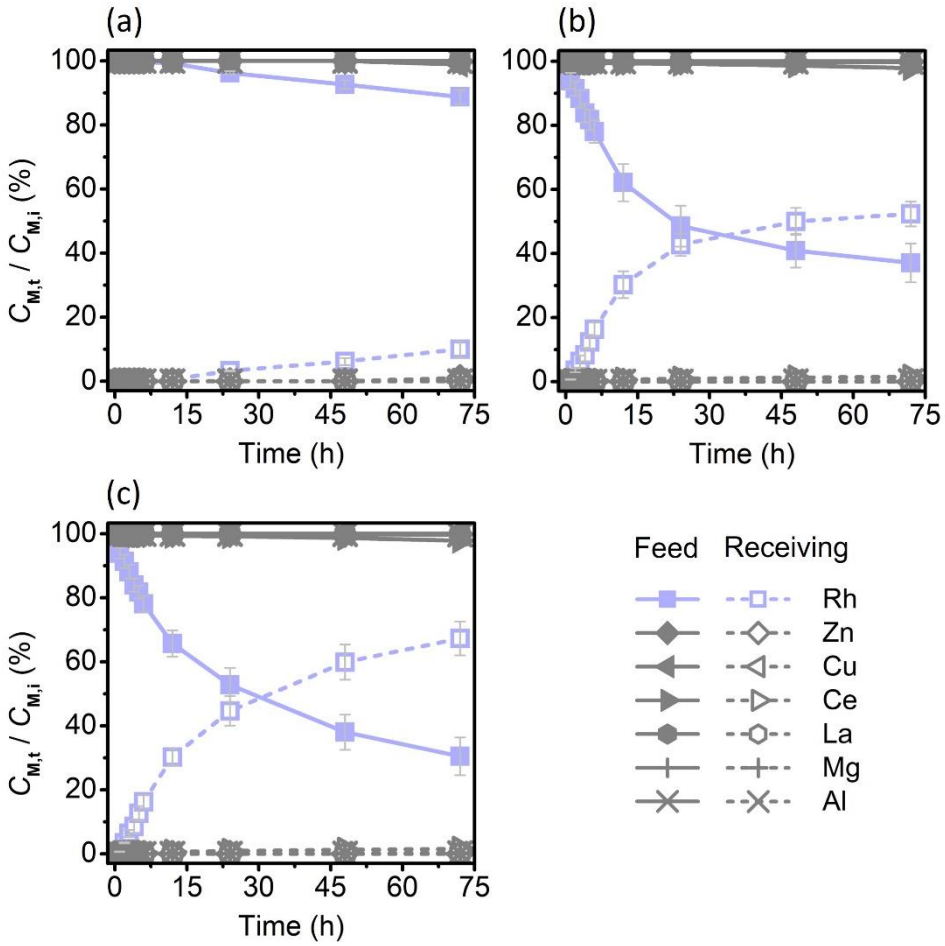

Figure 4.7. Selective Rh(III) transport from the SAC leachate solution through the (a) ID-PIM, (b) AP-PIM, and (c) AP-PIM at 35 ºC. Receiving solution: 4.9 M NH_4Cl in 0.1 M HCl.

In trials with Rh(III), very little was transported through the ID-PIM into a receiving solution consisting of 4.9 M NH_4Cl in 0.1 M HCl, even after 3 days of operation (Figure 4.7(a)). In previous work, Rh(III) could be transported through a dense PIM by decreasing the HCl concentration in the feed solution to 0.1 M and reducing the membrane thickness to less than 20 μm [14]. Unfortunately, leaching of the SAC was not possible using 0.1 M HCl, and this low thickness reduced the mechanical strength of the PIM. Using the AP-PIM, Rh(III) could be transported with an efficiency of approximately 50% after 3 days of operation (Figure 4.7(b)). The AP-PIM may have provided a greater concentration gradient (which provided the driving force for Rh(III) transport) together with a higher effective surface area compared with the ID-PIM, thus allowed the transport to occur. Even so, the AP-PIM also increased the concentrations of impurities in the receiving solution. Interestingly, Rh(III) transport through the AP-PIM could be improved to 67% (Figure 4.7(c) and Table 4.2) by increasing the operating temperature. Although not as effective as decreasing the HCl concentration, increasing the temperature increased the rate of hydration of $[RhCl_6]^{3-}$ ions, as described in equation (4.12) [25].

$$[RhCl_6]^{3-} + H_2O \rightleftharpoons [RhCl_5(H_2O)]^{2-} + Cl^- \qquad (4.12)$$

The extraction of $[RhCl_5(H_2O)]^{2-}$ by $P_{88812}Cl$ proceeds more readily than that of $[RhCl_6]^{3-}$ [23], and so the improved *RF* value at higher temperatures can presumably be ascribed to the greater availability of this extractable species in the feed solution. In addition, the dynamics of Rh(III) movement inside the PIM might also be improved with increases in temperature, assuming the fixed site jumping transport mechanism inside the membrane suggested by Li et al. [26].

4.3.4 Evaluation of membrane stability

The mechanical strengths of both the ID-PIM and AP-PIM were sufficient to enable easy handling and installation in the test apparatus. Because these membranes were not intended to operate under high pressure or gravitational force, the primary issue related to their use is their

resistance to various chemicals. To evaluate this resistance, small portions of each type of PIM were immersed in aqueous 5 M HCl, 1 M $NaClO_4$, 1 M thiourea + 1 M KSCN, and 5 M $NHClO_4$ solutions with continuous agitation for 10 days. These chemicals are representative of the feed and receiving solutions that might be encountered in practical applications, but were prepared at excessively high concentrations to exaggerate any deleterious effects. The membrane mass changes and the extent of leakage of the carrier from the membranes after these treatments are summarized in Figure S4.5 and Table S4.3 (Appendix C). The mass loss was relatively small for both the ID-PIM and AP-PIM, while the P concentrations in the solutions were less than 1 ppm for all the chemical treatments, indicating negligible loss of the ionic liquid.

Figure 4.8 shows the FTIR spectra obtained from the as-prepared membranes and from the specimens subjected to the stability tests. The as-prepared ID-PIM and AP-PIM generated similar spectra (Figure 4.8(a)), confirming that these membranes had the same compositions and chemical structures. Characteristic PVDF-*co*-HFP peaks are evident in the range of 500–1500 cm^{-1} in these spectra, whereas the C–H stretching, P–CH_2–R bending, C–C stretching, and P–C stretching peaks related to the $P_{88812}Cl$ can be seen at 2900, 1468, 1045 and 722 cm^{-1}, respectively. After the membranes were immersed in 5 M HCl (Figure 4.8(b)), the spectra of both types were relatively unchanged, demonstrating that these materials were resistant to a highly acidic environment. However, immersion in 1 M $NaClO_4$ (Figure 4.8(c)) altered the spectrum of the ID-PIM by removing the band in the range of 1170–1230 cm^{-1}, typically assigned to the C–F stretching vibration [27]. The fluoride moieties in the polymer base were evidently vulnerable to attack by ClO_4^- anions, in agreement with several prior studies [28–30]. Nevertheless, the partial damage to the polymer base did not lead to significant carrier leakage, because the characteristic ionic liquid peaks remained. The same result was obtained in previous research, which also determined that polymer damage could be suppressed by

adding HCl to the receiving solution [11]. Interestingly, the AP-PIM did not show a loss of the C–F band, which was possibly related to the reduced wetting properties of this membrane.

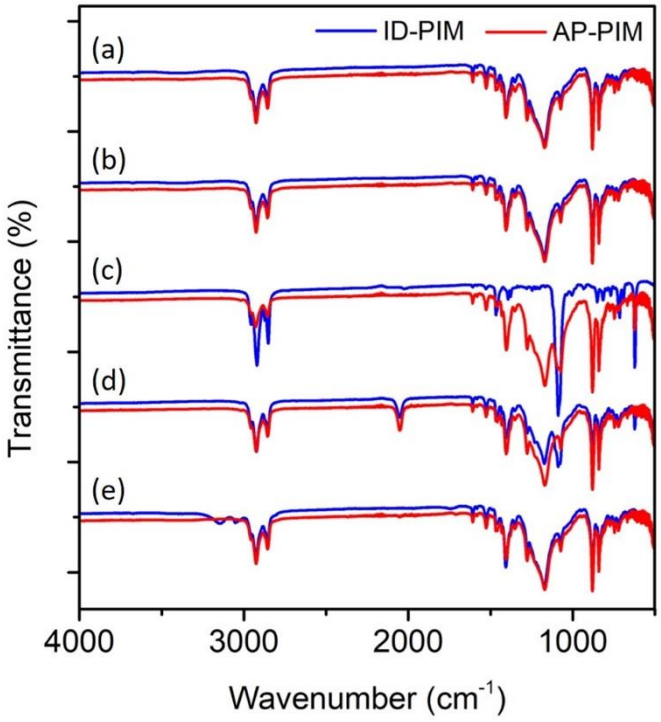

Figure 4.8. FTIR spectra obtained from the (a) as-prepared ID-PIM and AP-PIM, and from the membranes after being immersed in (b) 5 M HCl, (c) 1 M $NaClO_4$, (d) 1 M thiourea + 1 M KSCN, and (e) 5 M NH_4Cl for 10 days with constant shaking.

After being immersed in 1 M thiourea + 1 M KSCN, both membranes showed a new peak at 2109 cm^{-1} (Figure 4.8(d)) that was assigned to the S–C≡N stretching vibration. SCN^- ions from the KSCN were evidently trapped inside the membrane, either through ion exchange or simply adsorption. Nonetheless, despite the presence of these ions, the carrier was retained inside the PIM, because the characteristic peaks related to the ionic liquid remained unchanged. Following treatment with 5 M NH_4Cl, the ID-PIM generated a spectrum that was unchanged except for some small additional peaks in the range of 3100–3300 cm^{-1} that were assigned to N–H stretching vibrations (Figure 4.8(e)). Thus, a small quantity of NH_4^+ ions was absorbed into the ID-PIM. In the case of the AP-PIM, the spectrum was completely unchanged. These results established that both the ID-PIM and AP-PIM possessed remarkably good durability in

the presence of various harsh chemicals because the carrier molecules were not lost, although the AP-PIM showed slightly better chemical resistance. It should be noted that, in this study, the transport trials were carried out sequentially on the laboratory scale as a proof of concept to demonstrate the excellent performance of PIMs containing this ionic liquid with regard to the recovery of PGMs from a SAC. Nevertheless, for large scale applications, we would suggest using one dedicated membrane for each target metal to reduce unnecessary chemical exposures.

4.4 Conclusions

The recovery of PGMs from a SAC using two types of PIM containing the ionic liquid $P_{88812}Cl$ was demonstrated. The powdered SAC was pre-treated with HCOOH to allow extraction with a less concentrated acid (2 M HCl). A simple solvent casting method resulted in an isotropic, dense membrane (the ID-PIM), whereas a dual solvent process combined with the NIPS method gave an anisotropic, porous membrane (AP-PIM). The selective transport of Pt(IV) from the SAC leachate could be performed through both membranes with recoveries in excess of 90%. The ID-PIM transported Pd(II) to give a very high product purity of close to 100%, whereas the AP-PIM showed rapid transport kinetics (J_0 of 27.21 mmol m^{-2} h^{-1}). Rh(III) could not be transported using the ID-PIM but was found to migrate through the AP-PIM, which exhibited higher *RF* values at elevated temperatures. Both membranes were durable and withstood exposure to several harsh chemical treatments, although the AP-PIM showed slightly better endurance. PIMs containing an ionic liquid have significant potential as a greener and less expensive technology for PGM recycling. In the future development of more effective metal separation technologies, it would be beneficial to examine membrane transport modules with multiple receiving windows that can be operated simultaneously.

References

[1] D. Jasiński, J. Meredith, K. Kirwan, The life cycle impact for platinum group metals and lithium to 2070 via surplus cost potential, I*nt. J. Life Cycle Assess*. 23 (2018) 773–786.

[2] A. Cowley, Johnson Matthey PGM Market Report February, 2020.

[3] J. Kašpar, P. Fornasiero, N. Hickey, Automotive: catalytic converters current status, *Catal. Today*. 77 (2003) 419–449.

[4] M.L. Firmansyah, F. Kubota, M. Goto, Selective recovery of platinum group metals from spent automotive catalysts by leaching and solvent extraction, *J. Chem. Eng. Japan*. 52 (2019) 835–842.

[5] F.K. Crundwell, M.S. Moats, G. Robinson, G. William, Metallurgy of Nickel , Cobalt and Platinum-Group Metals, *Elsevier*, Oxford, 2011.

[6] D. Jimenez de Aberasturi, R. Pinedo, I. Ruiz de Larramendi, J.I. Ruiz de Larramendi, T. Rojo, Recovery by hydrometallurgical extraction of the platinum-group metals from car catalytic converters, *Miner. Eng*. 24 (2011) 505–513.

[7] H.B. Trinh, J. chun Lee, Y. jae Suh, J. Lee, A review on the recycling processes of spent auto-catalysts: Towards the development of sustainable metallurgy, *Waste Manag*. 114 (2020) 148–165.

[8] H.B. Trinh, J.C. Lee, R.R. Srivastava, S. Kim, S. Ilyas, Eco-threat Minimization in HCl Leaching of PGMs from Spent Automobile Catalysts by Formic Acid Prereduction, *ACS Sustain. Chem. Eng*. 5 (2017) 7302–7309.

[9] C. Saguru, S. Ndlovu, D. Moropeng, A review of recent studies into hydrometallurgical methods for recovering PGMs from used catalytic converters, *Hydrometallurgy*. 182 (2018) 44–56.

[10] A.T.N. Fajar, F. Kubota, M.L. Firmansyah, M. Goto, Separation of Pallaium(II) an Rhoium(III) Using a Polymer Inclusion Membrane Containing a Phosphonium-Base Ionic Liqui Carrier, *Ind. Eng. Chem. Res*. 58 (2019) 22334–22342.

[11] A.T.N. Fajar, T. Hanada, M.L. Firmansyah, F. Kubota, M. Goto, Selective Separation of Platinum Group Metals via Sequential Transport through Polymer Inclusion Membranes Containing an Ionic Liquid Carrier, *ACS Sustain. Chem. Eng*. 8 (2020) 11283–11291.

[12] L.D. Nghiem, P. Mornane, I.D. Potter, J.M. Perera, R.W. Cattrall, S.D. Kolev, Extraction and transport of metal ions and small organic compounds using polymer inclusion membranes (PIMs), *J. Memb. Sci*. 281 (2006) 7–41.

[13] E. Rynkowska, K. Fatyeyeva, W. Kujawski, Application of polymer-based membranes containing ionic liquids in membrane separation processes: A critical review, *Rev. Chem. Eng*. 34 (2018) 341–363.

[14] T. Hanada, M.L. Firmansyah, W. Yoshida, F. Kubota, S.D. Kolev, M. Goto, Transport of Rhodium(III) from Chloride Media across a Polymer Inclusion Membrane Containing an Ionic Liquid Metal Ion Carrier, *ACS Omega*. (2020).

[15] A.K. Upadhyay, J. chun Lee, E. young Kim, M. seuk Kim, B.S. Kim, V. Kumar, Leaching of

platinum group metals (PGMs) from spent automotive catalyst using electro-generated chlorine in HCl solution, *J. Chem. Technol. Biotechnol*. 88 (2013) 1991–1999.

[16] M.G. Buonomenna, P. Macchi, M. Davoli, E. Drioli, Poly(vinylidene fluoride) membranes by phase inversion: the role the casting and coagulation conditions play in their morphology, crystalline structure and properties, *Eur. Polym. J*. 43 (2007) 1557–1572.

[17] Q.T. Nguyen, O.T. Alaoui, H. Yang, C. Mbareck, Dry-cast process for synthetic microporous membranes: Physico-chemical analyses through morphological studies, *J. Memb. Sci*. 358 (2010) 13–25.

[18] E.A. Nagul, C.F. Croft, R.W. Cattrall, S.D. Kolev, Nanostructural characterisation of polymer inclusion membranes using X-ray scattering, *J. Memb. Sci*. 588 (2019) 117208.

[19] G.R. Guillen, Y. Pan, M. Li, E.M.V. Hoek, Preparation and characterization of membranes formed by nonsolvent induced phase separation: A review, *Ind. Eng. Chem. Res*. 50 (2011) 3798–3817.

[20] L. Chen, J. Chen, Asymmetric Membrane Containing Ionic Liquid [A336][P507] for the Preconcentration and Separation of Heavy Rare Earth Lutetium, *ACS Sustain. Chem. Eng*. 4 (2016) 2644–2650.

[21] S. Huang, J. Chen, L. Chen, D. Zou, C. Liu, A polymer inclusion membrane functionalized by di(2-ethylhexyl) phosphinic acid with hierarchically ordered porous structure for Lutetium(III) transport, *J. Memb. Sci*. 593 (2020) 117458.

[22] W. Yoshida, Y. Baba, F. Kubota, S.D. Kolev, M. Goto, Selective transport of scandium(III) across polymer inclusion membranes with improved stability which contain an amic acid carrier, *J. Memb. Sci*. 572 (2019) 291–299.

[23] M.L. Firmansyah, F. Kubota, M. Goto, Solvent extraction of Pt (IV), Pd (II), and Rh (III) with the ionic liquid trioctyl (dodecyl) phosphonium chloride, *J. Chem. Technol. Biotechnol*. 93 (2018) 1714–1721.

[24] M.L. Firmansyah, F. Kubota, W. Yoshida, M. Goto, Application of a Novel Phosphonium-Based Ionic Liquid to the Separation of Platinum Group Metals from Automobile Catalyst Leach Liquor, *Ind. Eng. Chem. Res*. 58 (2019) 3845–3852.

[25] E. Benguerel, G.P. Demopoulos, G.B. Harris, Speciation and separation of rhodium (III) from chloride solutions: A critical review, *Hydrometallurgy*. 40 (1996) 135–152.

[26] Z. Li, Y. Liu, B. Wang, Q. Lang, M. Tan, M. Lee, C. Peng, Y. Zhang, Insights into the facilitated transport mechanisms of Cr(VI) in ionic liquid-based polymer inclusion membrane – Electrodialysis (PIM-ED) process, *Chem. Eng. J*. 397 (2020) 125324.

[27] L.G. Bulusheva, Y. V. Fedoseeva, E. Flahaut, J. Rio, C.P. Ewels, V.O. Koroteev, G. Van Lier, D. V. Vyalikh, A. V. Okotrub, Effect of the fluorination technique on the surface-fluorination patterning of double-walled carbon nanotubes, *Beilstein J. Nanotechnol*. 8 (2017) 1688–1698.

[28] G.J. Ross, J.F. Watts, M.P. Hill, P. Morrissey, Surface modification of poly(vinylidene fluoride) by alkaline treatment: 1. The degradation mechanism, *Polymer*. 41 (2000) 1685–1696.

[29] S. Zhang, J. Shen, X. Qiu, D. Weng, W. Zhu, ESR and vibrational spectroscopy study on poly(vinylidene fluoride) membranes with alkaline treatment, *J. Power Sources*. 153 (2006) 234–238.

[30] X. Zhao, L. Song, J. Fu, P. Tang, F. Liu, Experimental and DFT investigation of surface degradation of polyvinylidene fluoride membrane in alkaline solution, *Surf. Sci*. 605 (2011) 1005–1015.

Appendix C. Supporting Information

Figure S4.1. Photograph of the SAC sample in the form of a fine powder.

Table S4.1. PGM content in the SAC sample and a comparison of leaching efficiency acquired with and without HCOOH pretreatment.

Metal	PGM content (g/kg SAC)[1]	Leaching efficiency (%)[2]		
		2M HCl with pretreatment	2M HCl	5M HCl
Pt	1.29	91	57	95
Pd	3.06	96	68	96
Rh	0.63	93	36	94

[1]The PGM content was determined by digestion method in *aqua regia*.

Digestion procedure

The aqua regia was prepared by mixing HCl (32%) and HNO_3 (60%) with a molar ratio of 3 : 1. In a typical experiment, 100 mg of the SAC powder was dispersed into 10 mL of aqua regia in a round-bottom flask. Subsequently, the mixture was stirred vigorously at 70 °C under reflux condition for 48 h. The product solution was then diluted using deionized water for safe handling and filtered to observe any residue. The metal concentration was measured using ICP-OES. Any solid residue was hardly observed during filtration; thus, it could be assumed the metals in the SAC, especially the PGMs, were almost completely dissolved.

[2]Calculated using the following equation.

$$L = \frac{C_L}{C_i} \times 100\% \qquad \text{(S1)}$$

Where L is the leaching efficiency (%), C_L is the metal concentration in the leaching solution per 1 g of SAC powder in 100 mL solution (ppm), and C_i is the metal concentration in the digestion product per 1 g of SAC powder in 100 mL solution (ppm). It should be noted that the leaching efficiency of 2 M HCl with HCOOH pretreatment was significantly higher than that of 2 M HCl without pretreatment, and it was also comparable to that of 5 M HCl.

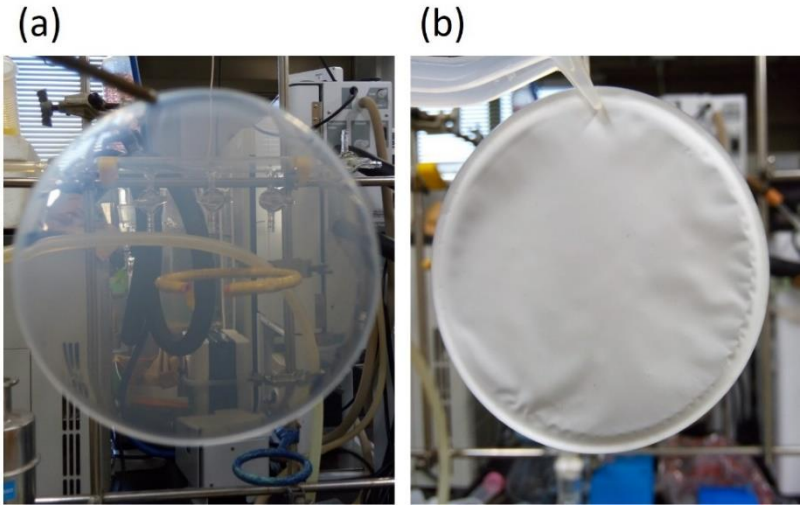

Figure S4.2. Photograph of the as-prepared (a) ID-PIM and (b) AP-PIM.

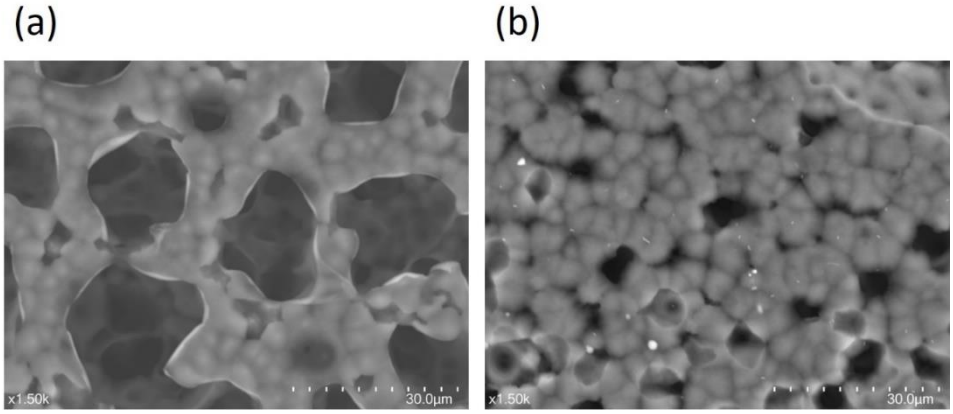

Figure S4.3. SEM images of the surfaces of AP-PIM on the (a) upper (in contact with air) and (b) lower (in contact with glass) side.

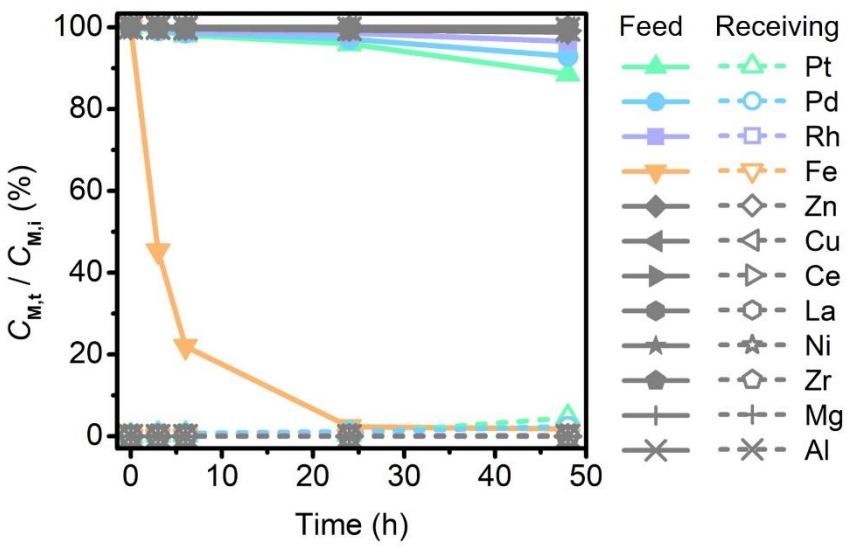

Figure S4.4. Adsorption behavior of Fe species from the SAC leachate solution.

Fe removal was conducted in a transport experiment apparatus with the following conditions:

Feed solution : SAC leachate

Receiving solution : 0.1 M Na_2SO_3

Membrane : ID-PIM

Fe ions were selectively adsorbed into the membrane due to the use of sodium sulfite (Na_2SO_3) solution—a commonly used solution for Fe scrubbing in solvent extraction processes—as the receiving solution. The optimum time for Fe removal was 24 h. Prolonging the operation time led to the transport of Pt and Pd into the receiving solution. The membrane containing Fe was not used for further operations.

Table S4.2. Metal concentrations in the SAC leachate solution after Fe removal.

Metal	Pt	Pd	Rh	*Fe*	Zn	Cu	Ce	La	*Ni*	*Zr*	Mg	Al
C (ppm)	56.1	143	29.1	*1.0*	16.9	8.6	150	750	*0.2*	*1.2*	1657	6174

Metals with concentrations of less than 1.5 ppm (in the present case: Fe, Ni, and Zr) were neglected when calculating the transport results for the sake of simplicity.

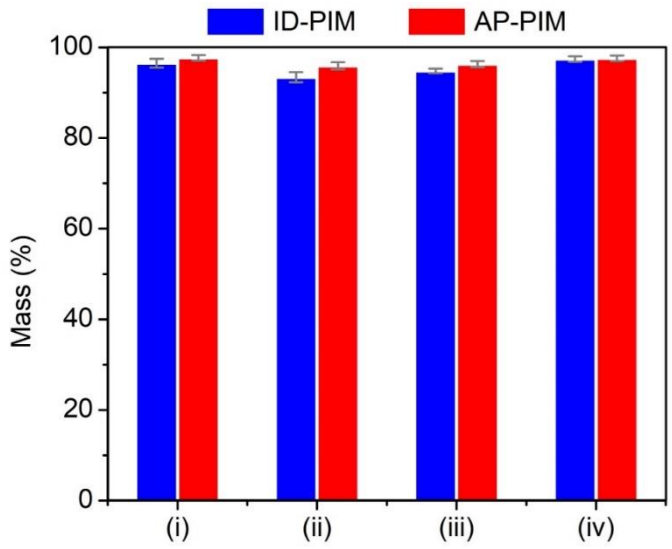

Figure S4.5. Remaining mass of the membranes after being immersed in (i) 5 M HCl, (ii) 1 M $NaClO_4$, (iii) 1 M thiourea + 1 M KSCN, and (iv) 5 M NH_4Cl for 10 days with constant shaking.

Table S4.3. Phosphorous (P) concentrations in the solutions after the membranes were immersed.

Solution	**P concentration (ppm)**	
	ID-PIM	**AP-PIM**
5 M HCl	0.061	0.003
1 M $NaClO_4$	0.118	0.077
1 M thiourea + 1 M KSCN	0.089	0.066
5 M NH_4Cl	0.041	0.008

~ End of Chapter 4 ~

CHAPTER 5. GENERAL CONCLUSIONS

5.1 Summary

The demand for PGMs was steadily rising in the past several years and is predicted it will be continuously growing in the future. Since the amount of primary ores is limited and the role of PGMs in the manufacture of various products is arguably irreplaceable, the need to recover PGMs from end-of-life products as a secondary source is inevitable. Furthermore, using wastes as resources is also favorable from the perspective of environmental ethics since it would decrease the necessity to excavate more mining sites and prevent harmful material disposal into landfill. As such, automotive catalyst wastes meet the criteria of secondary resources as they possess PGM-rich content and are widely available, i.e., proportional to the number of cars in the world. However, an adequate and green technology for the separation and recovery of PGMs is quite challenging issues. The present thesis addresses those issues by developing the PIM technology specifically designed to recover PGMs, using $P_{88812}Cl$ ionic liquid as the metal carrier.

In the Chapter 2, PIMs containing the $P_{88812}Cl$ ionic liquid was developed, and the transport performance in the separation of Pd(II) and Rh(III) was systematically investigated. The optimum PIM composition was 50 wt% PVDF-*co*-HFP (base-polymer), 40 wt% $P_{88812}Cl$ (carrier), and 10 wt% 2NPOE (plasticizer). In the experiments to selectively transport Pd(II) from the feed to receiving solutions, several factors affected the transport kinetics and selectivity, including the concentration of HCl in the feed solution, the concentration of thiourea in the receiving solution, and the initial metal concentration. At the optimized condition, selective transport of Pd(II) with a recovery yield of 98% and purity of 99% could be achieved, while Rh(III) remained in the feed solution. As a comparison, PIMs containing a commercially available $P_{66614}Cl$ ionic liquid were also prepared. The PIM containing $P_{88812}Cl$ demonstrated a stable performance over a 7-cycle of reusability test, while the PIM containing

$P_{66614}Cl$ exhibited approximately 30% depletion in the ability to transport Pd(II) selectively. The remarkable performance of $P_{88812}Cl$ ionic liquid to function as a carrier could be attributed to its higher hydrophobicity but lower viscosity compares to those of its commercially available counterpart. These promising results became a useful insight to carry out further investigation.

In the Chapter 3, a strategy to perform separation of three PGMs, i.e., Pt(IV), Pd(II), and Rh(III), using the PIM developed in the Chapter 2 was established. Sequential transports using a one-pot system with one membrane were carried out. In the first transport sequence, Pt(IV) could be selectively transported with the recovery of 96% and purity of 89.9%, while Pd(II) and Rh(III) stayed in the feed solution. The selective Pt(IV) transport was driven by an appropriate receiving solution, which was 0.1 M $NaClO_4$ in 1 M HCl. In the second transport sequence, Pd(II) could be transported into the receiving solution with a recovery of 96% and purity of 99.9%, while Rh(III) completely remained in the feed solution. This time, the receiving solution was a mixture of 10 mM thiourea, 0.1 M KSCN, and 1 M HCl. After the desired separation performances were achieved, transport mechanisms were studied by considering the transport behaviors and spectroscopy analyses. Pt(IV) was transported through the PIM via a coupled ion-exchange mechanism, and Pd(II) was transported via simultaneous ion exchange and ligand substitution. In addition, a membrane stability test demonstrated excellent durability of the PIM as it could maintain the stable performance over the course of 4 weeks, during which sequential transports of Pt(IV) and Pd(II) were continuously carried out.

In the Chapter 4, the PIMs and the transport strategy developed in the Chapter 2 and the Chapter 3 were applied to recover PGMs from an actual waste, i.e., a spent automotive catalyst. At first, metals were leached from the automotive catalyst matrix using 2 M HCl, preceded by pretreatment using HCOOH. The leachate solution, which contains 12 metals, was subjected to membrane transport operations to recover the PGMs selectively. To study the possibility to enhance transport performances further, two types of PIMs were prepared, which are

membranes with isotropic and dense morphology (ID-PIMs) and membranes with anisotropic and porous morphology (AP-PIMs). Selective transport of Pt(IV) from the leachate solution could be performed through both types of PIMs with recoveries of more than 90%. In the selective Pd(II) transport, ID-PIM showed a remarkable product purity (almost 100%), while AP-PIM showed rapid transport kinetics. As for Rh(III), the transport hardly occurred through ID-PIM, while it was observed to happen through AP-PIM. It was also found that the Rh(III) transport could be improved at elevated temperatures. ID-PIMs and AP-PIMs, although having the same chemical compositions, demonstrated distinctive features which are governed by the morphologies. This could be a helpful insight into the future development of PIMs. More importantly, the recovery of PGMs from the spent automotive catalyst using PIMs containing the ionic liquid was successfully performed, along with unraveling the chemistry phenomena that drive the transport of the metals through the membranes.

5.2 Outlook

The research findings in the present thesis may contribute to inspire developments of practical technologies in metal industries as well as membrane industries. From the industrial perspective, one of the concerns is probably related to the implementation of the current PIM technology on a large scale. The present study demonstrates all the transport achievements on the laboratory scale—the membranes at centimeter-scale and the feed and receiving solutions at milliliter scale. This is also the case for the majority of other reported studies. Thus, an attempt to perform transport experiments on a larger scale might be considered in future studies. Designing a membrane module to carry out this experiment would be one of the challenges, together with membrane preparation, handling, and the setup. In addition, some transport behaviors might change at a larger scale owing to the interplay between many forces, which needs to be considered at the fabrication of the module.

Some transport phenomena in the present study also arise intriguing questions from the theoretical viewpoints, particularly related to the role of carriers. Commonly, transport phenomena through membranes are classified into two models, i.e., pore flow and solution-diffusion models. The pore flow model is observed in porous membranes, and the transports are governed by Darcy's law. The solution-diffusion model is marked in a dense membrane, and the transports are governed by Fick's law. It is pretty standard that the calculation of transport kinetics in PIM experiments would be assumed to follow Fick's law since the membranes are typically dense. Nevertheless, it should be pointed out that the role of the carrier is not fully accounted for in this particular law. Thus, the accuracy of this approach might be further increased if the function of the carrier could be quantified into a tangible constant in the equation. Although it is evident that different carriers would lead to different transport behaviors, describing the feature into a mathematical formula is not an easy task. Modeling of PIM transport phenomena with thoroughly deliberating the role of the carrier would be exciting challenges in the future and perhaps would lead to a theoretical breakthrough in the field of the membrane science.

ACKNOWLEDGMENTS

Firstly, I would like to express my utmost gratitude to my supervisor, Prof. Masahiro Goto, for his guidance and support throughout the Ph.D. course at Kyushu University. It has been a privilege and a great honor to have you as my academic advisor. Your brilliant yet understandable ideas and admirable work ethic have been inspiring me in terms of research activities as well as life in general. Under your supervision, I felt much improvement in my knowledge, skills, attitude, and confidence, which led me to become a better scientist. I also would like to thank Prof. Noriho Kamiya, who is my co-advisor, for his support, advice, and encouragement during my Ph.D. study. I am thankful for the valuable comments and perspective that you gave during my stay in this lab. I am incredibly proud to be a member of Goto-Kamiya Laboratory. Also, I would like to express my gratitude to Prof. Masahiro Kishida as the thesis advisor and one of the thesis committee members. I really appreciate your constructive suggestions, critical questions, and noteworthy comments.

I would like to thank Assistant Prof. Fukiko Kubota, who has been retired as of April 2020, for her continuous help and advice, especially during my first year. Your expertise and insight have become my source of ideas in further developing my research. Have a nice retirement life, Kubota-sensei! I am indebted to Assistant Prof. Rie Wakabayashi for her continuous support during my research. I am really thankful for your helps every time I had trouble in the laboratory. I would also thank Assistant Prof. Kosuke Minamihata for his valuable and helpful comments during lab meetings. I really enjoy having a discussion with you. I appreciate the continuous support from all staff in Goto-Kamiya Laboratory.

I am really grateful to the Ministry of Education, Culture, Sport, Science and Technology (MEXT) of Japan for providing a scholarship. It has been a privilege to be a MEXT scholar. I am also indebted to many people who contribute to the success of my Ph.D. study. I gratefully acknowledge Prof. Aishah Abdul Jalil from University Teknologi Malaysia for introducing me

to Goto-sensei. This fantastic opportunity to join GK-Lab would not have occurred without your trust and kindness. I also gratefully thank my admirable senpai, Dr. M. Lutfi Firmansyah and Dr. Wataru Yoshida, for their tremendous support in technical experiments as well as discussion of ideas, particularly during my first year. I am also thankful to my genius lab mate and partner of discussion, Hanada-san. I really enjoy having a discussion and working together with you.

In addition, thanks to Indonesian GK-Lab members (Kak Alif, Mbak Patma, Kang Dani, Mas Wahyu, Mas Pugoh, Yovita, and Ghazian) for their support and togetherness. Thanks to international students and lab mates (Cai, Ali, Shihab, Moshikur, and others) for the support and friendship. Also, thank you to all members of GK-Lab, which I cannot mention one by one, for your continuous support, for warmly welcoming me, and for our memorable moments during my stay in Japan.

Lastly, I would like to thank my family: my mother, father, and brother, for their endless support and countless encouraging messages on pursuing my career. Alhamdulillah, all praise is to Allah, the almighty God who is always protecting me, guiding my soul, and blessing my life. I thank You with every breath I take.

In the midst of a global pandemic,

Fukuoka, June 2021

Adroit T.N. Fajar